STEM CELL-BASED OVARIAN CANCER SUICIDE GENE THERAPY

by

FARANAK SALMAN NOORI

A Dissertation submitted to the

Graduate School-New Brunswick

Rutgers, the State University of New Jersey

In partial fulfillment of the requirements

For the degree of

Doctor of Philosophy

Graduate Program in Pharmaceutical Sciences

Written under the direction of

Professor Arash Hatefi, PhD

And approved by

_____

_____

_____

_____

New Brunswick, New Jersey

October, 2015

ABSTRACT OF THE DISSERTATION

Stem cell-based ovarian cancer suicide gene therapy

By FARANAK SALMAN NOORI

Dissertation Director:

Arash Hatefi, PhD.

Cancer is a leading cause of death worldwide, resulting in 8.2 million deaths in 2012. Tumor suicide gene therapy is among the novel targeted therapeutics that has demonstrated promising results. There are two important factors that specify the efficiency and safety of the suicide gene therapy systems. One is vector safety and efficiency and the other enzyme/prodrug anticancer efficacy. Among the vectors employed for delivery of therapeutics, mesenchymal stem cells (MSCs) have attracted tremendous amount of attention due to their unique features such as inherent tumor tropism and low immunogenicity. The objective of this research was to take advantage of MSCs as cell-based vectors to develop an efficient and safe suicide gene therapy system for cancer. As a first step towards achieving the objective, I engineered a panel of MSCs that were genetically modified to express five different suicide genes and compared their anti-tumor efficiency in vitro and in vivo. Among the enzyme/prodrug systems tested, genetically modified MSCs that expressed yeast cytosine deaminase enzyme (yCD-UPRT) in combination with prodrug 5-fluorocytosine (5FC) demonstrated the highest anti-tumor efficacy. In the next step we focused on developing a safe and efficient method for stem cell engineering. Since current commercially available transfection

agents are inefficient and toxic to MSCs, I made an attempt to develop a safe and efficient gene delivery system suitable for MSC engineering. Using a previously developed vector in Dr. Hatefi's lab as a template, I recombinantly engineered a new vector for MSC transfection. This vector is comprised of a cell penetrating peptide for penetration into MSCs, four histone H2A repeats to condense plasmid DNA (pDNA) into nanosize particles and a fusogenic peptide named GALA to facilitate endosomal escape. The results of this study illustrated that the newly developed recombinant vector could efficiently and safely transfect MSCs. In conclusion we not only successfully developed a safe and efficient method for stem cell engineering but also identified an enzyme/prodrug system that could be used for effective treatment of ovarian cancer.

DEDICATION

To my grandmother, Masoumeh;

Who taught me humanity and love are the most important assets for life.

To my husband, Hamed;

Who supported me with his unlimited love during all tough moments.

To my parents, Mohammad and Mehri;

Who always sacrificed for me to achieve my dreams.

To my advisor, Dr Arash Hatefi;

Who instructed me to think more deeply and be a real scientist.

To my brothers, Mehrdad and Vahid;

Who encouraged me to be courageous enough to experience a challenging life.

Table of Contents

Figure List

Chapter 1

Introduction

Every year, cancer claims the lives of more than half a million Americans. Cancer is the second leading cause of death in the United States, exceeded only by heart disease. While conventional therapeutic systems have demonstrated successful anti-tumor effect, their systemic toxicity on the normal organs has prevented from raising the therapeutic doses. To overcome this limitation, several novel strategies have been proposed and studied to exert the therapeutic effect in a more efficient and targeted manner.

One of the popular targeted approaches for cancer therapy is the use of gene delivery system which is defined by two key components; therapeutic gene and tumor delivery vector. Among different categories of anti-tumor genes that have been studied, suicide genes have illustrated very promising results. This class of genes is able to express an enzyme inside the cell that converts a non-toxic prodrug to a toxic metabolite. Their significant benefit over the other therapeutic genes is exerting bystander effect that enables them not only kill the transfected cells but also the neighboring cells[1]. This is a very critical advantage considering that tumors have a very dense environment that prevents vectors from reaching to the deep sites of the tumors, however; drug molecules can easier penetrate to the tumors owing to their small molecular size. The success of suicide gene delivery system is highly dependent on the enzyme efficiency in prodrug conversion, the physicochemical properties of the prodrug and the strength of bystander effect[2]. Different types of suicide genes are available in the literature but there is no study to compare them side by side and determine the most efficient one for clinical applications. After reviewing the literature we found out that yeast cytosine deaminase-uracil phosphoribosyltransferase (yCD-UPRT), nitroreductase (NTR) and thymidine

kinase (TK) are among the most extensively used suicide genes; hence we decided to include them in our study.

The vectors used for gene delivery are classified in three major groups i.e. viral, non-viral and cell based vectors and each of them has its own benefits and drawbacks. Mesenchymal stem cells (MSCs) as a cell based vector are nowadays very popular for cancer therapy purposes owing to their distinct properties such as inherent tumor tropism and low immunogenicity[3]. As opposed to nanomedicines, they are also able to actively penetrate to the deeper part of the tumors by use of special movements called diapedesis[4]. All of these desirable features inspired us to select MSCs as the tumor delivery vector in our project.

After selecting suicide genes as the anti-tumor therapeutic gene and MSCs as the tumor delivery vector we prepared a panel of MSCs transfected with yCD-UPRT, NTR or TK and characterized their anti-tumor efficiency in vitro and in vivo in order to find the most efficient one. Transfection of the MSCs for this part of project was very challenging because MSCs can be maintained in an undifferentiated condition until a limited passage number (~8) and treating them in vitro for a long time can alter their properties[5]. Therefore, an efficient transfection reagent that is able to transfect a large number of MSCs each time while keeping their viability is inevitable. Consequently, we decided to develop an efficient and safe recombinant vector for stem cell transfection to fill this void.

In order to develop a vector for efficient and safe transfection of the stem cells, we used the recombinant vector previously developed in our lab as the template. This vector

is comprised of a tumor targeting moiety, four histon repeats (as a DNA condensing motif) and GALA (as the fusogenic peptide to facilitate endosomal escape)[6]. In the first step we replaced GALA with the other class of fusogenic peptides including RALA, KALA, H5WYG and INF7 to find the most appropriate one for our recombinant vector. In the second step we substituted the tumor targeting motif with penetrating peptide (Pep-1 or MPG) or VEGFR agonist. It is reported in some studies that Pep-1 and MPG are able to increase the cell internalization through direct translocation[7,8]. VEGFR is also highly expressed on the surface of the MSCs and its targeting can theoretically facilitate the cell uptake. All these constructs were developed and characterized in order to determine the most efficient and safest vector for MSCs transfection. At the end, this project is able to introduce an efficient and safe gene delivery system for cancer therapy purposes.

Chapter 2

Suicide Gene Therapy of Cancer

Cancer is generated by uncontrolled proliferation and abnormal growth of the cells which leads to tumor formation. Tumor environment has a complex pathophysiology consisting of abnormal lymphatic drainage, leaky blood vessels, and hypoxic environment. Poor lymphatic drainage increases the interstitial fluid pressure within the tumors. This pressure makes a resistance against the movement of the drug toward the core of the tumor and complicates the therapy[2]. The first attempts for cancer therapy was based on inhibition of cell proliferation by use of anti-metabolite agents. Unfortunately, the undesirable effect of this category of drugs on normal tissues specifically on high proliferating cells limited their application. Together with advances in biology and genetic of the cancer, in order to decrease systemic side effects, targeted cancer therapy enticed a lot of attention between scientists[2]. Imatinib mesylate (Gleevec®), approved in 1996, is the first targeted chemotherapy agent designed based on advances in genetics. Unfortunately, these rationally designed drugs may enter other organs which have the same biological attributes as tumors. For instance, Imatinib's can also inhibit c-fms tyrosine kinase in osteoclasts and osteoblasts which leads to hypophosphatemia and hypocalcemia[9].

Beside to antibody-based targeted therapy, numerous works was carried out simultaneously on different type of nanomedicines. The purpose was to increase efficiency and decrease toxicity by drug localization enhancement at tumor. Due to high leakiness of blood vessels, nanomedicines have a higher extravasation when reach to the tumor site relative to the other organs. Having considered the poor lymphatic drainage, this high leakiness can contribute to higher accumulation and retention of the drug in tumor site through passive targeting. This mechanism is called enhanced permeability

and retention (EPR) effect. Although this passively targeted formulations can increase drug concentration in tumor site but their efficacy is limited to the leakiness of blood vessels which is different based on the tumor size and tumor type. As a result neither of antibody-based therapeutics or nanomedicines are not sufficient to render an efficient and non-toxic therapy for cancer[2].

One of the other novel approaches that is extensively studied in recent years for targeted cancer therapy purposes is gene delivery. The success of this therapeutic system is highly dependent on the anti-tumor efficiency of the gene after expression and the efficacy of the vector for delivering the gene to the tumor site. Different categories of therapeutic genes and vectors are proposed for cancer therapy that are elaborated in further sections. The favorable outcomes could be achieved through the right selection of each and their combination.

2.1 Cancer Gene Therapy

Cancer gene therapy is based on the transfer of therapeutic genes into the tumor cells to stop or slow down the progression of the tumors. Three categories of therapeutic genes which are commonly used for cancer therapy are corrective gene therapy, toxin-apoptosis inducing gene therapy and suicide gene therapy. Corrective genes modify the gene expression profile of the tumor cells to stop or slow down cell proliferation. Tumor suppressor genes such as P53 are the examples of this group[10]. Toxin-apoptosis inducing genes express toxic proteins such as TNFα which can induce cell death in tumor cells [11]. The major problem attributed to these two groups of therapeutic genes is only the cancer cells that have received the genes are going under therapeutic effect. This would be a very critical problem because nanomedicines are not able to penetrate deep into the tumor

due to the dense physiological nature of the tumor and the high pressure of interstitial fluid[12]. Hence the tumor cells which were not affected by the therapeutic genes mediate recurrence of the disease.

2.2 Suicide Gene Therapy

One of the popular approaches to circumvent above mentioned hurdles is suicide gene therapy. This approach takes advantage of passive, active and transcriptional targeting to maximize the therapeutic effect in tumor and minimize the toxic effect in normal tissues. This approach is also known as gene directed enzyme prodrug therapy (GDEPT) in literature. In fact, GDEPT is a two steps process. In the first step, tumor cells are transduced with a gene encoding a non-toxic enzyme. This enzyme has the capability to convert a non-toxic prodrug to a toxic metabolite. In the second step, prodrug is administered and converted to a toxic metabolite. The toxic metabolite first kill the cell that is produced in it and then diffuse out and enter to the surrounding cancer cells[13]. This effect is called bystander effect **(Figure 2.1)**[1].

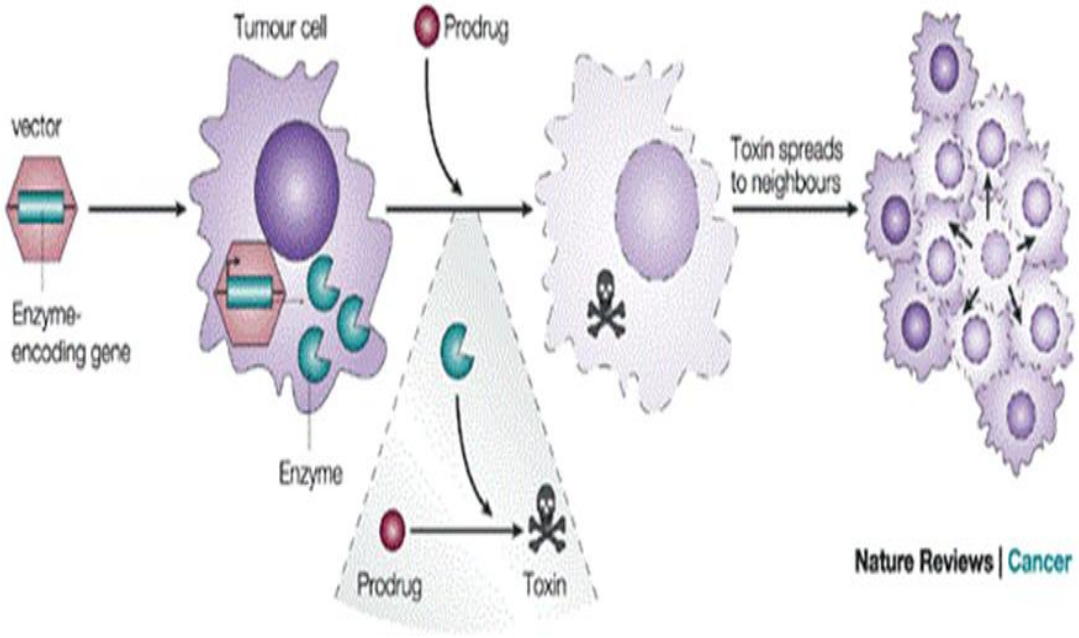

Figure 2.1: Suicide gene therapy and bystander effect, vector carries a gene that encodes a prodrug-converting enzyme to tumor cells. The prodrug is converted to the active, cytotoxic metabolite in the tumor cell, and diffusion to neighboring cells confers a potent bystander effect (Frank McCormick 2001).

This approach provides two distinct advantages over the conventional cancer treatments. The first advantage is the feasibility of transcriptional targeting in addition to passive and active targeting[14]. In this type of targeting suicide gene is located under the control of a tumor-specific promoter such as human telomerase reverse transcriptase promoter. Hence the gene expression occurs only in tumor cells but not in normal cells. The major factor preventing transcriptional targeting approaches from moving into the clinic is that the cancer-specific promoters usually have low transcriptional efficacy and are not able to produce sufficient amount of toxic metabolites.

The second advantage that makes a preference for suicide gene therapy over corrective and toxin-apoptosis inducing gene therapy is that by use of bystander effect not only the producing cells are killed but also the drug can diffuse to deeper part of the tumor and kill the un-transduced cells[2]. This diffusion may occur through gap junctional intercellular communication or endocytosis of apoptotic bodies released from dying cells. Another type of bystander effect, known as distant bystander effect, involves the activation of immune system by cancer antigens released from dead cells[15]. This mechanism is important in prevention of forming secondary tumors.

2.3 Important Factors that Impact the Success of Suicide Gene Therapy

The success of suicide gene therapy of cancer depends on three important factors, i.e. enzyme, prodrug and the delivery system (vector)[2]. The choice of each component is very critical to have a safe and efficient therapeutic system in clinical level. Enzymes that are used in GDEPT can be categorized into two groups. The first group of the enzymes can be found in normal human cells such as cytochrome P450. This group has less immunogenicity but their application may results in non-targeted toxicities in normal

tissues. The second group of enzymes is originated from viruses or bacteria such as bacterial nitroreductase. In contrast to the first group the probability of immunogenicity is higher in this category, however; non-targeted toxicities is less likely. In recent years many attempts has been made to develop new version of the enzymes with higher efficacy, more stability and less immunogenicity. Prodrugs should also own some specific properties to be tailored for efficient and safe therapy. The prodrug should be stable in the body, show low toxicity before and high toxicity after activation and own high bystander effect[2].

The third important component of suicide cancer gene therapy is the vector. The desirable properties of a suitable vector for clinical applications are low cytotoxicity/immunogenicity, high transfection efficiency, tissue specificity and cost-effectiveness[16]. Gene delivery vectors are generally categorized in three different groups consisting of synthetic (e.g., polymeric and lipid based), microorganism-based (viral, bacterial, yeast) and cell-based (e.g., stem cells or dendritic cells). These vectors will be elaborated in further sections.

2.3.1 Enzyme/prodrug systems

The most commonly used enzyme/prodrug systems are thymidine kinase/ganciclovir, cytosine deaminase/5-fluorocytosine, nitroreductase/CB1954, carboxypeptidase G2/nitrogen mustard, and purine nucleoside phosphorylase/6-methylpurine deoxyriboside.

Thymidine kinase/ganciclovir (TK/GCV): TK/GCV system is the most broadly used enzyme/prodrug in preclinical suicide gene therapy studies. GCV blocks DNA synthesis

and mediates cell death through necrosis or apoptosis induction. There are two major hurdles that limit this system application. Firstly the cytotoxic bystander effect of GCV is GJIC dependent; thereby, its anticancer activity is limited as GJIC is significantly compromised in many type of tumors[17]. Secondly HSVTK possess a high affinity to its natural substrate thymidine which can generate high nonspecific toxicities on normal tissues[18]. In order to solve this problem modified version of this enzyme were developed such as SR39 and TK007[19,20]. The needed dose to exert a therapeutic effect is significantly lower for these modified versions due to their higher affinity for GCV.

Cytosine deaminase/5-fluorocytosine (CD/5FC): This system has some important advantages over HSVTK/GCV including gap junction independent bystander effect and induction of significant distant bystander effect[21]. CD can be prepared from bacterial (bCD) or yeast (yCD) origin. It comparison to bCD, yCD has significantly higher affinity for 5-FC but it is more thermosensitive and has a shorter half-life in vivo, however; this problem is addresses with the new mutant of yCD[22]. In the other attempt, yCD is combined with uracil phosphoribosyltransferase (yCD-UPRT) which converts 5-FU to 5-fluorouridine 5′-monophosphate and generates a higher sensitivity to 5-FC in comparison to yCD alone[23]. 5FC is able to penetrate blood brain barrier, hence, this system is a good candidate for brain tumors.

Nitroreductase/CB1954 (NTR/CB1954): CB1954 is a DNA alkylating agent which becomes activated after conversion by nitroreductase originated from Escherichia coli[24]. After activation by cellular thioesterase, CB1954 becomes a potent DNA chelating agent which can freely diffuse to neighboring cells and induce extensive DNA damage and a P53 and cell cycle independent apoptosis[25]. This enzyme/prodrug system is able to kill

both dividing and non-dividing cells; however, dose-dependent hepatotoxicity and low conversion rate of prodrug has limited its application. This problem is partially address through development of new generation of prodrugs such as PR-104A and nitro-CBI-DEI in recent years[26]. Several new studies are underway to examine their therapeutic potential in clinical trials but the number of these studies is very limited due to restricted availability of these prodrugs as the commercial materials.

Carboxypeptidase G2/nitrogen mustard (CPG2/NM): In all enzyme/prodrug systems mentioned above, prodrug undergoes more than one step for activation. When one of these steps is dependent on intracellular enzymes, the conversion rate will be restricted by the activity of that enzyme. Bacterial enzyme CPG2 from Pseudomonas RS-16 separates glutamic acid from nitrogen mustard-based drugs to release the cognate drug. As opposed to the other enzyme/prodrug systems discussed before, this drug is activated by itself and doesn't need further activation. The final metabolites is lipophilic and independent of gap junction can easily diffuse to surrounding cells and make inter and intra DNA linkage[2]. The major disadvantage of this system is the toxicity and immunogenicity imposed by diffusion of the enzyme to blood circulation. To prevent this issue, the secretory tag of the enzyme has been cleaved to confine its activation to cytosol[27].

2.3.2 Gene Delivery Vehicles (Vectors)

Gene therapy was first employed for the treatment of single-gene defects but nowadays different category of disease such as cancer, cardiovascular disease and neurodegenerative disorders are the subject of most gene-therapy research. Having considered these various types of targets, it becomes obvious that there can be no single vector that is suitable for all applications. The hallmark features of a suitable vector for

clinical applications include low cytotoxicity/immunogenicity, high transfection efficiency, tissue specificity and cost-effectiveness. The most important vectors for gene therapy are consisting of viral, non-viral and cell based vectors. Each of these vectors has been broadly used for gene therapy of cancer and has its own advantage and disadvantage.

Viral vectors: The most common viral vectors in the field of gene therapy are lentivirus, retro-virus, adenovirus (Ads), adeno-associated virus (AAVs) and herpes simplex virus (HSV). The major advantages of viral vectors over the other vectors is high transduction efficiency[28]. Retrovirus and lentivirus are categorized as integrating viruses. The problem associated with this group is while they generate persistent gene transfer but the probability of oncogenesis increases due to genome integration. In contrast to retroviruses that are able to infect only dividing cells, lentiviruses does not have any restriction and have the capability of infecting both dividing and non-dividing cells. The big advantage of this group is inducing low immunogenicity response. The other important point worth mentioning is that the assembly and production of such viruses is considered easy, whereas their production in high titers (> 108 pfu/ml) is time-consuming and difficult[29].

Ads, AAVs and HSV are categorized as non-integrating viruses and in contrast to previous group doesn't have the problem of oncogenesis. Ads and AAV are able to infect a broad range of cells but their packaging capacity is low. On the other hand HSV has a high tropism only for neurons but own the highest packaging capacity among all viral vectors. From this group Ads and HSV can elicit strong immune response but AAV is similar to previous group and induce low immunogenicity. Although viral vectors are

distinct because of having an efficient transduction capability compared to the other groups, high manufacturing cost, tissue targeting constraints and life threatening immune response has confined their application[29].

Non-viral vectors: They are classified into two groups: cationic lipids such as 1,2-dioleyloxy-3-trimethylammonium propane (DOTAP) and cationic polymers such as polyethylenimine (PEI). These cationic lipids and polymers bear positive charges on their surfaces which confers them the ability to condense DNA through electrostatic interactions[30].

Cationic lipids are able to condense DNA plasmids and form stable particles that are called lipoplexes. The gene transfer efficiency of lipoplexes is dependent on the structure of the cationic lipid; lipid-to-DNA charge ratio; the structure and proportion of the helper lipid in the complexes; the complex size and surface charge; the total amount of lipoplexes applied; and the cell type[31]. While this positive surface charge can increase the probability of the membrane binding and internalization, it can generate high toxicities and aggregation with negatively charges serum proteins. To alleviate these problems, lipoplexes are modified with poly ethylene glycol (PEG) on their surface to mitigate their surface charge density and minimize their toxic effects[32]. However, two different groups have recently demonstrated that repeated injection of PEGylated liposomes in rats and mice evoked PEG-specific IgM/IgG antibodies production[33,34]. The other drawback of this group is size heterogeneity of targeted lipoplexes. Particle size is a determining factor in the mechanism of particle entry into cells. Studies have revealed that receptor mediated internalization is mediated through clathrin-coated pathway for particles with the size

distribution less than 150 nm. Above 150 nm particle size, the cellular uptake is carried out towards other nonspecific pathways[35].

Cationic polymers are the other type of non-viral vectors. PEI has been found to be an efficient vector for gene delivery. However, it has been demonstrated that PEI-based polyplexes induce molecular weight, zeta-potential, particle size and a degree of branched-dependent cytotoxicity which stems from their non-biodegradability[36]. PEI is generally believed to be non-immunogenic mostly owing to the lack of structural hierarchy. PEI has also the potential to bind negatively charged blood components after systemic administration and therefore be eliminated from the blood circulation before reaching the target tissue. Again, polymers such as PEG, are able to mitigate this problem[37]. One of the shortcomings of this type of vectors is as most conventional polymers are synthesized using free radical addition or similar methods, the resulting product is heterogeneous. Consequently, the structure/function relationship has been difficult to elucidate[30].

In conclusion, non-viral gene delivery vectors have some disadvantages including poor gene transfer rates, lack of reproducibility, heterogeneity and cytotoxicity which has kept them in the second priority after viral vectors.

Cell based vectors: Dendritic cells and mesenchymal stem cells are among the most broadly used cell based vectors. Dendritic cells (DCs) are able to efficiently uptake, process and present antigen to initiate adaptive immune responses. Antigen captured by interstitial DCs mediates humoral immunity whereas the one captured by Langerhans cells (LCs) trigger cellular immunity. Hence, targeting LC is important for designing of

vaccines that the final target is inducing strong cellular immune-response[38]. In order to produce ex vivo derived DC-based vaccines, several methods have been reported for loading of DCs with antigens. These methods consist of autologous inactivated or recombinant virus, peptides and proteins, mRNA and nanoparticles. In order to prepare in vivo DC based vaccines antigens are delivered to DCs using chimeric proteins made of anti-DC receptor antibody fused to a selected antigen. The most frequent outcome of the current DC vaccination trials is a demonstration of expanded antigen-specific immunity, but no long lasting tumor regression. Therefore, it is highly required to build on DC subsets for improving cancer vaccines[39].

Recent progress in mesenchymal stem cell (MSC) research has sparked great interest among scientists because these cells are taken from the patient's own body and can act as an easily accessible cell source for cell transplantation in cancer therapies. One of the attractive attributes of the stem cells is their inherent tumor tropism. This characteristic of stem cells could be exploited to develop effective treatments for patients with tumors that are hard to access or treat (e.g., glioblastoma)[40]. For this purpose, stem cells are first genetically modified ex-vivo to stably express a therapeutic molecule and then are injected back into the body to migrate into tumors and exert their therapeutic effect in the targeted site.

2.4 Conclusion

Suicide gene delivery systems encompass some specifications that tailors them for targeted cancer therapy purposes. They are able to exert extensive anti-tumor effects through bystander effect. In order to design and develop an efficient and safe suicide

gene therapy system two important factors needs to be precisely selected; tumor delivery vector and enzyme/prodrug system.

Selecting a suitable vector for gene delivery purposes is one of the critical steps toward developing a successful gene therapy system for cancer. It appears that MSCs own specific qualifications that highlights them among all different types of vectors. MSCs are easily isolated from the body (bone marrow or adipose tissue) and expanded in vitro. They don't evoke immune response owing to lack of MHCII expression and low demonstration of MHCI. MSCs own intrinsic tumor tropism that confers them targeted tumor delivery and tailors them for therapy of hard to access tumors[3]. At last but not least, in contrast to nanomedicines, they can actively penetrate deep inside the tumor by special movements known as diapedesis[4]. All the mentioned above properties that are discussed in more details in next chapter inspired us to pick MSCs as the most appropriate vector for our cancer gene therapy project.

Chapter 3

Use of Stem Cells for Cancer Suicide Gene Therapy[1]

[1] A version of this chapter has been published in Stem Cell Reviews and Reports. Please see "Practical Issues with the Use of Stem Cells for Cancer Gene Therapy", PMID: 26123358.

Recent progress in stem cell research has sparked great interest among scientists because these cells are taken from the patient's own body and can act as an easily accessible cell source for cell transplantation in cancer therapies. One of the attractive attributes of the stem cells is their inherent tumor tropism. This characteristic of stem cells could be exploited to develop effective treatments for patients with tumors that are hard to access or treat (e.g., glioblastoma)[40]. For this purpose, stem cells need to be genetically modified ex-vivo to stably express a therapeutic molecule.

In comparison to some of the current nanotechnology-based targeted drug delivery systems (nanomedicines) that exist for cancer treatment, stem cell-mediated therapies are believed to provide some distinct advantages. To date, numerous nanomedicines such as viruses, liposomes and polymeric nanoparticles have been developed and utilized to target cancer[41-44]. These drug carriers are known to be able to target tumor cells passively by taking advantage of tumor's leaky vessels to accumulate and then release the cytotoxic drugs in the tumor environment. This mechanism is termed enhanced permeability and retention (EPR) effect[45,46]. Because of a better understanding of tumor physiology in recent years, we now know that taking advantage of the EPR effect as the primary source for tumor targeting and treatment may not be applicable to all tumors [16]. For example, it is well-understood that the degree of leakiness of blood vessels significantly varies depending on the tumor type and size, which in turn complicates dose-response correlation studies in patients. In contrast to nanomedicines, the extravasation of stem cells to move from circulating blood to the tumor environment is an active process and not EPR dependent[47]. Diapedesis is the combination of several consecutive cell movements that finally results in the escape of stem cells from blood vessel to

surrounding tissues[4]. Therefore, the difference in leakiness of the tumors may not significantly influence the efficiency of the treatment. The emergence of stem cell-mediated cancer therapy as an alternative or complementary approach to current cancer therapeutics has sparked great enthusiasm among scientists because it may be used to carry therapeutic agents actively deep inside the tumor hypoxic environment[47].

This chapter starts by examining a number of proof-of-concept studies that demonstrate the potential application of stem cells in cancer therapy. Then, it highlights the studies that illustrate stem cells' tumor tropism, followed by discussing the reports that provide evidence to argue otherwise. Subsequently, it delineates various imaging methods for stem cell tracking as it is necessary for performing reliable dose-response studies at both preclinical and clinical levels. In each section, the pros and cons associated with each method are highlighted; weaknesses underlined and potential solutions are discussed.

3.1 Stem Cells in Cancer Therapy: Proof-of-Concept

Several groups in the past decade have performed proof-of-concept studies to demonstrate potential use of stem cells in cancer therapy. In these studies, stem cells were first genetically modified to express therapeutic genes such as interferons (INFs)[48], interleukins (ILs)[49], tumor necrosis factor-related apoptosis-inducing ligand (TRAIL)[50] or suicide genes[51]. Then, they were mixed with tumor cells at different ratios in vitro to co-culture or co-inject in vivo and study the impact of genetically modified stem cells on stimulation/inhibition of tumor growth. For example, Studeny et al. (2002), engineered INF-β expressing mesenchymal stem cells (MSC-INFβ) and co-cultured them with A375SM melanoma cells at 1:10, 1:5 and 5:1 ratios to evaluate their cancer cell growth

inhibitory effects in vitro [52]. The number of cells was measured after 72 hours and the results demonstrated significant decrease in number of co-cultured MSC-INFβ and A375SM cells as compared to the control group. In another approach, Uhl et al. (2005), used thymidine kinase expressing neural stem cells (NSC-TK) and co-cultured with glioma cells at ratios ranging from 1:1 to 1:20 [53]. GCV treatment was started after 24 h and continued for 48h. The results of this study showed significant levels of toxicity in the co-cultured cells that were treated with GCV as compared to untreated control. Overall, the highest level of toxicity was observed at 1:1 ratio and lowest at 1:20 ratio as expected.

While the studies mentioned above demonstrated the potential use of stem cells in cancer therapy in vitro, others evaluated their use in animal models. Benedetti et al. (2000), were among the first groups who examined the tumor inhibitory effects of genetically modified stem cells in animal models [54]. They first transduced neural progenitor cells with IL4 followed by mixing with C6 glioma cells at 10:1 ratio in vitro. Then, the mixture was injected to the left striatum of the Sprague-Dawley rats. The results revealed long term survival of 50% of rats in co-injection groups as compared to control group that only received C6 glioma cells. Later, Kucerova et al. (2008), performed a similar experiment but with different stem to cancer cell ratios[55]. They first mixed yeast fusion cytosine deaminase:uracil phosphoribosyl transferase expressing mesenchymal stem cells (MSC-yCD:UPRT) with A375 melanoma cells at ratios of 1:10 and 1:5 and then injected into mice. All groups were treated with prodrug 5-fluorocytosine. Although all mice in 1:10 ratio treatment group developed tumors by the study's end point, but the tumor onset was twice longer than the control group. This

difference was even more pronounced in treatment group which received stem to cancer cells at ratio of 1:5. At this ratio, 89% of animals in treatment group were tumor free at the end of the study. The ratio of the stem cells to the tumor cells in these studies also proved to be of paramount importance and a determining factor.

3.2 Tumor Tropism of Stem Cells

3.2.1 Evaluation of tumor tropism of stem cells in vitro

Stem cells are derived from different parts in the body such as embryo, fetus, cord blood and adipose tissues among others [56]. Regardless of the source, it is broadly claimed in literature that stem cells possess intrinsic tropism towards tumors. However, it needs to be emphasized that factors such as tumor type and stem cell lineage and size could impact the number of stem cells that reach tumors [57]. This tumor tropism is attributed to many factors including tumor cell-specific receptors and soluble tumor derived factors such as stromal cell-derived factor-1, tumor necrosis factor (TNFα), and interleukins among other inflammatory mediators [58,59]. The most commonly used test for in vitro demonstration of the tumor tropism of stem cells is migration assay **(Figure 3.1)**. Using this assay, many groups have shown that stem cells have preference to migrate toward cancer cells relative to normal cells [60,61]. Although informative, but migration assay may not be a perfect experiment to prove tumor tropism of the stem cells because it is extremely difficult to mimic the in vivo conditions and include all the factors which may alter the fate of the stem cells in the body. Therefore, more studies at the in vivo level are required.

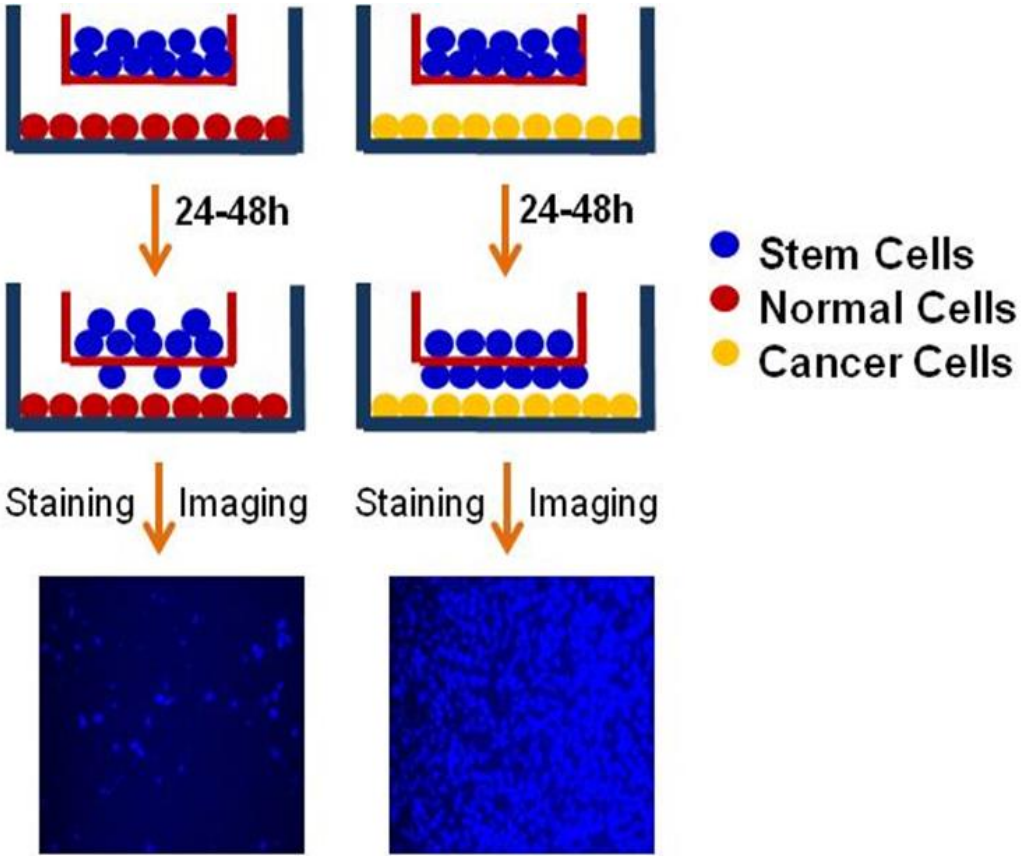

Figure 3.1: Migration assay, stem cells are seeded on the upper layer of a permeable membrane (upper chamber) and the cancer cells are seeded in the bottom chamber. If tropism exists, it is expected that the stem cells migrate through the membrane towards the tumor cells in the lower chamber. A non-cancer cell line is used as control.

3.2.2 Evaluation of tumor tropism of stem cells after injection in tumor vicinity

In the past decade, tumor tropism of the stem cells has been studied in animal models after local injection of stem cells in close proximity of tumors. One very well-studied cancer model using this approach is glioma where stem cells are injected intracranially in the contralateral hemisphere relative to tumor site followed by evaluation of their migration toward tumors [62]. In majority of the studies, it has been observed that stem cells migrated from the injection site to contralateral hemisphere and successfully reached the tumors [63,64]. Similar observations have also been reported with tumors of peritoneal cavity such as ovarian. For example, Kidd et al. (2009), used HEY cell line to induce intraperitoneal (IP) ovarian tumors in SCID mice [65]. Two weeks later, luciferase expressing MSCs were injected IP into tumor-bearing and tumor-free (control) mice. Live animal imaging was performed on days 1, 7 and 14 to track stem cells' migration. In both cancerous and normal mice, stem cells dispersed initially in peritoneal cavity but after 14 days the signal was only detectable in tumor bearing mice. In this study, the presence of the stem cells in tumors was confirmed by detecting luciferase signal followed by immuno-histochemistry assays after euthanizing the animals and dissecting the tumor and other organs **(Figure 3.2)**[65]. Similar observations with breast cancer and SKOV3 ovarian cancer models have also been reported [66,67]. In all the above mentioned studies, the results illustrated tropism of stem cells towards tumors.

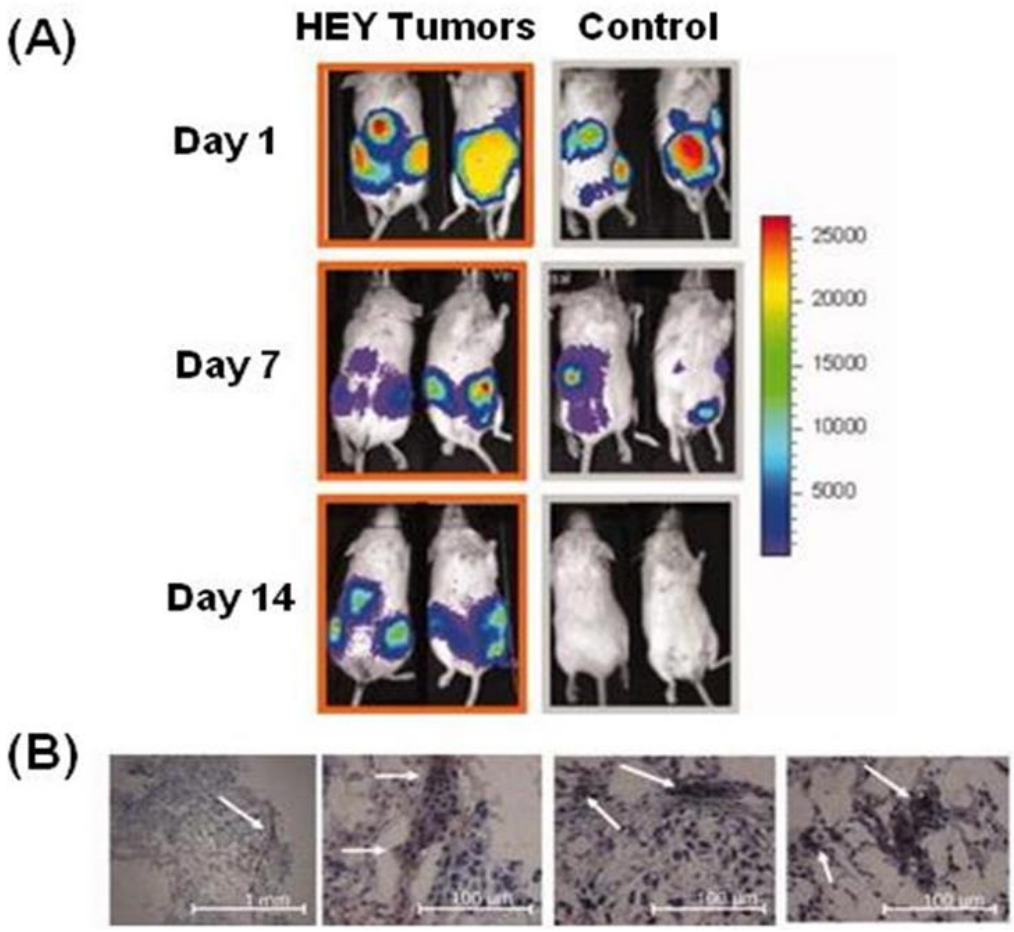

Figure 3.2: Tropism of MSCs toward HEY ovarian carcinoma. A) On day 1, 1 × 106 MSCs were injected into the peritoneal cavity and their localization in tumors was monitored over 14 days. The MSCs which were injected into mice without tumors did not localize; hence, undetectable. B) Immunohistochemistry study demonstrated the presence of luciferase protein in tumor tissue sections. (Kid et al. 2009)

In contrast to what we discussed above, there are studies that have argued otherwise and reported that no evidence of MSC migration towards tumors has been observed. For example, in a very interesting study by Bexell et al. (2011), rat bone marrow-derived green fluorescent protein expressing MSCs were injected extra-tumorally in syngeneic rat models of glioma [68]. The authors found no evidence of long-distance MSC migration across the corpus callosum or through the striatum toward malignant gliomas. However, their results suggested that intratumoral implantation may be the method of choice for MSC-based treatment approaches of malignant brain tumors [68].

3.2.3 Evaluation of tumor tropism of stem cells after intravenous injection

While injection of the MSCs close to the tumor site has produced promising results, but this approach may not be applicable in many types of cancer due to tumor inaccessibility. The most reliable injection route with widespread application in the clinic is intravenous (IV). After IV injection, it has been shown that stem cells first accumulate in lungs. Understandably, the application of stem cells in treating tumors that are localized in lung has been extensively studied. In a study by Song et al. (2011), lung metastasis models of PC-3 prostate and RIF-1 fibrosarcoma were examined by injecting cancer cells via tail vein to induce lung tumors [69]. Seven days later, rat luciferase expressing bone marrow-derived MSCs (Luc-BMSCs) were injected IV. In both PC-3 and RIF-1 lung metastasis models, Luc-BMSCs were detected mainly in the lung one day after injection and remained detectable over a 30 day period. A new batch of BMSCs was then genetically modified to express thymidine kinase enzyme (TK-BMSC) and used in combination with GCV to treat lung tumors. The results demonstrated significant tumor size reduction in lung tumors when TK-BMSCs were administered with GCV. Other

groups have also used IV route to inject stem cells and target tumors that are located in the lungs [70,71]. One important point to highlight is that after IV injection, accumulation of stem cells in lungs is due to their large sizes (~15 microns) and not necessarily their inherent tumor tropism. This is due to the fact that lung is part of reticuloendothelial system and responsible for the entrapment and then clearance of large particles with sizes bigger than 6 microns [72]. Given that tumor tropism of stem cells is dependent on both stem cell lineage and tumor type, it may be somewhat premature at this point to conclude that MSCs have tropism toward all lung tumors [57]. However, there are still considerable numbers of studies which have induced tumors in regions other than lung and have shown tumor tropism of the stem cells after IV injection. For example, in a study by Xia et al (2011), the tumor tropism was evaluated after IV injection of SPIO-labeled MSCs in mice bearing orthotopic breast xenografts [73]. Using Prussian blue staining technique, the results revealed accumulation of MSCs mainly in tumors and to a significantly less degrees in other organs. This tissue staining technique is also used to illustrate tumor tropism of stem cells in other types of cancers such as human colon cancer [74], primary and metastatic breast cancer [66,75] and neuroblastoma metastatic tumors [76]. Although tissue sectioning is one way of observing stem cells in various tissues at specific time points, but it does not allow continuous tracking over a long period of time. To overcome this limitation, several groups have used live animal imaging systems to track stem cells inside animals at different time intervals. In a study by Hung et al (2005), human MSCs were transduced with Herpes Simplex Virus-Thymidine Kinase gene (hMSC-HSVTK) for tracking by Positron Emission Tomography (PET) imaging[77]. HT-29 Inv2 colon carcinoma cells were injected subcutaneous (SC) in the flank region of the SCID mice to

induce tumors. After 3 days, 5×10^5 hMSC-HSVTK cells were injected via tail vain. Then Micro PET imaging was performed after infusion of [^{18}F]-FHBG to evaluate the biodistribution of hMSC-HSVTK. Live animal imaging data demonstrated the localization of hMSC-HSVTK cells in the tumors. Later, Yang et al. (2012), studied tumor tropism of IV injected DiR-labeled neural stem cells (NSCs) in immunodeficient NSG and immunocompetent BALB/c mice [78]. Tumors were induced by injecting luciferase expressing 4T1 breast cancer cells in the mammary fat pads. Seven days post tumor induction, DiR-labeled NSCs were injected via tail vein and live animal imaging was performed on days 0, 1, 2, 7, 14. The results displayed the localization of NSCs in 4T1 breast tumor regions within two weeks.

In contrast to the studies that we discussed in this section, there are studies with contradictory results which challenge the tumor tropism of the stem cells after IV injection. In a study by Luetzkendorf et al. (2010), TRAIL expressing MSCs were engineered to induce apoptosis in tumor cells [79]. Even though the in vitro co-culture studies and in vivo co-injection of MSCs and tumor cells clearly demonstrated inhibitory effects of stem cells on tumor growth but there was no significant effect after systemic injection of MSCs. Ex vivo studies revealed entrapment of the MSCs in lung and presence of just 0.1% of stem cells in tumors which was not enough to inhibit tumor growth.

In another study, Eggenhofer et al (2012), investigated the fate of MSCs after IV infusion [80]. Mouse MSCs expressing DsRed-fluorescent protein and also radioactively labeled with Cr-51 were IV injected in C57BL/6 mice. After 5 min, 1, 24, or 72h, mice were euthanized and blood, lungs, liver, spleen, kidneys, and bone marrow removed to

detect viable MSCs. In vivo and ex vivo tracking studies demonstrated the presence of viable MSCs only in lungs indicating that viable MSCs do not pass lung after IV injection. These results are in agreement with the results of another study which used radiolabeled stem cells to track their biodistribution [81]. Such conflicting results in different studies may be indicative of the impact of different factors such as tumor size, tumor type, stem cell source and stem cell passage number on tumor tropism of stem cells [57]. To help identify the determining factors in stem cell tropism, it may be necessary to ask investigators to include all these relevant information in their publications in order to help identify the critical factors that impact stem cells' tumor tropism. One approach which could help overcome this hurdle is intra-arterial injection which simply bypasses the lungs. In a study by Doucette et al. (2011), it has been demonstrated that syngeneic bone marrow derived MSCs after intra-arterial injection could effectively localize in tumors and kill the cancer cells while they failed to reach tumors after i.v. administration[82].

Overall, it appears that for effective cancer therapy, significant numbers of stem cells are needed to reach tumors so that they can make an impact on tumor growth. In recent years, several groups have looked at various factors such as radiation, ultra sound, and cell surface modification and their impact on increasing tumor tropism. They have illustrated local radiation or ultrasound exposure of one region can enhance the tropism of the stem cells by increasing the chemokine gradient [83,84]. Other factors such as cell surface receptors may also play a significant role in stem cell tropism towards tumors. In a study by Nystedt et al. (2013), the cell surface profiles of the MSCs from two origins of bone marrow and umbilical cord blood were compared [85]. They linked the higher lung

clearance rate of the umbilical cord blood MSCs to higher expression of the CD49D and CD49f on the cell surfaces. They suggested that modification of the cell surface can be a practical approach to change the lung clearance of the stem cells which is a significant limiting factor to the efficacy of this approach.

So far, the most successful studies that have reached clinical trials been performed by Aboody's group at the City of Hope where they have used suicide gene expressing neural stem cells for the treatment of glioma (Clinicaltrials.gov, NCT02015819 and NCT01172964). These clinical trials are ongoing and no data have been reported yet.

3.3 Tracking the Stem Cells

As the number of stem cells that reach tumors plays a significant role in anti-cancer activity, it is important to validate the stem cell delivery process and quantify the number of stem cells that reach the target so that a reliable dose-response study can be performed. One method that could facilitate such studies is the live imaging of stem cells in vivo. The most broadly used methods for stem cell tracking are bioluminescence imaging (BLI), florescence imaging (FLI), magnetic resonance imaging (MRI) and radionuclide imaging. FLI is performed by exposing a florescent compound to an external light for excitation and is categorized as a high sensitive and non-invasive imaging method. This technique is confined to small animals due to scattering and absorbance of the light by tissues. Ruan et al. (2012), developed murine DiR-labeled embryonic stem cells (DiR-mES) and detected a strong florescence signal within 24 hours in vitro [86]. Then, DiR-mES were injected IV to tumor bearing mice and the florescence signal was tracked over a 24 hour period. The results revealed the accumulation of the stem cells in tumors. As presented in this study, one of the major problems with using FLI is the short stability of

the fluorescent signal due to dilution of the labeling agent with each cell division and particle shedding. Other groups that used quantum dots (QD) for FLI observed similar results in their experiments where the number of QD labeled cells decreased from 72.2% to 4.3% in a four day period [87]. In another study, the percentage of the QD labeled stem cells dropped from 93% to 25% three days post labeling[88]. Overall, it appears that using fluorescent dyes for FLI can be an acceptable approach for tracking stem cells in small animals only when the duration of study is short (<24hrs). However, the major disadvantage of FLI with fluorescent dyes is that detection of fluorescent signal under microscope or in animals does not necessarily mean that the cells are alive. As a result, the probability of making wrong conclusions with FLI with fluorescent dyes is high. One approach that could help overcome this shortcoming associated with cell viability is the use of fluorescence-based imaging with MSCs that express fluorescent proteins such as enhanced green or red fluorescent protein family (e.g., EGFP and DsRed)[89]. While use of EGFP and DsRed may be useful in in vitro studies, they may not be as attractive in fluorescence imaging of deep tumors due to limited penetration of light, tissue absorption and scattering. Recently, Jiguet-Jiglaire et al. (2014), reported the use of an infrared fluorescent protein with fluorescence characteristics laying within a near IR transparency of mammalian tissues[90]. This approach helped overcome issues related to fluorescent light tissue penetration, absorption and scattering in small animals such as mice facilitating more reliable preclinical studies; however, the application of this approach in larger animals or humans has not been investigated yet.

One method that has a significant advantage over FLI is BLI. BLI measures the emitted light generated from conversion of a substrate (e.g., luciferin) by an enzyme

(luciferase) in live stem cells. This imaging technique has high sensitivity, exclusive to live stem cells and suitable for quantitative studies [91,92]. For example, our studies demonstrate the ability to image small number of stem cells in mice which could facilitate dose-response studies **(Figure 3.3)** [93]. In addition to our work, others have also used BLI technique to track stem cells in live animals [82]. Wang et al (2009), modified MSCs to express firefly luciferase in fusion with green fluorescent protein (fLuc-eGFP) to investigate trafficking of the stem cells in 4T1 breast tumor bearing mice[94]. They injected MSCs via tail vein and demonstrated localization of the stem cells in both subcutaneous tumor and lung metastasis model by two dimensional BLI (2D BLI) and histological analysis. The drawback of using 2D BLI is its inability to pinpoint the exact location of bioluminescence source; hence, a complementary histological analysis is needed to identify the anatomical location. In recent years, more refined optical imaging techniques such as three-dimensional BLI (3D BLI) have been utilized which allow us identify the exact source and brightness of bioluminescence foci[95,96]. While BLI possesses several advantages over FLI, but there are some drawbacks that needs to be considered. One of the shortcomings of this method which has restricted its use to small animals is the absorption and scattering of the emitted light by the tissues and potential immunogenicity of the substrate and enzyme [97]. Therefore, BLI may be a great and reliable technique for performing dose-response studies at the pre-clinical level but for clinical studies other imaging techniques such as MRI are more applicable.

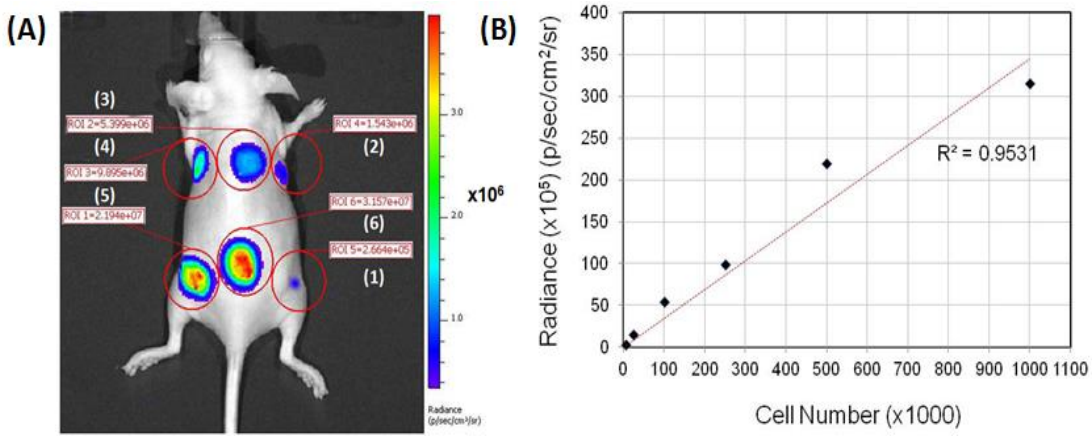

Figure 3.3: Bioluminescence imaging. A) Various number of luciferase expressing stem cells were injected subcutaneously into a nude mouse and then imaged by IVIS live animal imaging system. Numbers 1 to 6 correspond to 5000, 25,000, 100,000, 250,000, 500,000, and 1,000,000 cells, respectively. B) The luminescence intensity was plotted against cells numbers and a good linear correlation between cell number and luminescence intensity was obtained. Adapted with permission from reference

MRI is one of the most commonly used methods in clinic with markers such as gadolinium (Gd3+) and manganese for T1 system and super paramagnetic iron oxide (SPIO) and micron sized particles of iron oxide (MPIOs) for T2 system [98,99]. The benefits of MRI are high resolution, three dimensional imaging and clinical application. In this imaging technique, stem cells are labeled directly with a contrast agent (e.g., SPIO) or transduced with a gene such as ferritin which can produce magnetic contrast in the cell [100]. The advantage of using ferritin expressing stem cells over labeled ones is that the potential for generation of fake signals by dead cells or engulfed stem cells by scavenger macrophages is eliminated [101]. There are also some studies which have reported the toxic effects of labeling compounds on stem cells properties. Nohroudi et al (2010), demonstrated that the viability and migratory potential of the BM-MSC decrease as MPIOs incorporation in stem cells increases [102]. In another study, it was shown that SPIO loading of the fetal stem cells impairs cell movements in a dose dependent manner [103]. In terms of application, MRI is broadly used in Glioma cancer model [104], although other types of cancer have also been studied. For example Lee et al (2013), used MRI to track migration of the genetically modified NSCs toward prostate tumors [105]. Despite its significant clinical applications, the drawbacks of using MRI include low sensitivity as compared to the other imaging techniques such as BLI and PET [106], unsuitability for quantitative studies [107] and contraindication in patients with implantable devices.

Currently, methods such as radionuclide imaging provide significant benefits over MRI which makes it suitable for in vivo tracking of stem cells. These advantages include high sensitivity, application at the clinical level and suitability for quantitative studies [108]. Radionuclide imaging employs gamma ray emitting radioisotopes for imaging cells in

vivo and contains two types of single photon emission computed tomography (SPECT) and positron emission tomography (PET). While in SPECT radioisotopes send one gamma photon in one direction; in PET radiotracers emit two gamma photons in opposite directions. The most commonly used radiotracers for SPECT are indium-111 (^{111}In) and Technetium-99m (^{99m}Tc), whereas in PET it is usually fluorine-18 (^{18}F) and copper-64 (^{64}Cu). For direct stem cell labeling, ^{18}F can be incorporated into a glucose analog, 2-deoxy-2-^{18}F-fluoro-D-glucose (^{18}F-FDG), or into a modified thymidine analog, 3′-deoxy-3′-^{18}F-fluorothymidine (^{18}F-FLT) both of which could be trapped inside the cells after phosphorylation [109,110]. These radioisotopes have a short half-life making them suitable for short-term tracking. To extend the stem cells tracking period up to two months, they can be genetically modified to express HSV-TK [111]. HSV-TK can phosphorylate and retain pyrimidine analog derivatives such as 2′-fluoro-2′-deoxy-β-D-arabinofuranosyl-5-iodouracil (FIAU) and acycloguanosine derivatives such as 9-(4-fluoro-3-hydroxy-methyl-butyl) guanine (FHBG) inside the cells [112,113]. Another commonly used reporter gene is the sodium iodide symporter (NIS), a trans-membrane protein normally expressed in thyroid cells and responsible for iodine uptake. Stem cells modified to express this transporter are suitable for PET imaging with ^{124}I and SPECT imaging with ^{123}I or ^{99m}Tc. Dwyer et al (2011), evaluated the use of genetically modified MSCs that could express NIS for imaging and therapy of MDA-MB-231 breast cancer tumors in nude mice [114]. Modified MSCs were injected IV when tumor reached appropriate size and SPECT was performed through use of ^{99m}Tc injection on days 3 and 14. To quantify, accumulation of the radioisotope in each region was calculated and reported as the percentage of the total dose administered. The results revealed enhancement in radiotracer accumulation at the

tumor site starting from 1.2% on day 3 up to 9.4% on day 14. The results also showed the suitability of the method for quantitative evaluation of the therapeutic efficacy. However, it is important to mention that radiations from radionuclides could induce toxic effects in stem cells and normal tissues. Other drawbacks with the use of radionuclides include release of radiotracers into non-target cells, short half-life of the tracers necessitating repeated injections and lower spatial resolution as compared to MRI [115,116].

Knowing that each of these imaging techniques has its own advantages and disadvantages, scientists occasionally employ a combination of these methods for tracking stem cells. For example, Wang et al. (2012), used a dual probe approach (Gd^{+} and Cy5.5) for MRI and FLI [117]. Here, MRI provided information regarding spatial distribution of stem cells in tumors, whereas FLI showed presence of stem cells in other non-target organs such as liver with higher sensitivity, a task which could not be achieved by MRI alone because of the homogenous distribution of MSCs.

3.4 Conclusion

Although MSCs are attracting tumor delivery vectors owing to their distinct properties, their systemic delivery is a bottleneck due to pulmonary first pass effect that limits the number of viable cells that can reach the tumor. Since this shortcoming directly impacts the efficacy of the treatment protocols, future studies may need to focus on overcoming this obstacle in order to facilitate translation of this science into the clinic. The first solution is to investigate the impact of different factors such as tumor size, tumor type, stem cell source and stem cell passage number on lung entrapment and tumor tropism of stem cells. Perhaps, more emphasis may need to be placed on intra-arterial

administration of MSCs rather than intravenous. As the second solution, given that a significant number of MSCs are cleared in pulmonary first pass effect, finding the most efficient enzyme/prodrug system in preclinical level has a great value. In this case the MSCs which are able to reach the tumor site can exert the highest possible therapeutic effect. Therefore, as the first part of this project we utilized MSCs to compare different Enzyme/Prodrug systems.

Chapter 4

Evaluation of the Anticancer Efficacy of Enzyme/Prodrug Systems by Use of Genetically Modified MSCs [2]

[2] A version of this chapter has been published in Journal of Control Release. Please see "Genetically engineered theranostic mesenchymal stem cells for the evaluation of the anticancer efficacy of enzyme/prodrug systems.", PMID: 25575867.

Stem cell mediated gene delivery is emerging as a new strategy to improve the safety and efficacy of current cancer gene therapy methods. Recent evidence indicates that systemically administered mesencymal stem cells (MSCs) can migrate and deliver therapeutic genes to tumors[118]. It is envisioned that this inherent tumor tropism of MSCs can be exploited to develop effective and well-tolerated treatments for patients with malignant solid tumors [74,119]. For this purpose, MSCs are first genetically modified ex-vivo to stably express a prodrug-converting enzyme (e.g., thymidine kinase, cytosine deaminase, nitroreductase, etc.) and then injected back into the body to migrate into tumors. Subsequently, a prodrug is administered which gets converted into its cytotoxic form by the enzyme inside the MSCs. This in turn results in the death of the stem cells as well as neighboring cancer cells through a phenomenon known as "bystander effect" [55,69,120]. Therefore, in addition to the number of MSCs that reach the tumor target, prodrug's bystander effect also plays a major role in the success of this approach. This effect become more valuable considering that a large portion of MSCs are cleared in pulmonary first pass effect; hence, it would be very critical that the cells which reach to the tumor site demonstrate the highest anti-cancer effect. Although in the past decade several different enzyme/prodrug systems are utilized for this purpose, literature search shows that thymidine kinase/ganciclovir (TK/GCV) and yeast cytosine deaminase/5-fluorocytosine (yCD/5-FC) are the most widely used systems [40,121-123]. Unfortunately, in many cases no clear rationale is provided to justify the use of one enzyme/prodrug system over another and it has been unclear which enzyme/prodrug system is the most effective one. As each enzyme/prodrug system has its own strengths and weaknesses[124], it is important to be able to perform a study at the preclinical level that can reliably illustrate

the strengths and weaknesses of using different enzyme/prodrug systems and/or compare the efficacies of different enzyme mutants.

The overall *objective* of this project was to genetically engineer a panel of MSCs that stably express TK (TK_{007} and TK_{SR39} mutants), yCD:UPRT and nitroreductase (NTR) suicide genes and evaluate their anticancer efficacies side-by-side by using a sensitive tumor model. To achieve the objective, we genetically modified bone-marrow derived MSCs to stably express the aforementioned suicide genes and evaluated their ability to kill xenografts of SKOV3 ovarian cancer tumors after administration of an appropriate prodrug. This model cancer cell line was chosen because of its sensitivity to the enzyme/prodrugs systems used in this study [6]. The use of a cancer cell line that is sensitive to the enzyme/prodrug systems is essential as it helps to eliminate the cell-related bias. As a result, the observed differences in terms of therapeutic outcome will not be due to the cell's biological traits but the enzyme/prodrug systems' properties. Therefore, cell lines that are not sensitive (resistant) to one system or another will not be suitable for such comparative studies.

TK_{007} and TK_{SR39} are the most efficient mutants of wild-type TK with the ability to rapidly convert GCV into its cytotoxic form inside the TK expressing cells [19,20]. Bacterial nitroreductase (NTR) is able to convert CB1954 prodrug into its potent cytotoxic form [125]. In comparison to yCD alone, yCD:UPRT, which is a combination of yCD and UPRT, has a higher sensitivity to 5-FC. Therefore, yCD:UPRT can convert this prodrug into its cytotoxic form in a faster rate resulting in higher efficacy [126]. Using an in vitro cell toxicity assay, we first examined the sensitivity of the suicide gene expressing MSCs to prodrugs followed by studying their ability to kill SKOV3 cancer cells through their

bystander effects. From the in vitro studies, three of the most efficient suicide gene expressing MSCs were selected and then used to evaluate their ability in killing SKOV3 xenograft tumors in nude mice. To correlate dose with response, all MSCs were engineered to stably express luciferase gene and the in vivo viability of MSCs were tracked and monitored before and after prodrug administration.

4.1 Materials and Methods

4.1.1 Genetic engineering of suicide gene expressing MSCs

All the recombinant DNA work presented here has been reviewed and approved by the Rutgers University Environmental Health and Safety office. The genes encoding yCD:UPRT and wild-type herpes simplex virus thymidine kinase (HSVTK) were purchased from Invivogen (San Diego, CA). Using site-directed mutagenesis wild-type HSVTK was mutated into TK_{SR39} as previously reported [20]. The full length NTR gene based on previously published data was synthesized by IDTDNA technologies (Coralville, IA) [127]. The gene encoding TK_{007} enzyme was obtained from Professor B. Fehse (University Medical Centre Hamburg-Eppendorf, Germany) through Material Transfer Agreement. Using pBudCE4.1 dual promoter mammalian expression vector (Invitrogen), all suicide genes were cloned separately under EF1α promoter, whereas a firefly luciferase-GFP fusion gene was cloned under CMV promoter to facilitate colony selection and in vivo imaging. The sequences of all genes and fidelity to the original design were verified by DNA sequencing.

In the next step, human bone-marrow derived MSCs were first seeded in 58 cm^2 culture dishes at 3000-6000 cells/cm^2 density and propagated in DMEM media supplemented with 10% fetal bovine serum, 10,000 units/ml of penicillin and 10,000

µg/ml of streptomycin (Caisson, UT, USA). These cells were originally purchased from the Texas A&M Health Science Center College of Medicine and a generous gift from Professor P. Moghe at Rutgers University to our lab. MSCs were then transfected with the constructed mammalian expression vectors by using GeneIn™ reagent (GlobalStem®, MD, USA) to make MSC-TK_{007}-Luc, MSC-TK_{SR39}-Luc, MSC-yCD:UPRT-Luc, and MSC-NTR-Luc. Transfected MSCs were maintained in full media and treated with 150 µl/ml Zeocin (Invitrogen, NY, USA) for 3-4 weeks to eliminate the non-transfected cells. Several colonies from each plate were picked and then propagated for further analysis.

4.1.2 In vitro and in vivo analysis of luciferase expression in genetically modified MSCs

The levels and stable expression of luciferase in all colonies were first evaluated in vitro by using luciferase assay kit and protocol (Promega). MSC-TK_{007}-Luc, MSC-TK_{SR39}-Luc, MSC-yCD:UPRT-Luc and MSC-NTR-Luc were seeded separately in 96 well plates at the density of 2×10^4 cells per well. After 24 h the media were removed, cells were washed with Dulbecco's Phosphate Buffer Saline (DPBS) and 20 µl of lysis buffer was added to each well. Equal amounts of lysate were mixed with 50 µl of D-luciferin (Promega, WI, USA) in glass tubes and luminescence was measured by a luminometer (Berthold, Germany). Colonies with statistically similar luciferase expression were selected and propagated for in vivo evaluation.

The minimum number of genetically modified MSCs that can be detected in mice by IVIS imaging system (PerkinElmer, Waltham, MA, USA) after subcutaneous (SC) injection was examined by using MSC-TK_{SR39} clone. This was done by first suspending different number of cells ranging from 5×10^3 to 1×10^6 in 100 µl of DPBS:Matrigel

(Corning, MA, USA) (50:50 v/v) and injecting it subcutaneously (SC) in the dorsal regions of female nude mice. D-luciferin (Goldbio®, St. Louis, MO, USA) was then injected intraperitoneally (IP) into the mice at the dose of 150 mg/kg. Five minutes after D-luciferin injection, mice were anesthetized by isoflurane inhalation and placed in IVIS imaging system to detect the cells. The in vivo bioluminescent images were displayed in "photon" mode; therefore, the signal intensity is represented by radiance (p/sec/cm2/sr), which refers to the number of photons per second that are leaving a square centimeter of tissue and radiating into a solid angle of one steradian (sr).

4.1.3 Evaluation of the sensitivity of suicide gene expressing MSCs to prodrugs

To study the expression and sensitivity of the suicide gene expressing MSCs to prodrugs, they were first seeded in 96-well plates at the density of 1×10^4 cells per well. The next day, the corresponding prodrug for each suicide gene expressing MSC; i.e., 5-FC for MSC-yCD:UPRT-Luc; CB1954 for MSC-NTR-Luc; and GCV for MSC-TK_{007}-Luc and MSC-TK_{SR39}-Luc were added to each well. 5-FC (PureChems™, TX, USA), CB1954 (Medkoo Biosciences, NC, USA) and GCV (PureChems™, TX, USA) prodrugs were added and incubated with the cells for 5 days in the following ranges: 0.1-1.5 µM, 10-200 µM and 0.1-5.0 µM, respectively. Cell viability was evaluated by WST-1 assay (Roche, Nutley, NJ) after addition of the reagent and measuring the absorbance at 450 nm. The viability of untransfected MSCs (naïve) treated with prodrug was used as control. The data are reported as mean±SD (n=3).

4.1.4 Evaluation of MSC tropism towards cancer cells by migration assay

The tropism of genetically modified MSCs towards cancer cells was studied by using migration assay. SKOV3 ovarian cancer cells and HEK 293 human embryonic kidney

cells (control) were seeded in 24-well plates at the density of 1×10^5 cells per well. After 24 hours, inserts of 8-µm pore size (Greiner bio-one, NC, USA) were placed on the wells followed by transferring 2×10^4 genetically modified MSCs to each insert. After 48 hours, the inserts were taken out for staining and visualization. Briefly, cells inside each insert were removed with a cotton tip and the inserts were soaked in cold methanol for 10-20 min to fix the cells on the outer layer. The membrane was carefully cut off after washing with PBS and placed on a slide with the bottom side up. DAPI solution (Southern Biotech, Alabama, USA) was added onto the membranes to stain cells' nucleus. The cells were then visualized using a fluorescent microscope (Olympus, USA). The number of migrated cells was measured by counting five random fields of view per well under the microscope (ocular lens 10x, objective 10x, field of view 220 µm). The data are reported as mean±SD (n=5).

4.1.5 In vitro evaluation of the cancer cell killing efficiency of suicide gene expressing MSCs

Using a previously published method, we evaluated the ability of the suicide gene expressing MSC clones to kill SKOV3 cancer cells through the bystander effect [74,119]. In brief, SKOV3 cells (doubling time: ~35 hours) were seeded in 96-well plates either alone or mixed with suicide gene expressing MSCs (doubling time: ~40 hours) at the density of 5×10^3 cells per well to generate MSC to SKOV3 ratios of 0:100 (SKOV3 alone), 1:50, 1:10, 1:5, and 1:2. The next day, the corresponding prodrugs at the concentrations of 50, 100 or 200 µM for each suicide gene were added to the wells. WST-1 assay was performed after 5 days to measure the cell viability. The absorbance of each MSC to

SKOV3 co-culture without any prodrug treatment was considered as 100% viable. The data are reported as mean±SD (n=3).

4.1.6 In vivo evaluation of the tumor killing efficiency of the suicide gene expressing MSCs

Five-week old female nude mice were purchased from Jackson laboratory (Bar Harbor, ME) and used for the in vivo studies. All animals were cared for in accordance with the Rutgers Institutional Animal Care and Use Committee approved protocols. Mice were anesthetized by isoflurane inhalation and 3×10^6 SKOV3 cells suspended in 100 µl DPBS (50% Matrigel®) were injected SC in dorsal flank regions (two tumors per mouse). The tumor size growth was monitored by pressure sensitive caliper and when reached 100-150 mm^3 all mice were randomly distributed into 10 groups each containing 5 mice. First treatment group received intratumoral injection of 1×10^6 MSC-TK_{SR39}-Luc cells once a week plus daily injection of GCV (25 mg/kg). Second treatment group received intratumoral injection of 1×10^6 MSC-yCD:UPRT-Luc cells once a week plus daily injection of 5-FC (600 mg/kg). Third treatment group received intratumoral injection of 1×10^6 MSC-NTR-Luc cells once a week plus daily injection of CB1954 (20 mg/kg). Cell control groups received intratumoral injection of 1×10^6 MSC-TK_{SR39}-Luc, MSC-yCD:UPRT-Luc and MSC-NTR-Luc once a week, respectively (without prodrug). Prodrug control groups received daily injections of GCV (25 mg/kg), 5-FC (600 mg/kg) and CB1954 (20 mg/kg), respectively. Vehicle control group received intra-tumoral injection of PBS once a week. Genetically modified MSCs were administered intratumorally on days 0, 6, 12, 18, 24 and 30 (6 doses). Before each cell injection, tumor sizes and body weights were measured, D-luciferin injected (150 mg/Kg) and mice were

imaged by IVIS imaging system. Five minutes after each cell injection, animals were imaged again to determine the total luciferase expression from the viable MSCs. In each weekly cycle, the prodrugs were administered one day post cell injection, continued for six days and stopped on the day of cell injection before the next cycle. The data are reported as mean±SD (n=10).

4.2 Results and Discussion

Intrinsic tumor tropism of stem cells has provided this opportunity for scientists to use them as a tool for delivery of various anticancer agents into the tumor environment [48]. There are two important factors that play significant roles in determining the success of stem cell mediated suicide gene therapy. One is the number of viable MSCs that come in contact with the tumor cells and the other is the potency of the drug's bystander effect. Similar to viral and non-viral vectors which get trapped in non-tumor tissues such as liver, a significant portion of the MSCs gets trapped in lungs after IV administration and only a subpopulation of them can reach the tumors [128,129]. Therefore, the drug's bystander effect becomes the most prominent factor that could determine the rate of success. To compare the efficiency of the four enzyme/prodrug systems in stem cell mediated suicide gene therapy of cancer, we used a dual promoter mammalian expression vector. This was done by cloning four different suicide genes separately (i.e., TK_{007}, TK_{SR39}, yCD:UPRT and NTR) under an EF1α promoter and a luciferase gene under CMV promoter. The fidelity of the each sequence to the original design was verified by DNA sequencing and translation into the corresponding amino acid sequence. The plasmids were then used to create stably transfected MSC-TK_{007}-Luc, MSC-TK_{SR39}-Luc, MSC-yCD:UPRT-Luc and MSC-NTR-Luc clones suitable for simultaneous therapy and quantitative in vivo

imaging. In the next step, we determined the expression of luciferase protein in all four stably transfected clones and selected those with statistically similar luciferase expression levels. As it can be observed in **Figure 4.1A**, all four selected clones could express luciferase gene at statistically similar levels (ANOVA, $p>0.05$). To examine whether this level of luciferase expression is high enough to be detected in nude mice, one clone was selected (i.e., MSC-TK_{SR39}-Luc) and various numbers of MSCs were injected subcutaneously. The results showed that the expression of luciferase was sufficient to allow us detect as low as 5,000 MSCs and there was a good correlation between the cell number and Radiance **(Figure 4.1B and C)**. The ability to detect MSCs in vivo with high degree of sensitivity is important because it makes it possible to perform more accurate dose-response relationship studies.

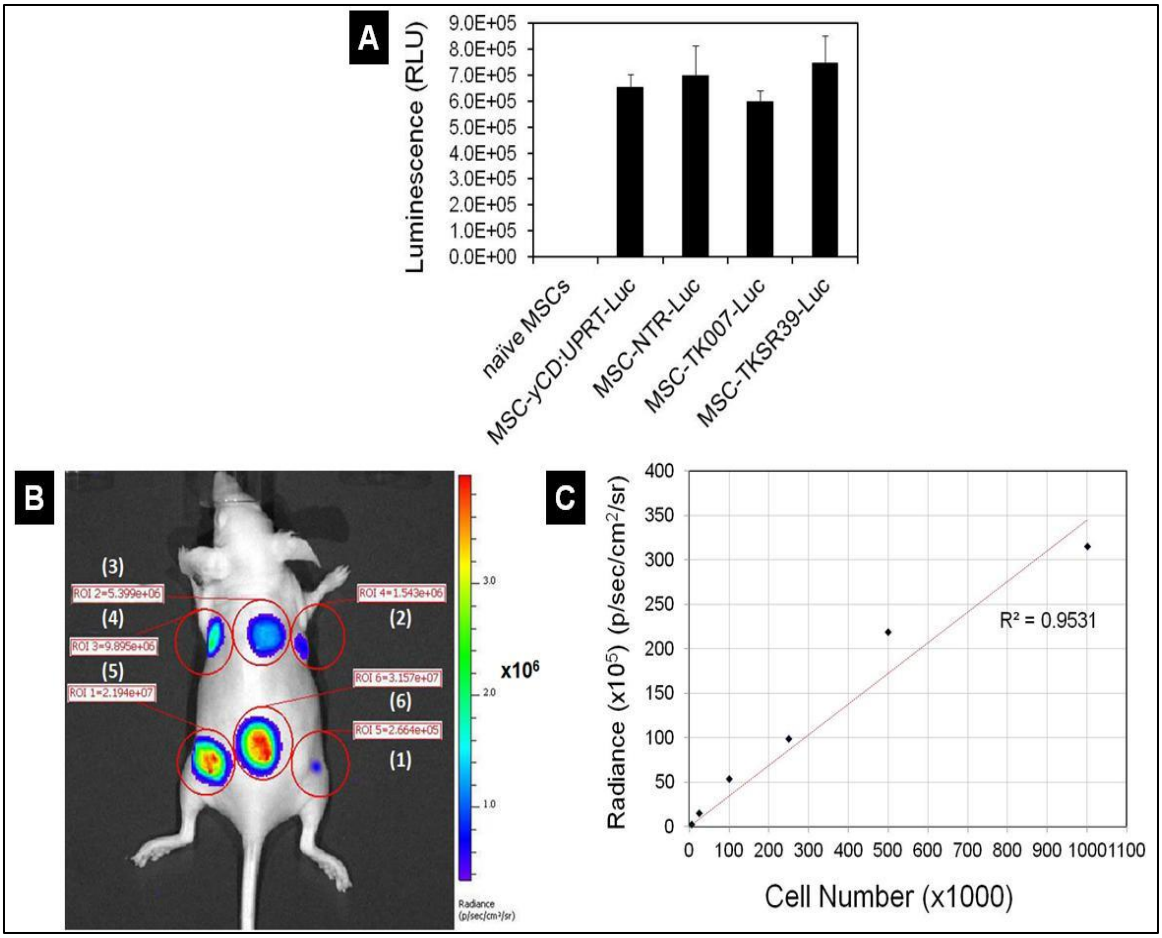

Figure 4.1: Measurement of bioluminescence intensity of luciferase expressing MSCs in vitro and in vivo. A) In vitro measurement of the bioluminescence of MSC-TK007-Luc, MSC-TKSR39-Luc, MSC-yCD:UPRT-Luc and MSC-NTR-Luc clones. B) Radiance of various numbers of subcutaneously injected MSCs in nude mouse. Numbers 1 to 6 correspond to 5000, 25,000, 100,000, 250,000, 500,000, and 1,000,000 cells, respectively. C) Plot of Cell Number versus Radiance and its correlation.

We then examined the sensitivity of the genetically modified MSCs to prodrugs using a cell toxicity assay. This was to verify that the engineered MSCs could express suicide genes at levels sufficiently high that could induce significant cell death in the presence of the corresponding prodrug. The results of this study showed that all four suicide gene expressing MSC clones were sensitive to prodrugs in a dose-dependent manner while naïve MSCs remained insensitive **(Figure 4.2)**. Among all MSC clones, it was apparent that the MSC-yCD:UPRT-Luc was the most sensitive one (5-FC IC_{50} 0.2 μM). In addition, we did not observe any significant difference between MSC-TK_{007}-Luc and MSC-TK_{SR39}-Luc clones in terms of sensitivity to GCV (IC_{50} ~0.5 μM). Overall, the results of the cytotoxicity study show that all four genetically modified MSCs were able to convert prodrugs into their cytotoxic forms which resulted in the death of suicide gene expressing MSCs. Although in many cases it may be desirable to see MSCs die as a result of prodrug conversion but it is worth noting that in some cases it may even be advantageous for the MSCs not to die and remain active so that they can produce more cytotoxic drugs in the tumor environment.

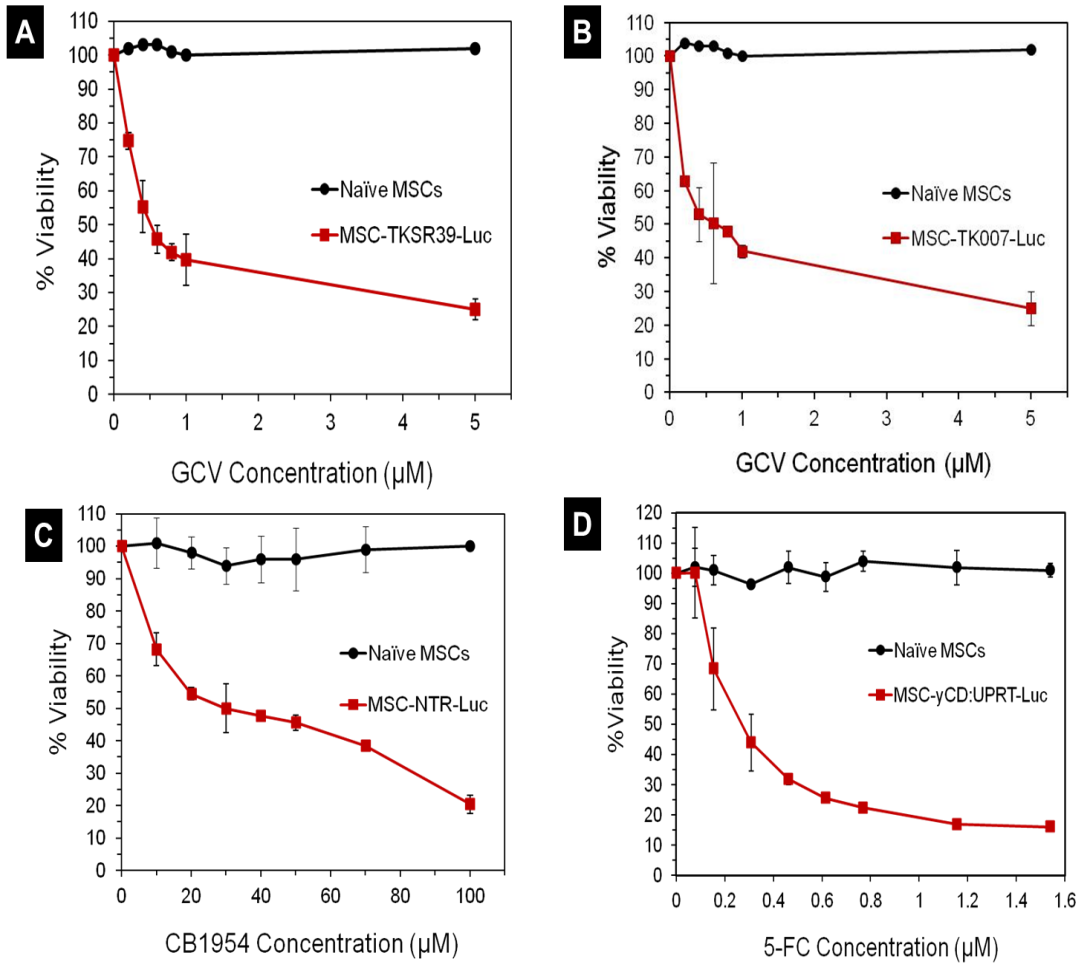

Figure 4.2: Sensitivity of the MSC-TK_{SR39}-Luc, MSC-TK_{007}-Luc, MSC-NTR-Luc and MSC-yCD:UPRT-Luc clones to prodrugs as measured by a cell toxicity assay. Naïve unmodified MSCs which do not express any suicide gene were used as control.

Learning that all the genetically modified MSC clones could efficiently express not only the luciferase gene but also the suicide genes, we utilized a migration assay to examine whether the genetic manipulation of MSCs affected their inherent tropism towards cancer cells. Thus, we studied the tropism of MSCs towards SKOV3 cancer cells and compared it with tropism towards HEK293 normal cells. The results of this assay demonstrated that all genetically modified MSC clones maintained their cancer tropism by migrating at significantly higher numbers towards cancer cells in comparison to HEK293 cells (t-test, $p<0.05$) **(Figure 4.3)**. Based on published data by other groups, this observation was expected [60].

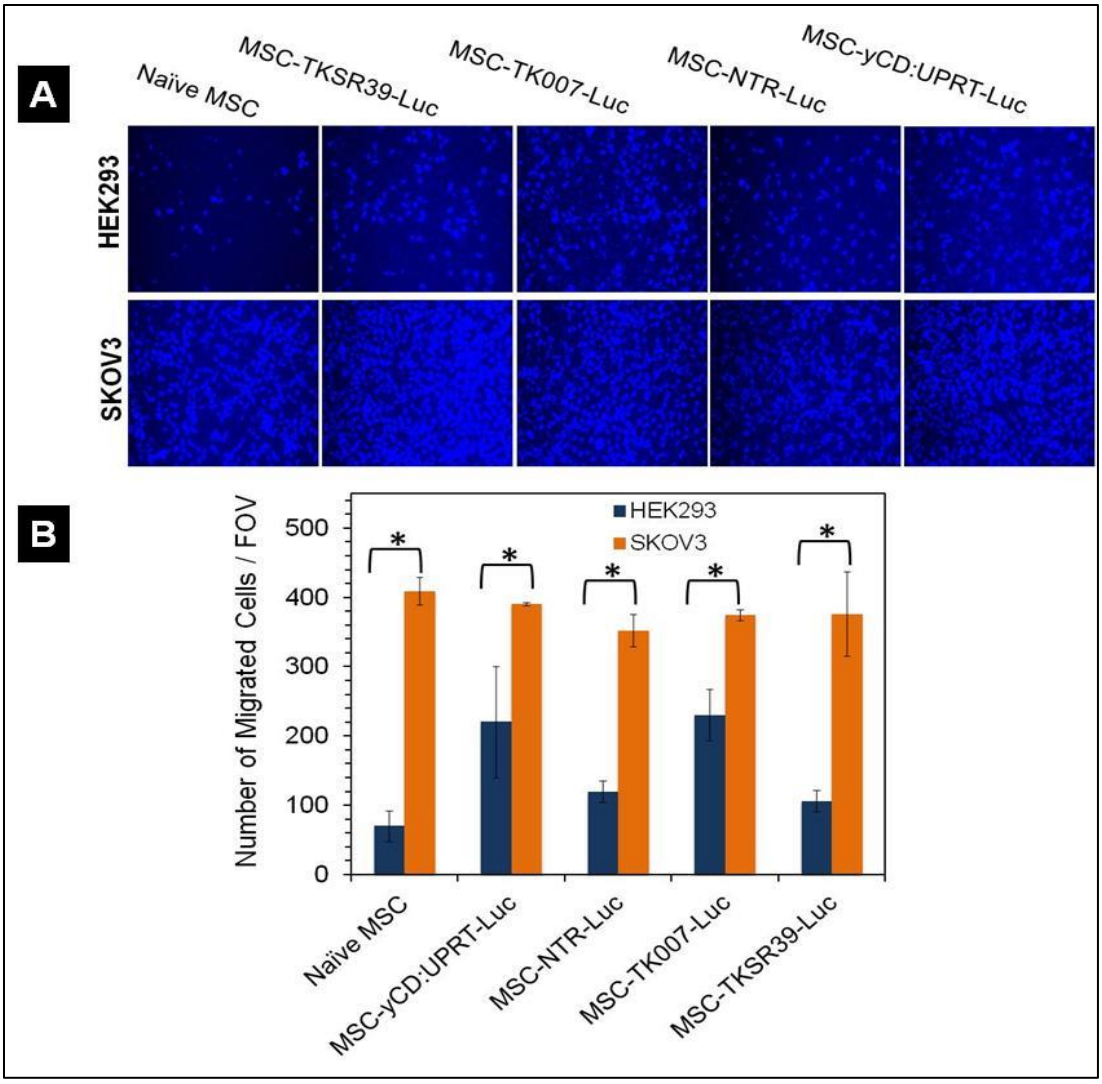

Figure 4.3: Qualitative and quantitative analysis of MSCs' cancer tropism by using Migration assay. A) Representative fluorescent images of the MSCs that migrated towards normal HEK293 and SKOV3 cancer cells. B) Quantitative analysis of the number of migrated cells per field of view (FOV) towards SKOV3 cancer cells and HEK293 cells.

Next, we examined whether the prodrugs after conversion into their cytotoxic form inside the MSCs can diffuse out and kill neighboring cancer cells (bystander effect). For this purpose, we separately co-cultured each suicide gene expressing MSC clone with SKOV3 ovarian cancer cells at different MSC to cancer cell ratios followed by administration of prodrugs. The results of this study illustrated that all genetically modified MSCs could significantly induce cell death in SKOV3 cancer cells **(Figure 4.4A-D)**.

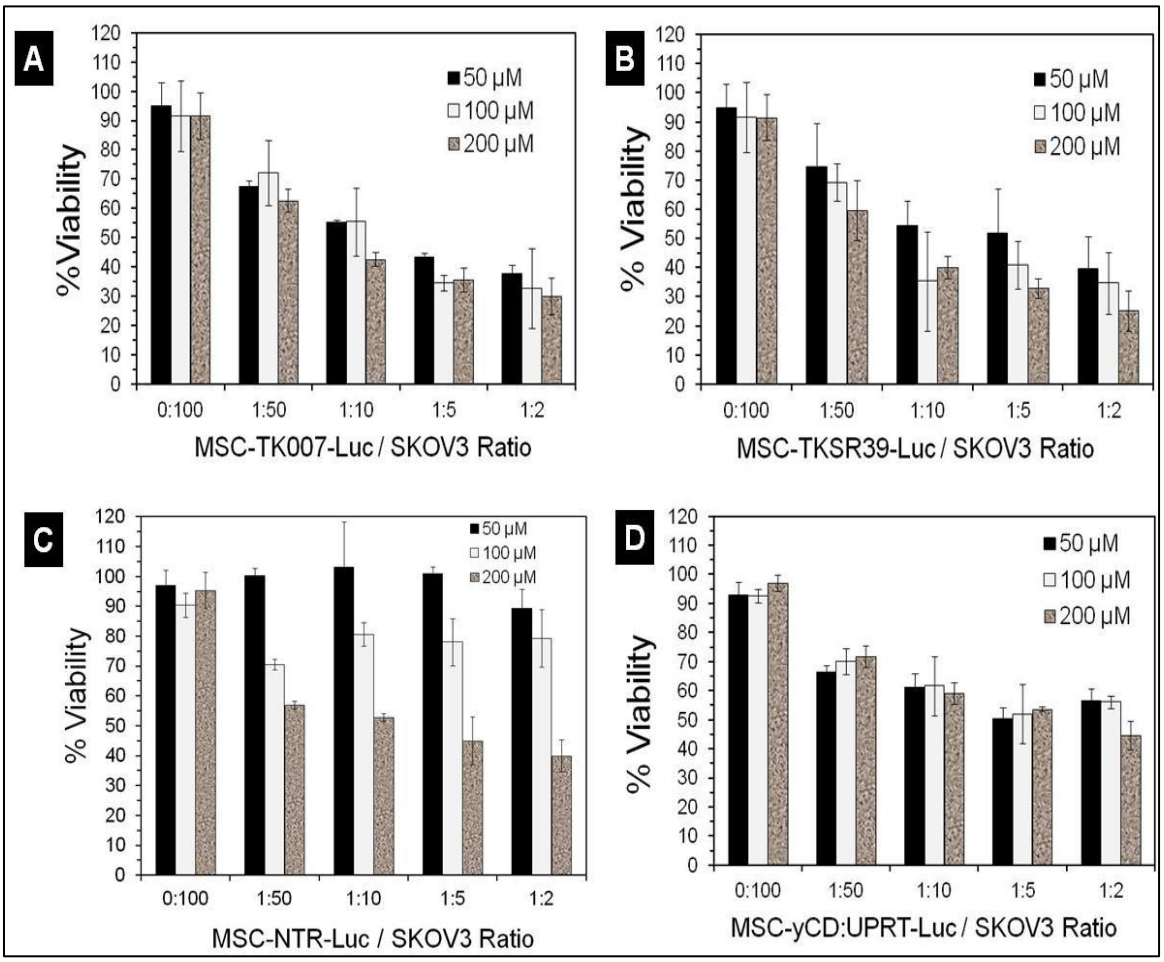

Figure 4.4: Evaluation of the bystander effect. A-D) Cancer cell killing efficiency of MSCs that were co-cultured with SKOV3 cancer cells at different MSC/cancer cell ratios and prodrug concentrations.

More specifically, we did not observe any significant increase in cancer cell killing efficiency by MSC-TK_{SR39}-Luc, MSC-TK_{007}-Luc and MSC-yCD:UPRT-Luc clones when prodrug concentration increased from 50 μM to 200 μM. This could be due to the fact that the IC_{50} of GCV and 5-FC for all these clones as shown in **Figure 4.2** were less than 1 μM. In contrast, MSC-NTR-Luc clone showed dose dependent cancer cell killing efficiency with maximum efficacy at 200 μM of prodrug. This observation correlates very well with the results in **Figure 4.2** which showed more than 100 μM of CB1954 is needed to kill at least 70% of MSC-NTR-Luc cells. To evaluate the potency of the bystander effect with these enzyme/prodrug systems, we used the data in **Figure 4.4** and plotted the best curve fit for all four clones when exposed to 200 μM of prodrug. Comparison of the slopes of the lines and statistical analysis of data revealed the following order of the bystander effect: TK_{SR39}=TK_{007}>NTR>yCD:UPRT (ANOVA followed by posthoc Tukey test, p<0.05) **(Figure 4.5)**. The similarity of sensitivity to prodrug and bystander effects for MSC-TK_{SR39}-Luc and MSC-TK_{007}-Luc clones signifies that both suicide genes could effectively convert GCV into its charged cytotoxic form GCV-triphosphate (GCV-TP). Moreover, it indirectly suggests that gap junctions were present in between MSCs and SKOV3 cells because the bystander effect induced by GCV-TP is largely dependent on active transport via gap junctional intercellular communication (GJIC) [130]. In a mechanistic study by Matuskova et al. (2010), the formation of gap junctions between MSCs and cancer cells after co-culturing is demonstrated [120].

As we mentioned in the introduction section, in previous published studies with suicide gene expressing MSCs no clear rationale is provided to justify the use of one

enzyme/prodrug system over another. The data in **Figure 4.5** which shows the high anticancer activity of TK/GCV system provides the rationale for using this system to effectively kill cancer cells at least at the in vitro level. However, this observation does not explain why the only ongoing two MSC mediated suicide gene therapy protocols in the clinic are based on CD/5-FC system and not TK/GCV or NTR/CB1954. Therefore, we continued the evaluation of these systems at the in vivo level to get a better understanding of the limiting factors.

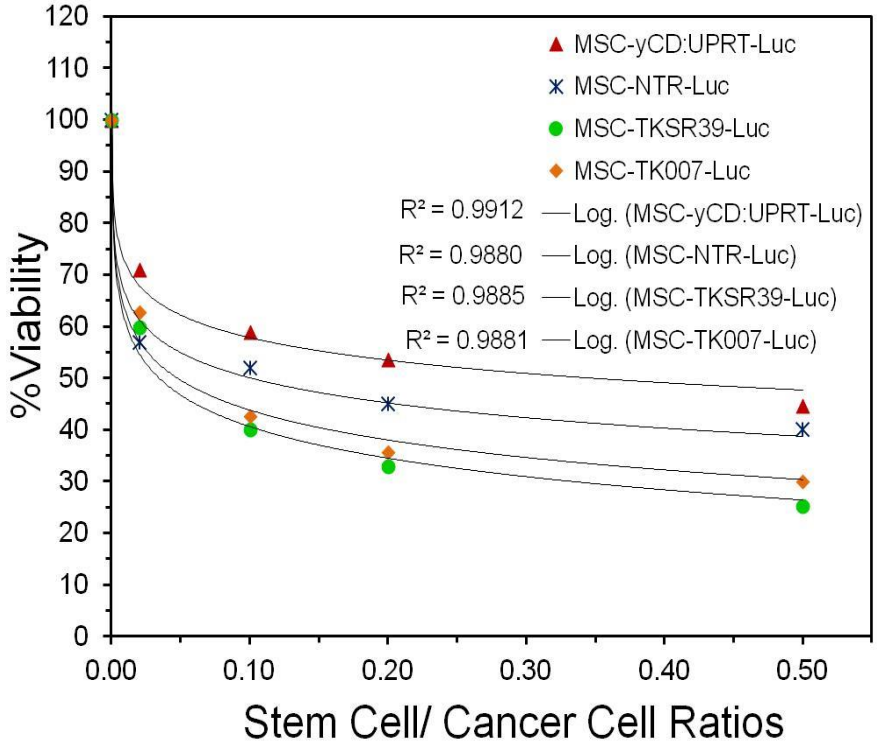

Figure 4.5: Plot of cell viability versus cell ratios for all clones treated with 200 μM prodrug and comparison of the best curve fits.

Based on these results which showed no significant difference between MSC-TK_{SR39}-Luc and MSC-TK_{007}-Luc clones, we selected MSC-TK_{SR39}-Luc as a candidate along with MSC-NTR-Luc for the in vivo studies. Although MSC-yCD:UPRT-Luc clone showed lower levels of anticancer efficacy in comparison to others, but we decided to evaluate its in vivo efficacy since its bystander effect is not GJIC dependent. Therefore, MSC-TK_{SR39}-Luc, MSC-NTR-Luc and MSC-yCD:UPRT-Luc were propagated and used to evaluate their efficacy in killing SKOV3 tumors in nude mice.

Besides the prodrug's bystander effect the number of MSCs that come in contact with tumor cells plays a crucial role in determining the therapeutic outcome of the MSC mediated suicide gene therapy [128]. Therefore, we had to choose the most appropriate route of administration to ensure that all tumors receive equal number of MSCs. It has been shown that after each systemic administration a significant number of MSCs get cleared by pulmonary first pass effect [129]. In addition to pulmonary clearance, other factors such as tumor type and stem cell lineage and size could also impact the number of stem cells that reach tumors [131]. Therefore, to eliminate the impact of stem cell lineage/size and pulmonary first pass effect on the number of MSCs that reach tumors we injected all MSC clones intratumorally. This ensures that all tumors receive consistent and known number of MSCs. Since our data in **Figure 4.3** show that all the genetically modified MSCs maintained their cancer tropism, therefore it is highly likely that the MSCs after intratumoral injection remain in the tumor vicinity. To validate the delivery of viable MSCs to the tumors, all mice were imaged and luciferase expression quantified immediately after receiving one million MSCs intratumorally. After treatment with prodrugs for six days, all mice were imaged again and luciferase expression quantified to

examine whether the MSCs responded to prodrugs. As soon as the effect of prodrug on MSC viability was measured, the next doses of viable MSCs were injected. For each treatment group (MSC plus prodrug) we used the corresponding cell treated group (no prodrug) as a control. This was to evaluate whether MSCs can remain alive in mice and confirm that the decrease in bioluminescent signal is due to prodrug treatment and not other factors such as clearance by the mice natural killer cells. Qualitative and quantitative analysis of the luciferase signal before and after treatment with prodrugs demonstrated that the GCV and 5-FC at the administered dose could significantly kill the MSC-TK_{SR39}-Luc and MSC-yCD:UPRT-Luc clones, respectively **(Figure 4.6A and B)**. However, the MSC-NTR-Luc was mildly responsive to the maximum tolerable dose of CB1954 and the luciferase signal did not change as significant as others before and after prodrug administration **(Figure 4.6C)**. It is worth noting that the bioluminescent signal did not increase overtime in the group treated with MSC-NTR-Luc plus CB1954 suggesting that a portion of the MSCs were responding to prodrug treatment although it was not sufficient to cause dramatic change in signal strengths similar to other groups. Unfortunately, we could not exceed the 20 mg/Kg/day for CB1954 because at higher concentrations mice showed significant hepatotoxicity and started to lose weight. Dose-dependent hepatotoxicity is one of the major side effects of CB1954 which has limited its use [132].

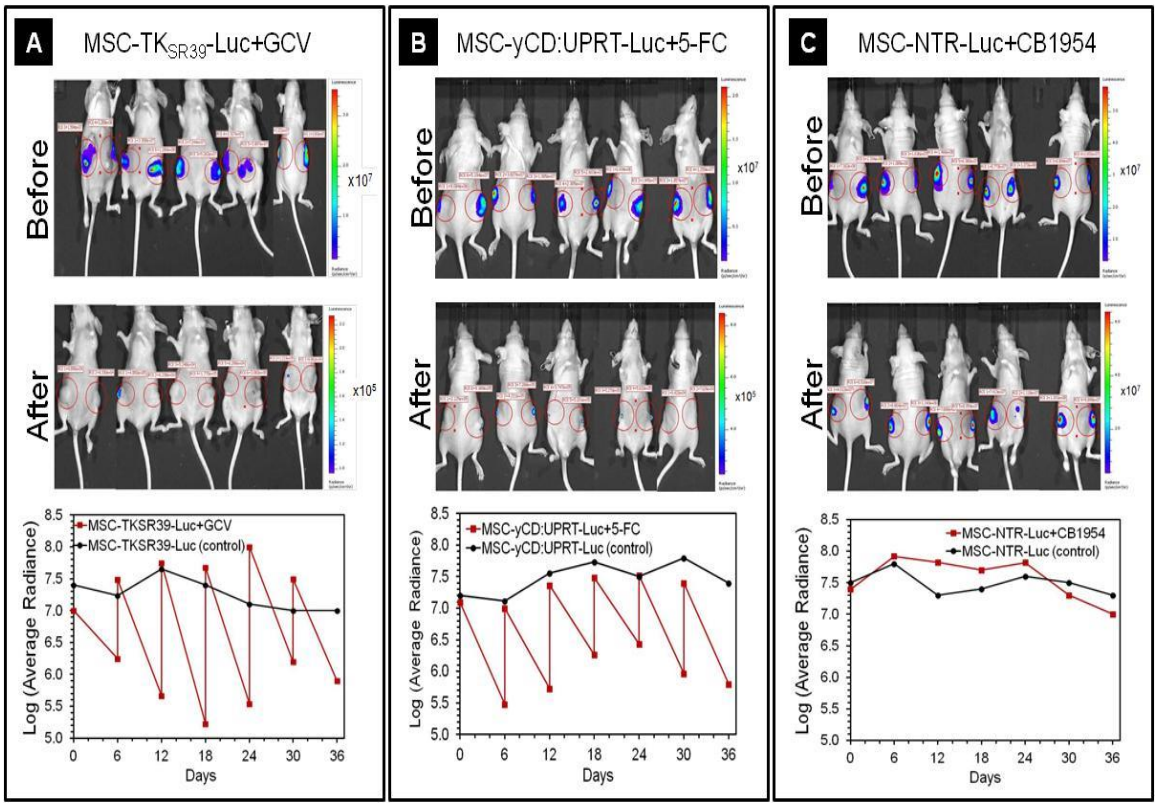

Figure 4.6: Evaluation of luciferase expression before and after prodrug treatment. A-C) Representative images of mice before (top panels) and after (mid panels) receiving the genetically modified MSCs plus prodrugs. The bottom panels show the quantitative analysis of luciferase expression over the 36 days treatment period. This figure shows that after each intratumoral MSC injection, the luciferase signal significantly increased. It also shows that in each 6 day prodrug treatment (GCV and 5-FC) cycle, the luciferase signal in MSCs significantly dropped.

It is well-documented that CB1954 is a potent DNA chelating agent which can freely diffuse to surrounding cells and trigger extensive DNA damage and P53-independent apoptosis in both replicating and non-replicating cells [133]. However, it has also been reported that the conversion rate of CB1954 by NTR is somewhat low as CB1954 is not the natural substrate of NTR [125]. Therefore, the fact that we didn't observe significant reduction in luciferase signal before and after treatment with CB1954 in MSC-NTR-Luc treated mice was explicable. As a result of this observation, we reduced the number of injected MSC-NTR-Luc to 500,000 cells after day 12 because the majority of the injected MSC-NTR-Luc cells from previous dose were still alive. Nonetheless, we continued the treatment of all mice for 36 days until the size of tumors in control groups exceeded the $1000mm^3$ limits. At this point, the tumor sizes were big enough to interfere with the mice natural movements causing distress. Therefore, mice were euthanized at this point and the study was stopped on day 36.

The tumor measurement studies during the period of treatment showed that in comparison to the control groups, mice treated with MSC-TK_{SR39}-Luc plus GCV or MSC-NTR-Luc plus CB1954 did not respond to therapy and the tumor size growth did not get affected significantly (Repeated measure analysis, $p>0.05$) **(Figure 4.7A and C)**. Based on the data in **Figure 4.6**, the lack of response to therapy with MSC-NTR-Luc plus CB1954 was expected since the conversion rate of CB1954 into its cytotoxic form was not high enough to induce significant MSC death. The fact that we did not observe any significant difference between groups treated with MSC-TK_{SR39}-Luc plus GCV or GCV alone indicates that significantly higher numbers of MSCs are required to come in contact and cause considerable damage to cancer cells in a fast growing tumor model. It appears

that to slow down the growth of a tumor that has surpassed the 200mm^3 volume, administration of more than 1 million MSCs per week is necessary. This is sensible as the efficacy of GCV-TP is entirely dependent on GJIC and in tumors gap junctions in between cancer cells are either highly compromised or in many cases non-existent [17,130]. Literature search also shows that TK/GCV enzyme/prodrug therapy has been effective when tumors were small (<100mm^3) and treated early [134,135]. Most importantly, these results could also explain why despite significant success at the preclinical level [69,120,136], no MSC mediated suicide gene therapy protocol with TK/GCV system has reached the clinic. This is also consistent with the results of virus-based suicide gene therapy protocols with TK/GCV system which passed Phase I clinical trials (safety) but later failed at efficacy [124,137].

In contrast to TK/GCV system, mice that were treated with 1 million per week MSC-yCD:UPRT-Luc plus daily administration of 5-FC responded well to therapy and the tumor growth could be inhibited significantly (Repeated measure analysis, $*p<0.05$) **(Figure 4.7B and D)**. This response could be attributed to two important factors; one is GJIC-independent diffusion of 5-FU which significantly enhances drug's bystander effect and the other is the efficiency of yCD:UPRT enzyme in converting 5-FC to 5-FU. Here, we administered one million MSCs to each tumor once a week which could inhibit tumor growth but not eradicate completely. It is worth mentioning that at low concentrations 5-FU has been shown to kill mostly dividing cancer cells; however, at high concentrations it could kill even non-dividing cancer cells through disruption of mRNA processing and protein synthesis [138]. Therefore, a combination of enzyme efficiency and prodrug's physicochemical properties has been responsible for effective killing of the tumor cells.

To achieve complete tumor remission, either injection of higher doses of MSCs or use of other enzyme/prodrug systems with better bystander effect may be needed. The fact that the only MSC mediated suicide gene therapy protocols that have reached clinical trials are based on CD/5-FC system (NCT02015819 and NCT01172964), points at the potentially higher efficacy of this system over others and in line with our findings. Since there are several other enzyme/prodrug systems also available, use of theranostic MSCs for preclinical screening could be expanded to compare the anticancer efficacy of yCD:UPRT/5-FC with other potentially effective systems such as carboxylesterase/irinotecan. For preclinical screening, it is important to choose a cell line that is sensitive to all the enzyme/prodrug systems of interest so that the outcome is not biased. The sensitivity test as shown in Figures 4.4 and 4.5 ensures the chosen cell line is suitable for screening process and identification of a system that can cause maximum damage to cancer cells. Non-sensitive cell lines (resistant) can be used in cases where enzyme/prodrug systems are being screened to find one that can generate sufficiently high concentrations of activated prodrug to overcome resistance. For example, non-dividing breast cancer cells are shown to be resistant to therapy with low concentrations of 5-FU but responsive when the 5-FU concentration is high [138]. Therefore, various yCD mutants can be screened through use of theranostic MSCs as shown in this study to find one that can generate high concentrations of 5-FU and overcome resistance.

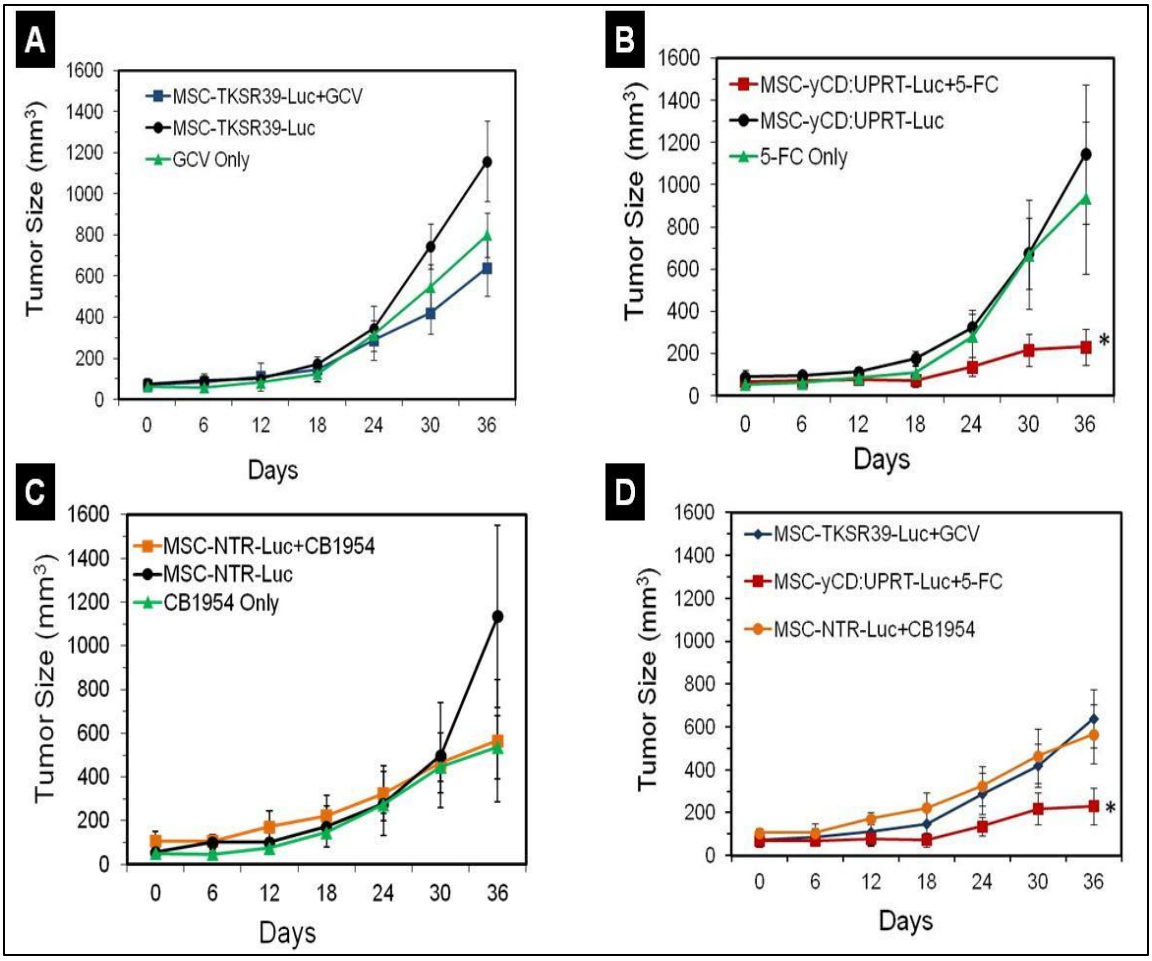

Figure 4.7: Evaluation of tumor size growth in mice treated with suicide gene expressing MSCs and corresponding prodrugs. A) Tumor size growth in mice treated with MSC-TKSR39-Luc cells plus GCV and associated control groups. B) Tumor size growth in mice treated with MSC-yCD:UPRT-Luc cells plus 5-FC and associated control groups. C) Tumor size growth in mice treated with MSC-NTR-Luc cells plus CB1954 and associated control groups. D) Comparison of tumor size growth in mice treated with suicide gene expressing MSCs plus prodrugs and statistical difference among groups.

4.3 Conclusions

Success of stem cell mediated suicide gene therapy of cancer is dependent to a large extent on the conversion rate of the prodrug into its cytotoxic form and also the bystander effect. Among the enzyme/prodrug systems tested in this study, our quantitative imaging and tumor size measurement studies show that yCD:UPRT/5-FC is the most effective system. This study also provides evidence that genetically modified MSCs can be used as a means for side-by-side evaluation of the efficacy of enzyme/prodrug systems.

After selecting the most efficient enzyme/prodrug system, the next step would be delivering a sufficient number of MSCs to the tumor site. It is demonstrated in different studies that a large number of MSCs are trapped in the lung after IV injection, hence multiple injections are needed[85]. Preparing large number of MSCs for multiple injections is a challenging step considering the difficulties of treating MSCs in vitro. The problem is MSCs can be maintained in an undifferentiated condition until a limited number of passages (~8) and they change in cell culture over time which may alter their properties such as proliferation and tumor tropism[5]. As the consequence, the transfection reagent that is used for MSCs should be efficient enough to produce enough number of transfected cells within the shortest time possible by keeping their viability.

For this purpose, both viral and non-viral vectors have been utilized. Lentiviral vectors transfect stem cells relatively efficiently but are not suitable for cancer therapy due to potential for insertional mutagenesis. Adenoviral vectors at high MOI (~100) are also used to achieve high efficiency, but have generated high levels of toxicity to stem cells (>90% death). Non-viral vectors are also available in different categories in the market but there is no study to evaluate and compare their stem cell transfection

efficiency and toxicity profile. As the second part of this project we evaluated transfection efficiency and toxicity of the most commonly used commercially available vectors on MSCs.

Chapter 5

Efficiency and Safety of Commercially Available Vectors

One of the major barrier against stem cell based cancer therapy is that a significant portion of MSCs are cleared in first pass pulmonary effect; therefore, a large number of transfected MSCs needs to be administered in order to reach the sufficient number in the tumor. Since cell culture condition may alter stem cell's properties such as proliferation and tumor tropism, highly efficient vectors are required to produce sufficient number of transfected cells in the lowest number of passages and shortest time [5].

While high efficiency is a critical feature for vectors used in stem cells transfection, safety is also an unavoidable property. Transfection vectors need to be non-toxic and non-oncogenic to maintain the cell viability and genome integrity. Genotoxic vectors could potentially transform normal stem cells into cancer initiating cells (CICs) and result in tumor formation. Therefore, high levels of safety are expected from vectors that are used in stem cell engineering.

Commercially available non-viral vectors are constructed from polymer or lipid and bear a positive charge on their surface. They are able to condense plasmid DNA (pDNA) into nanosize particles suitable for cellular uptake. Among various type of commercial transfection vectors available in the market GeneIn™, Lipofectamine® LTX with Plus™ Reagent, PolyFect, jetPRIME®, and FuGENE® HD are among the mostly used ones. The following description are brought by the manufacturers for each construct,

- GlobalStem®: "GeneIn® is a novel cationic transfection reagent that delivers high transfection efficiency in stem cells and hard-to-transfect primary cells with exceptionally low cellular toxicity to maintain optimal cell health and viability."

- Life Technologies: “Lipofectamine® LTX with Plus™ Reagent is a plasmid transfection reagent that offers a balance of potency and gentleness for your cells, resulting in high transfection efficiencies and viabilities. This reagent provides an advanced solution for gene expression in common cell lines, particularly Chinese Hampster Ovary (CHO), and challenging cell types such as primary neural progenitor cells, primary fibroblasts and primary epithelial cells.”
- QIAGEN: “PolyFect Transfection Reagent is a solution of specifically designed activated-dendrimers. The reagent consists of dendrimer molecules of a defined spherical architecture with branches radiating from a central core. The branches terminate at charged amino groups, which can interact with negatively charged phosphate groups of nucleic acids. PolyFect Reagent assembles DNA into compact structures, that bind to the cell surface and are taken into the cell by nonspecific endocytosis. The reagent buffers the pH of the endosome, leading to pH inhibition of endosomal nucleases, which ensures stability of PolyFect–DNA complexes. The procedure is fast with low cytotoxicity.”
- Polyplus transfection™: “jetPRIME® is a new powerful and versatile DNA and siRNA transfection reagent for day-to-day experiments. jetPRIME® ensures high DNA transfection efficiency and excellent gene silencing in a variety of adherent cells. jetPRIME® is ideal for DNA/siRNA co-transfection. jetPRIME® is very gentle on cells since it requires low amounts of reagent and

nucleic acid during transfection. Effective and nontoxic DNA and siRNA delivery is essential for reliable scientific results."

- Promega: "FuGENE® HD Transfection Reagent is a nonliposomal formulation designed to transfect DNA into a wide variety of cell lines with high efficiency and low toxicity. The protocol does not require removal of serum or culture medium and does not require washing or changing of medium after introducing the reagent/DNA complex. Additionally, the FuGENE® HD Transfection Reagent has been shown to support transfection in chemically defined media and does not contain any animal-derived components."

Even though all the manufacturers have claimed the high efficiency and low cytotoxicity of their commercial vectors, after reviewing the supporting materials presented by them, it appears that there is not sufficient data supporting the efficiency and safety of these commercial vectors on MSCs. To examine whether theses available vectors own the suitable criteria for stem cell based gene delivery, we performed a side-by-side efficiency and cytotoxicity study for all these five commercial vectors.

5.1 Methods and Materials

5.1.1 Transfection of AD-MSCs

Adiposed-derived MSCs (AD-MSCs) (Lonza) were seeded in 24-well plates at 12000 cells/well and incubated overnight at 37 °C to reach ca. 80% confluency. At the time of transfection, the old medium was removed and replaced with 500 μL of ADSC growth medium supplemented with FBS. Commercial reagents were complexed with 0.25, 0.5, 1

and 2 µg of pEGFP according to the manufacturers' instruction. Preparation instructions are brought in the following briefly,

1. GeneIn®: 300 µl of Opti-MEM® was mixed with 1.5 µg of DNA and 6 µl of Red reagent and vortexed for 2-3 second. The mixture was incubated for 5 min. Then 6 µl of the Blue reagent was added to the first mixture and vortexed for 2-3 second. The mixture was incubated for 10 min. Finally 100 µl of the mixture was added to each well for 0.5 µg of DNA transfection. For transfection of 0.25, 1 and 2 µg of DNA the volume of the nanoparticles was adjusted.

2. Lipofectamine® LTX with Plus™: Two tubes were prepared. In the first one 75 µl of Opti-MEM® was mixed with 6 µl of Lipofectamine® LTX. In the second one 75 µl of Opti-MEM® was mixed with 1.5 µg of DNA and 1.5 µl of Plus™ reagent. Two tubes were mixed and incubated for 5 min. 50 µl of the mixture was added to each well for 0.5 µg of DNA transfection. For transfection of 0.25, 1 and 2 µg of DNA the volume of the nanoparticles was adjusted.

3. PolyFect: 1.5 µg of DNA was mixed with 100 µl of Opti-MEM®. 10 µl of PolyFect transfection reagent was added to the mixture and vortexed for 10 seconds. The mixture was incubated for 10 min. Then 200 µl of ADSC growth medium was added to the complex. 100 µl of the mixture was added to each well for 0.5 µg of DNA transfection. For transfection of 0.25, 1 and 2 µg of DNA the volume of the nanoparticles was adjusted.

4. jetPRIME®: 1.5 µg of DNA was added to 150 µl of jetPRIME® buffer and vortexed for 10 second. 3 µl of the jetPRIME® reagent was added to the mixture and

vortexed for 10 seconds. The mixture was incubated for 10 min and 50 µl of that was added to each well for 0.5 µg of DNA transfection. For transfection of 0.25, 1 and 2 µg of DNA the volume of the nanoparticles was adjusted.

5. FuGENE® HD: 2 µg of DNA was added to 98 µl of Opti-MEM® and vortexed for 2-5 second. Then 6 µl of FuGENE® HD reagent was added. The mixture was incubated for 10 min and 25 µl of that was added to each well for 0.5 µg of DNA transfection. For transfection of 0.25, 1 and 2 µg of DNA the volume of the nanoparticles was adjusted.

To visualize green fluorescent protein (GFP) expression, an epifluorescent microscope (Olympus, USA) was used. To prepare the samples for FACS analysis, cells were trypsinized in each well and, after detachment and neutralization, collected by centrifugation at 300g for 6 min. The supernatant was removed, and formaldehyde at 2% in PBS was added to fix the cells. Then, a F500 flow cytometer (Beckman Coulter, USA) was used to measure percent transfected cells as well as GFP expression (transfection efficiency). Each time, 1000 cells were counted and the total fluorescence intensity of positive cells was normalized against the total fluorescence intensity of untransfected cells (background control). The data are presented as mean ± SD (n = 3).

5.1.2 Cell Viability Assay

For WST-1 assay AD-MSCs were seeded in 24-well plates at 12000 cells/well. GeneIn™, Lipofectamine® LTX with Plus™ Reagent, PolyFect, jetPRIME®, and FuGENE® HD were complexed with 0.25, 0.5, 1 and 2 µg of pEGFP and used to transfect AD-MSCs according to manufacturers' instruction. After 24 h incubation, WST-1 reagent was added to the cells. Cytotoxicity was evaluated by measuring the

absorbance of each well at 450 nm after 3 hours. The absorbance of untransfected cells was considered as %100 viable. Data are reported as mean ± SD (n = 3).

5.2 Results and Discussion

High efficiency and lack of toxicity are two requirements for vectors that are used for stem cells transfection. Various types of non-viral vectors are commercially available. Although manufacturers state that these vectors possess high efficiency and low toxicity in stem cell transfection, the materials supporting this claim are missing. In order to evaluate the suitability of these vectors for MSCs transfection, we carried out a side-by-side transfection and cell viability studies on AD-MSCs. In the first step AD-MSCs were transfected with five broadly used commercial transfection reagents including GeneIn™, Lipofectamine® LTX with Plus™ Reagent, PolyFect, jetPRIME®, and FuGENE® HD complexed with different amounts of DNA. The transfected cells were visualized with epiflourescent microscope and analyzed with FACS 48 hours after transfection **(Figure 5.1 & 5.2)**. In the next step AD-MSCs were transfected again with above mentioned commercial vectors and after 24 cell viability was measured by WST-1 assay **(Figure 5.2)**. These studies will help to identify the highest efficiency of the vectors before they start negatively affecting metabolic activity of the MSCs.

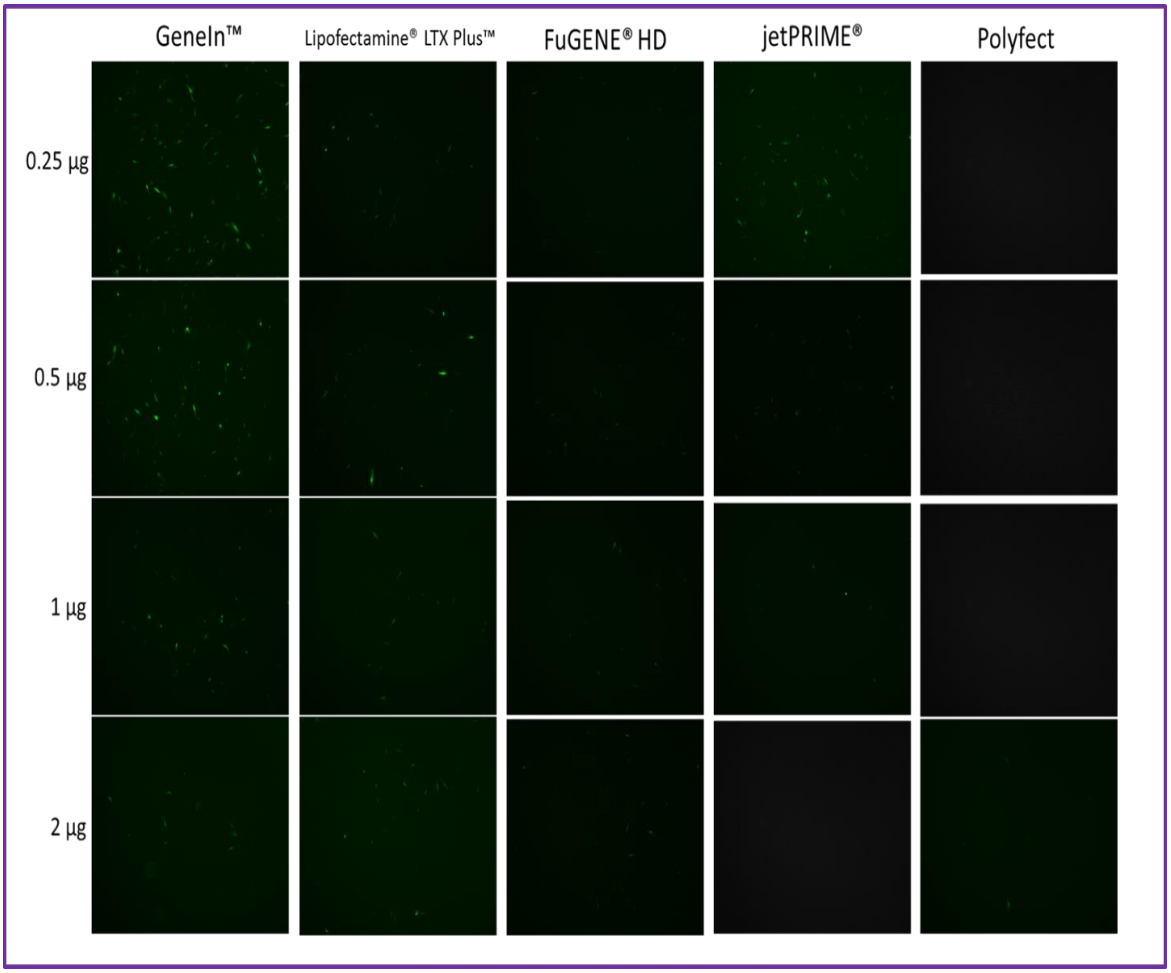

Figure 5.1: Epifluorescence imaging of AD-MSCs transfected with GeneIn™, Lipofectamine® LTX with Plus™ Reagent, PolyFect, jetPRIME®, and FuGENE® HD in 0.25, 0.5, 1 and 2 µg of pEGFP.

As depicted in the epifluorescence images and graphs **(Figure 5.1 & 5.2)**, GeneIn™ in 0.5 and 1 µg of DNA transfection had the highest efficiency among all different conditions of transfection. This reagent was able to transfect MSCs with the total fluorescence intensity (TFI) of ca. 27000 unit that was correlated with 80% cell viability. Transfection percentage was also calculated for GeneIn™ that was ca. 35 to 40 % in the best condition **(Figure 5.3)**. While GeneIn™ demonstrated the highest efficiency, its progressive cytotoxicity in 2 µg DNA transfection diminished its efficiency significantly. FuGENE® and Polyfect indicated the lowest efficiency among all vectors with the TFI of less than 5000 unit in different DNA amounts. As opposed to FuGENE® that its low transfection was correlated to high cell viability (>90%), Polyfect illustrated high toxicity of ~60% in 1 µg of DNA transfection. It might be indicative that the low transfection of FuGENE® is corresponded to its low inherent transfection efficiency, whereas in Polyfect the high toxicity has restricted transfection efficiency. Lipofectamine® LTX with Plus™ Reagent depicted its highest efficiency in 0.5 µg of DNA with TFI of ca. 13000 unit correlated with cell viability of less than 80%. jetPRIME® also showed its highest efficiency in 0.25 µg of DNA with TFI of ca. 15000 correlated with cell viability of less than 80%.

It appears that GeneIn™ is the best candidate for stem cell transfection among these five commercial vectors examined in this study due to showing the significantly higher efficiency, although its efficiency is confined by its cytotoxicity.

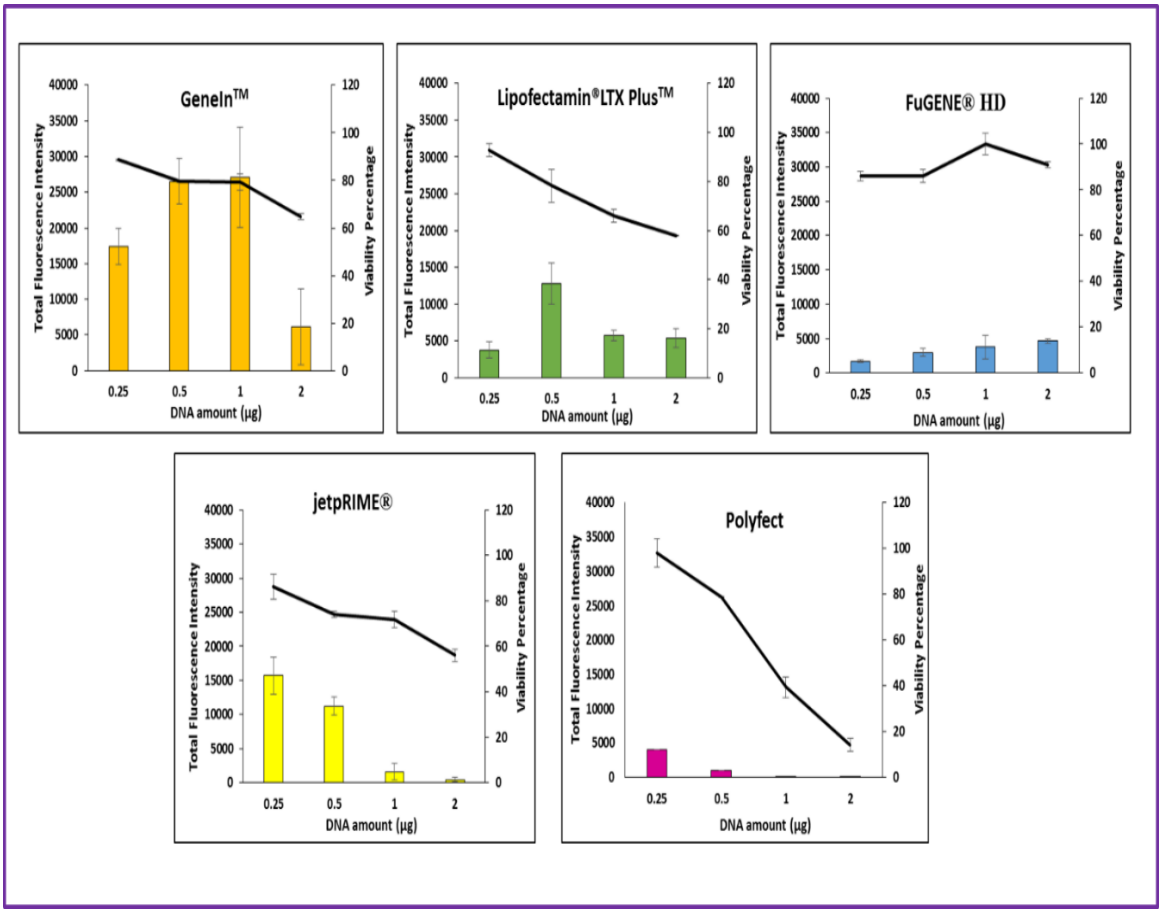

Figure 5.2: Total fluorescence intensity (bar chart) and cell viability percentage (line) of AD-MSCs transfected with GeneIn™, Lipofectamine® LTX with Plus™ Reagent, PolyFect, jetPRIME®, and FuGENE® HD in 0.25, 0.5, 1 and 2 µg of pEGFP.

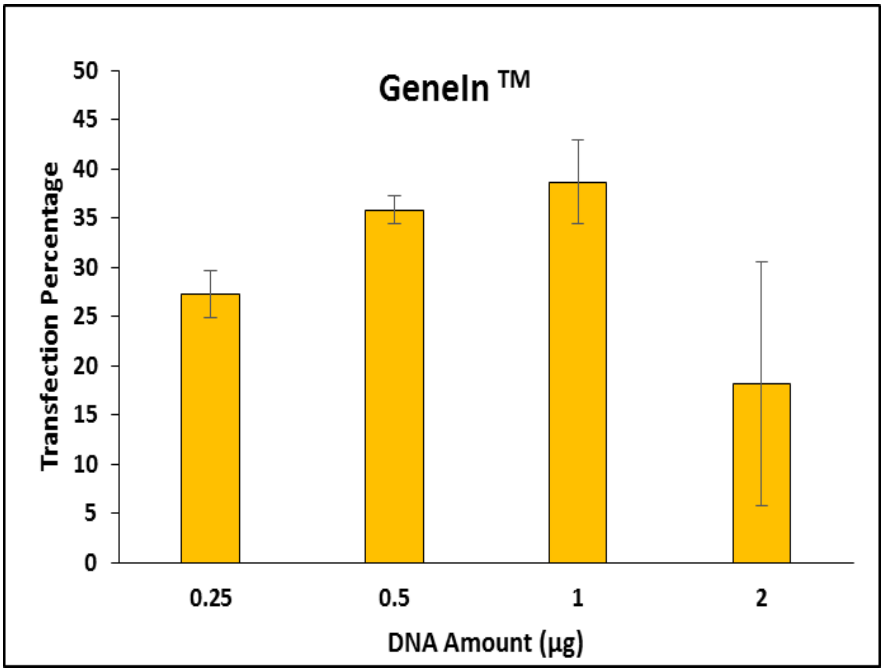

Figure 5.3: Percentage of transfection for MSCs transfected with GeneIn™ in 0.25, 0.5, 1 and 2 µg of pEGFP.

5.3 Conclusion

We conducted a side-by-side transfection and cell viability study for five of the most broadly used commercial transfection reagents including, GeneIn™, Lipofectamine® LTX with Plus™ Reagent, PolyFect, jetPRIME®, and FuGENE® HD. The results indicated that GeneIn™ is the most efficient vector with the transfection percentage of ~ 40% that was correlated with ~ 80% cell viability. While GeneIn™ displayed an acceptable gene transfection efficiency, its increasing cytotoxicity prevents from dose enhancement. To circumvent this type of cytotoxicity and achieve higher efficiency we decided to design and develop a recombinant vector for stem cell transfection. We employed the recombinant vector previously developed in our lab as the template and strived to optimize its structure to achieve the highest level of safety and efficiency for stem cell transfection.

Chapter 6

Vector Design for Efficient and Safe Gene Delivery [3]

[3] A version of this chapter has been published in Journal of Biomacromolecule. Please see "A recombinant biopolymeric platform for reliable evaluation of the activity of pH-responsive amphiphile fusogenic peptides.", PMID: 23682625.

Nonviral delivery systems potentially have several advantage over viral counterparts because of easier production in large scales, capability of delivering transgenes in various sizes, and lower immunogenicity, however; their lower efficiency of gene delivery has significantly limited their application[139]. This inefficiency of gene delivery mostly comes from the inability of these vectors to circumvent the numerous intra- and extracellular barriers. The most important barriers encountered efficient nonviral gene delivery are (1) complex formation and characterization, (2) transport in blood circulation, (3) uptake/entry into the cell, (4) release from endosome, (5) dissociation from synthetic vector, (6) transit from cytoplasm to nucleus, (7) uptake/entry into nucleus and (8) transgene expression[140]. Unfortunately, none of the peptide motifs of biological origin (e.g., TAT, Mu, SV40-NLS, etc.) were able to independently overcome the major cellular barriers to exert successful targeted gene delivery[141]. In contrast, recombinant multifunctional vectors, which are the fusion of multiple biological motifs, have been successful in overcoming these hurdles by performing several independent functions such as cell targeting, DNA condensation, endosome disruption, and nuclear localization. We have previously developed a recombinant multifunctional vector in our lab composed of a HER2-targeting affibody, four repeating units of histone H2A, and a pH-responsive fusogenic peptide (GALA). We reported that this vector has the ability to condense plasmid DNA into nanosize particles and protect from serum endonucleases, target HER2-positive cancer cells (i.e., SKOV-3) but not HER2-negative ones (e.g., MDA-MB-231), escape from the endosomal compartment into cytosol with the help of the fusogenic peptide, utilize microtubules to transfer genetic material toward the cell nucleus, and

mediate efficient gene expression[142]. We used this recombinant biopolymer as the template for developing an efficient and safe vector for MSC transfection.

In targeted gene delivery, for an internalized gene delivery system to effectively shuttle its cargo into the cell nucleus, it must overcome a major biological barrier, the endosomal membrane. While an intact endosomal membrane is critical for proper cell function, it is also one of the major hurdles for the delivery of therapeutic agents into the cytosol. Use of fusogenic peptides (FP) as part of gene delivery systems is one of the most promising approaches to assist endosomal escape and therefore improve gene transfection. FPs are amphiphilic molecules that can interact with phospholipid membranes to form pores or induce membrane fusion and/or lysis. Amphiphile pH-responsive FPs are derived from the sequence of the N-terminal segment of the HA-2 subunit of the influenza virus hemagglutinin (GLFGAIAGFIENGWEGMIDGWYG), which is involved in the fusion of the viral envelope with the endosomal membrane. These peptides exhibit endosome membrane disrupting properties in acidic media and are used in the development of synthetic gene delivery systems. The pH-dependent lytic activity of amphiphilic FPs is one of their important attributes because it minimizes the possibility of causing damage to normal cell membranes under physiological conditions. Several pH-responsive FPs, classified as anionic and cationic, have been reported in literature. While the cationic FPs have the ability to bind directly and condense plasmid DNA (pDNA) into nanosize particles suitable for cellular uptake, the anionic ones are unable to interact with pDNA directly. As a result, in many studies, anionic FPs have been used in conjunction with a cationic vector for gene delivery[49,143,144]. Due to this charge property difference between anionic and cationic FPs, no accurate comparative

study has been performed to date to establish the precise correlation between FP sequence and cytotoxicity, endosomolytic activity and impact on gene transfer efficiency. Therefore, there has been no clear rationale for selecting one FP over another in the past, and it is still unclear which FP is the most suitable and efficient construct for use in drug/gene delivery system design. The *objective* of this study was to utilize a biopolymeric platform as a tool to accurately evaluate and compare the pH-dependent membrane disruption activity, cell toxicity and impact on gene transfer efficiency of five most widely used cationic and anionic pH-responsive FPs, INF7, GALA, KALA, H5WYG and RALA.

INF7 (GLFEAIEGFIENGWEGMIDGWYG)[145] and GALA (WEAALAEALAEALAEHLAEALAEALEALAA)[49] peptides are anionic and glutamic acid-enriched HA-2 analogs whereas KALA (WEAKLAKALAKALAKHLAKALAKALKAGEA)[146], RALA (WEARLARALARALARHLARALARALRAGEA) and H5WYG (GLFHAIAHFIHGGWHGLIHGWYG)[147] are cationic and enriched in lysine, arginine, and histidine, respectively. The biopolymeric platform used in this study is a single chain multifunctional fusion biopolymer composed of four repeating units of Histone H2A with an inherent nuclear localization signal (H) and a human epidermal growth factor receptor 2 (HER2) targeting affibody (T).[144] In a series of mechanistic studies, our group has previously demonstrated that all motifs in the TH biopolymer are functional and when equipped with fusogenic peptide GALA can efficiently transfect SKOV-3 ($HER2^+$) cancer cells.[144] We used the TH biopolymer as a base to engineer five multifunctional fusion biopolymers with similar sequences that were different only in FP sequence.

Therefore, the designed recombinant biopolymers are single chain peptides composed of an affibody to target HER2, four repeating units of histone H2A with an inherent nuclear localization signal to condense pDNA into nanosize particles and facilitate active translocation of pDNA towards nucleus, and a fusogenic peptide GALA (G), KALA (K), RALA (R), H5WYG (H) or INF7 (I) to disrupt endosomal membranes. For simplicity the biopolymers will be shown as THG, THK, THR, THH and THI **(Figure 6.1)**.

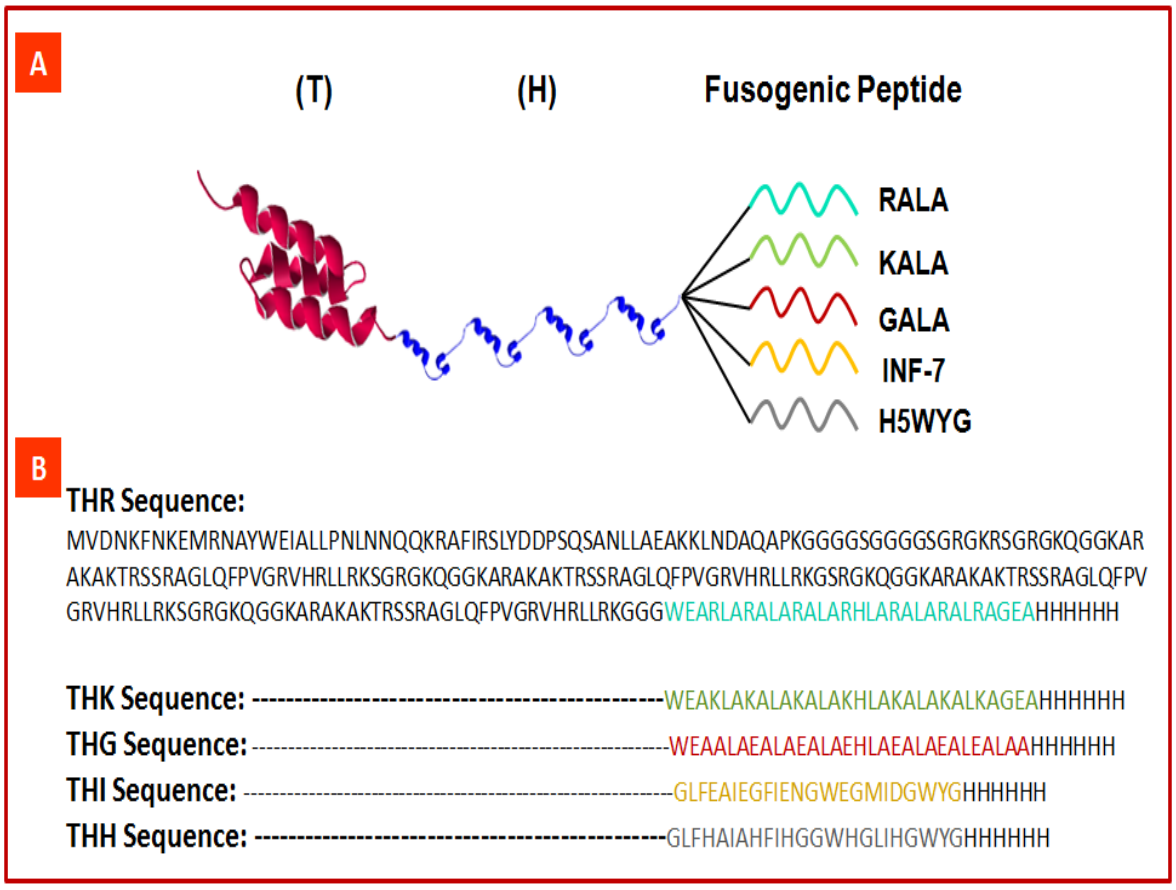

Figure 6.1: A) Schematic representation of recombinant biopolymers composed of a targeting motif (T), four repeating units of Histone H2A with an inherent nuclear localization signal (H) and a fusogenic peptide (e.g., INF7, GALA, KALA, RALA and H5WYG). The 3D structures of T and one repeat of histone H2A are predicted by SWISS-MODEL program. B) The full amino acid sequence of THR and other biopolymers with C-terminal histags. In THK, THG, THI and THH, only the amino acid sequence of FP is shown.

6.1 Materials and Methods

6.1.1 Cloning and expression of the recombinant fusion biopolymers

The genes encoding THG, THK, THR, THH and THI with C-terminal histags were designed by our group and synthesized by Integrated DNA Technologies (Coralville, Iowa). A C-terminal NdeI and N-terminal XhoI restriction sites were also designed for cloning purposes. The synthesized genes were double digested with NdeI and XhoI restriction enzymes (New England Biolabs, Ipswich, MA) and cloned into the pET21b expression vector (Novagen, Billerica, MA). After verification by DNA sequencing, each construct was transformed into an E.coli expression host for production. Plasmid encoding THH was transformed into E.coli BL21(DE3) pLysS (Novagen, Billerica, MA) and those encoding THG, THK, THR and THI were transformed into E.coli BL21AI (Invitrogen, Life Technologies, Grand Island, NY).

For THG, THK, THR and THI production, starter cultures were prepared by inoculation of a single fresh colony of BL21AI harboring expression plasmids in 5 ml LB media containing 50 µg/ml carbenicillin incubated at 30 ˚C overnight. The next day, 5 ml of the starter culture was used to inoculate 500 ml Circlegrow media (MP Biomedicals) containing 50 µg/ml carbenicillin which resulted in OD_{600} of 0.1. The culture was grown at 30 ˚C for 3 hours to reach the OD_{600} of 1.2. Gene expression was induced by isopropyl β-D-1-thiogalactopyranoside (IPTG) 1 mM and L-arabinose (0.2%) at 30 ˚C. The cells were harvested after 5 hours by centrifugation at 5000 g for 20 min.

For the production of THH, a single fresh colony of BL21(DE3)pLysS harboring expression plasmids was inoculated in 10 ml TB media containing 200 µg/ml carbenicillin and incubated at 37 ˚C for 3 hours to reach the OD_{600} of 0.4-0.6. The cells

were collected by centrifugation at 1000 g for 5 min. The soluble fraction (supernatant) was removed and cells were resuspended in 10 ml fresh TB media with 200 µg/ml carbenicillin and 6 ml of that was used to inoculate 500 ml of TB media containing 200 µg/ml carbenicillin. The cells were incubated at 37 ^{o}C for 3 hours to grow and reach the OD_{600} of 0.5. The cells were collected by centrifugation at 1000 g for 5 min and after removing the supernatant were resuspended in the same volume of fresh TB media (i.e., 500 ml). Expression was induced by IPTG to a final concentration of 1 mM. Cells were incubated at 37 ^{o}C for 2 hours with vigorous shaking to express THH. Then, the cells were pelleted by centrifugation at 5000 g for 20 min.

6.1.2 Purification of recombinant fusion biopolymers

All biopolymers were purified using Ni-NTA affinity chromatography. The cell pellets were suspended in lysis buffer (Urea 8M, NaCl 2M, NaH_2PO_4 100mM, Tris 10mM, Triton 1%, Imidazole 10 mM) and stirred for 30 min. The lysates were centrifuged at 37,000 g for 1 hour to sediment the insoluble fractions. The supernatant was transferred to another tube and incubated with Ni-NTA resins equilibrated with lysis buffer for 1 hour with gentle shaking on ice. The resins were loaded onto a column and first washed with 70 ml of lysis buffer and then 45 ml of wash buffer (Urea 5M, NaCl 1.5M, NaH_2PO_4 100mM, Tris 10mM, Imidazole 40 mM) to remove the impurities. Finally, the peptides were eluted with elution buffer (Urea 3M, NaCl 0.5M, NaH_2PO_4 100mM, Tris 10mM, Imidazole 200 mM). The expression and purity of the biopolymers were analyzed by western blot analysis with anti-histag antibody and SDS-PAGE, respectively.

6.1.3 Biopolymer desalting and preparation of stock solution

Prior to use in experiments, the purified biopolymer solutions were desalted. The G-25 sepharose column (GE Heathcare) was first conditioned with HEPES buffer (100 mM, pH 7.4) plus saline (5 mM) and then loaded with the biopolymer solution. The elute fractions were collected and the final concentrations of the desalted biopolymers were measured by Nanodrop 2000 spectrophotometer (Thermoscientific).

6.1.4 Particle size and charge analysis

Different amounts of each biopolymer were mixed with 1 µg of pEGFP (plasmid encoding green fluorescent protein) to make nanoparticles at N:P ratios (the ratio of positive nitrogen atoms in biopolymer to negative phosphate groups in pDNA) of 1, 4, 8, 10 and 12. In N:P calculations, each K and R in the biopolymer sequence was considered as +1 while H was considered zero. Therefore, for preparation of nanoparticles at N:P 1, 1.4 µg of THG, 1.38 µg of THI, 1.25 µg of THK, 1.26 µg of THR or 1.37 µg of THH was used to complex with 1 µg of DNA. Desired amounts of biopolymer and pEGFP were diluted each to 50 µl with HEPES buffer (100 mM pH 7.4) in separate tubes. Nanoparticles were formed by addition of biopolymer to pEGFP solution through flash mixing method. In this method, biopolymer solution is added to pEGFP solution rapidly all at once. Nanoparticles were incubated at room temperature for 15 min before measuring particle size and surface charge using Nano-ZS Zetasizer (Malvern Instruments, U.K). Three independent batches for each N:P ratio were prepared and the results are presented as mean ± s.d (n=3).

6.1.5 Particle shape analysis by transmission electron microscopy

To study the shape of the nanoparticles, one drop of sample was put on a carbon type B coated copper grid (Ted Pella, USA) for 5 minutes. The sample was dried and the grid was stained for ca. 2 minutes with 1% sodium phosphotungstate solution. The grids were imaged using transmission electron microscope (1200EX electron microscope, JEOL®, USA) at RUMDNJ TEM core imaging facility. This method was adapted with slight modifications from a previously published method for imaging viruses.[148]

6.1.6 Cell transfection studies

The transfection protocol is similar to that used as a standard for transfecting cells with adenoviruses, which are targeted nanoparticles with sizes of less than 100 nm. For more information please see the standard protocol of cell transfection with adenovirus from MP Biomedicals (Solon, Ohio). In brief, SKOV-3 ovarian cancer cells ($HER2^+$) were seeded in 96-well plates at 4×10^4 cells/well and incubated overnight at 37 ^oC to reach ca. 80% confluency. At the time of transfection, the old media was removed and replaced with 200 µl of McCoy's 5A medium supplemented with insulin, transferrin, selenium, ovalbumin, dexamethasone, and fibronectin and incubated at 37 ^oC for 2 hours. Each biopolymer was complexed with 0.5 µg pEGFP at N:P ratios of 1, 4, 8, 10 and 12 to form nanoparticles. They were then added to each well and incubated with SKOV-3 cells. After four hours of incubation, the media was removed and replaced with 300 µl of McCoy's 5A medium supplemented with 10% FBS. When used, 100 nM of Bafilomycin A1 (Sigma-Aldrich St. Louis, MO, USA) or 100 µM of chloroquine was added to cells at the time of transfection.

To visualize green fluorescent protein (GFP) expression, an epifluorescent microscope (Olympus, USA) was used. To prepare the samples for FACS analysis, cells were trypsinized in each well and, after detachment and neutralization, collected by centrifugation at 300 g for 6 min. The supernatant was removed and formaldehyde at 2% in PBS was added to fix the cells. Then, a F500 flowcytometer (Beckman Coulter®, USA) was used to measure percent transfected cells as well as GFP expression (transfection efficiency). Each time, 5000 cells were counted and the total fluorescence intensity of positive cells was normalized against the total fluorescence intensity of untransfected cells (background control). The percentage of GFP positive cells was determined by Kaluza flow analysis software (Beckman Coulter, USA) using 99% gating. Total green fluorescence intensity (TFI), which is a measure of green fluorescent protein expression, was calculated using the following formula: TFI= mean fluorescence value of each GFP positive cell (measured by flowcytometer) × total number of transfected GFP positive cells. The data are presented as mean ± s.d (n=3).

6.1.7 Hemolysis assay

Sheep red blood cells were purchased from Innovative Research Inc. (Novi, MI). Cells were washed 3 times with phosphate buffer saline with pH adjusted to 5.5 and 7.4. The final number of cells was 1.5×10^9 cells/ml and from that 250 µl of cell suspension was transferred into two separate microfuge tubes. 30 µg of each biopolymer was added to each tube and incubated at 37^oC while shaking at 175 RPM. After 1 hour, cells were centrifuged at 1500 RPM for 1.5 min to pellet the cells. The absorbance (Abs) of the supernatant was measured at 540 nm to calculate percent hemolysis. Triton 1% was used as positive control and phosphate buffer saline at pH 5.5 and 7.4 were used as negative

controls. The following formula was used to calculate hemolytic activity of each biopolymer: (Abs of sample - Abs of negative control) × 100 / (Abs of positive control - Abs of negative control). Data are reported as mean±s.d (n=3).

6.1.8 Cell viability assay

The biopolymer related cytotoxicity was evaluated by WST-1 assay (Roche, Nutley, NJ). SKOV-3 cells were seeded in 96-well plates at 2×10^4 cells/well. THG, THK, THH, THI and THR biopolymers were complexed with 0.5 μg of pEGFP and used to transfect SKOV-3 cells as mentioned above. After 24 hours incubation, WST-1 reagent was added to the cells and cytotoxicity was evaluated by measuring the absorbance of each well at 450 nm. The absorbance of untransfected cells was considered as %100 viable. Data are reported as mean±s.d (n=3).

6.2 Results and Discussion

Since the 1980s, the sequences and activities of various pH-responsive amphiphile FPs have been reported in literature.[49,145,149-152] It has been shown that such FPs are effective in disrupting endosomal membranes at low pH facilitating the escape of gene cargo from endosomes into cytosol and resulting in a significant increase in the transfection efficiency of vectors. However, there have been no studies reliably correlating the FP sequences with their impact on vectors' cell transfection efficiency. To minimize the impact of vector heterogeneity in terms of polydispersity and sequence variability on gene transfer efficiency, we used a recombinant biopolymer as base vector. Because recombinant biopolymers can be made as monodisperse with precise compositions, molecular weights and specified functions, conducting structure activity studies is achievable with higher degrees of accuracy. In this study, we engineered five

multifunctional biopolymers with identical sequences that differed only in FPs **(Figure 6.1)**. The four functional motifs in the biopolymer structure were combined into a single chain vector rather than four separate ones in order to reduce considerably the number of variables that needs to be optimized in structure/activity correlation studies.

We characterized these biopolymers in terms of pH-dependent lytic activity, ability to condense pDNA, transfection efficiency and toxicity in order to identify the most efficient construct. First, the genes encoding the biopolymers were constructed and cloned into the pET21b expression vector. The cloned vectors were then transformed into suitable expression hosts (i.e., BL21AI or BL21(DE3) pLysS) for expression. Due to the cationic nature of the biopolymers and lytic activity of the fusogenic peptides, they are usually toxic to biological expression systems. Therefore, we had to develop specific and stringent protein expression conditions for their expression. Because the level of THH biopolymer toxicity to E.coli during expression was significantly higher than that for other biopolymers, we developed a specific method for its production as described in the methods section. All biopolymers were expressed as soluble proteins and purified. Western blot analysis and SDS-PAGE confirmed the expression and purity of biopolymers after Ni-NTA affinity chromatography **(Figure 6.2)**. From each liter of culture we were able to purify ca. 2 mg of THK, THR and THH and ca. 3 mg of THG and THI with >98% purity. Overall, toxicity of biopolymers with cationic FPs (THH, THK, and THR) was higher than those with anionic FPs (THI and THG).

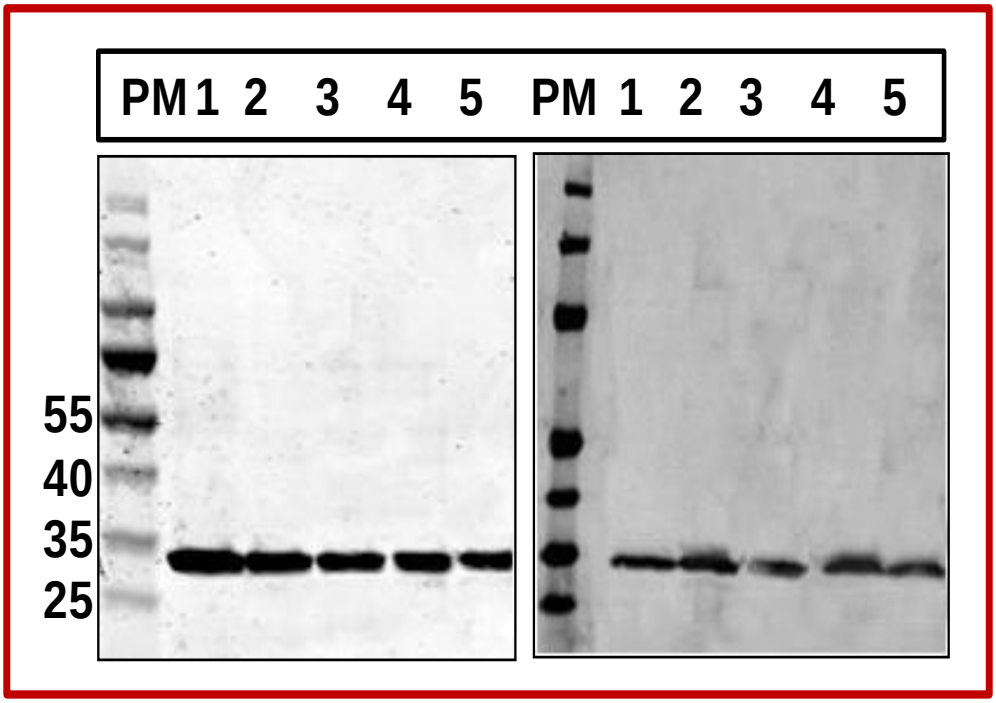

Figure 6.2: SDS PAGE (left panel) and western blot analysis (right panel) of the purified biopolymers. PM stands for protein marker. Lanes 1 through 5 are THG, THR, THK, THH and THI, respectively.

In the next step, all five biopolymers were desalted to remove the excess salt and used to complex with pEGFP at various N:P ratios to form nanoparticles, which were then characterized in terms of hydrodynamic particle size and charge. The results of this study revealed that the sizes of the nanoparticles formed at N:P ratios of 8, 10, and 12 were below 100 nm and not statistically different from each other ($p<0.05$) **(Figure 6.3)**.

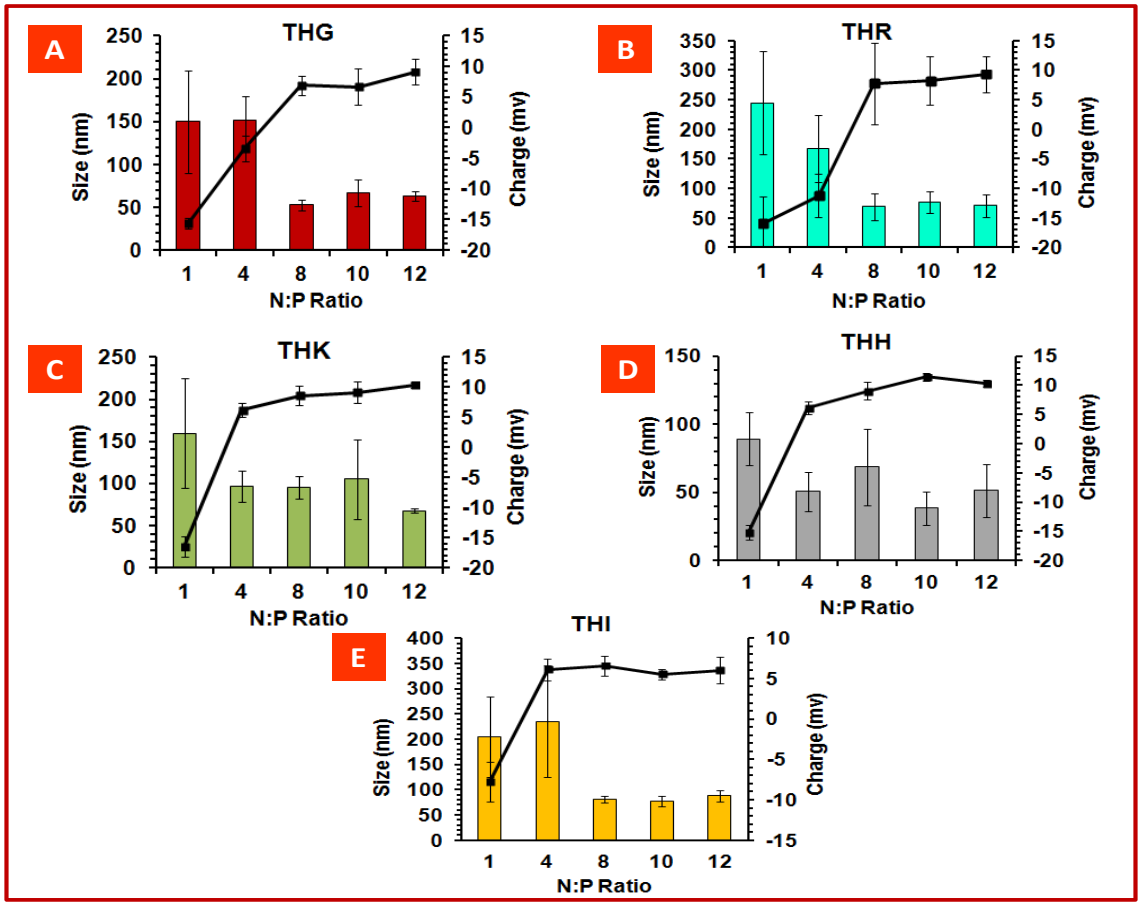

Figure 6.3: The particle size and charge analysis of THG, THR, THK, THH and THI biopolymers in complexation with pEGFP at various N:P ratio

The desalting step is highly important because it helps to remove the excess ions from the system and stabilize the particles' sizes by minimizing the potential for salt bridge formation in between nanoparticles and consequent aggregation. It is noteworthy that nanoparticles in this size range (<150nm) are known to be suitable for receptor mediated endocytosis as they can fit into clathrin-coated vesicles.[35] The results of the zeta potential study revealed that the nanoparticles' surface charge increased to a stable ca. +10mV at N:P ratios 8 or higher for all biopolymer/pEGFP complexes **(Figure 6.3)**. Overall, these results indicate that nanoparticles at N:P ratios of 8, 10 and 12 are statistically similar in terms of size and charge (p>0.05).

We then investigated the ability of all five biopolymer/pEGFP nanocomplexes to internalize and transfect SKOV-3 cancer cells. This cell line was used as a model $HER2^+$ mammalian cell line because our group has previously demonstrated that the targeting ligand (affibody) in the THG structure could recognize the HER2 on the surface of the cells and internalize.[144] Affibodies are small antibody mimetics composed of a three-helix bundle based on the scaffold of one of the IgG-binding domains of Protein A. [153,154] To make a more accurate comparison among the biopolymers, we have deliberately included a targeting motif in the biopolymer structure so that the biopolymer/pDNA complexes enter the cells via receptor-mediated endocytosis. Therefore, entrapped nanoparticles will require an active pH-responsive FP for efficient escape from the endosomal compartment. Without a targeting peptide, nanoparticles may enter the cells via other non-specific routes such as cavaolae where there may not need a pH-responsive FP for escape.[155] In order to find the N:P ratio at which the nanoparticles have the highest rate of transfection efficiency, we transfected SKOV-3 cells with biopolymer/pEGFP complexes

at N:P ratios of 1 to 12. The results of the transfection studies showed that the transfection efficiencies of all biopolymers were the highest at N:P ratios of 8, 10 and 12 **(Figure 6.4)**. However, THG showed not only a statistically higher percentage of transfected cells in comparison to other biopolymers but also higher rates of green fluorescent protein expression ($p<0.05$).

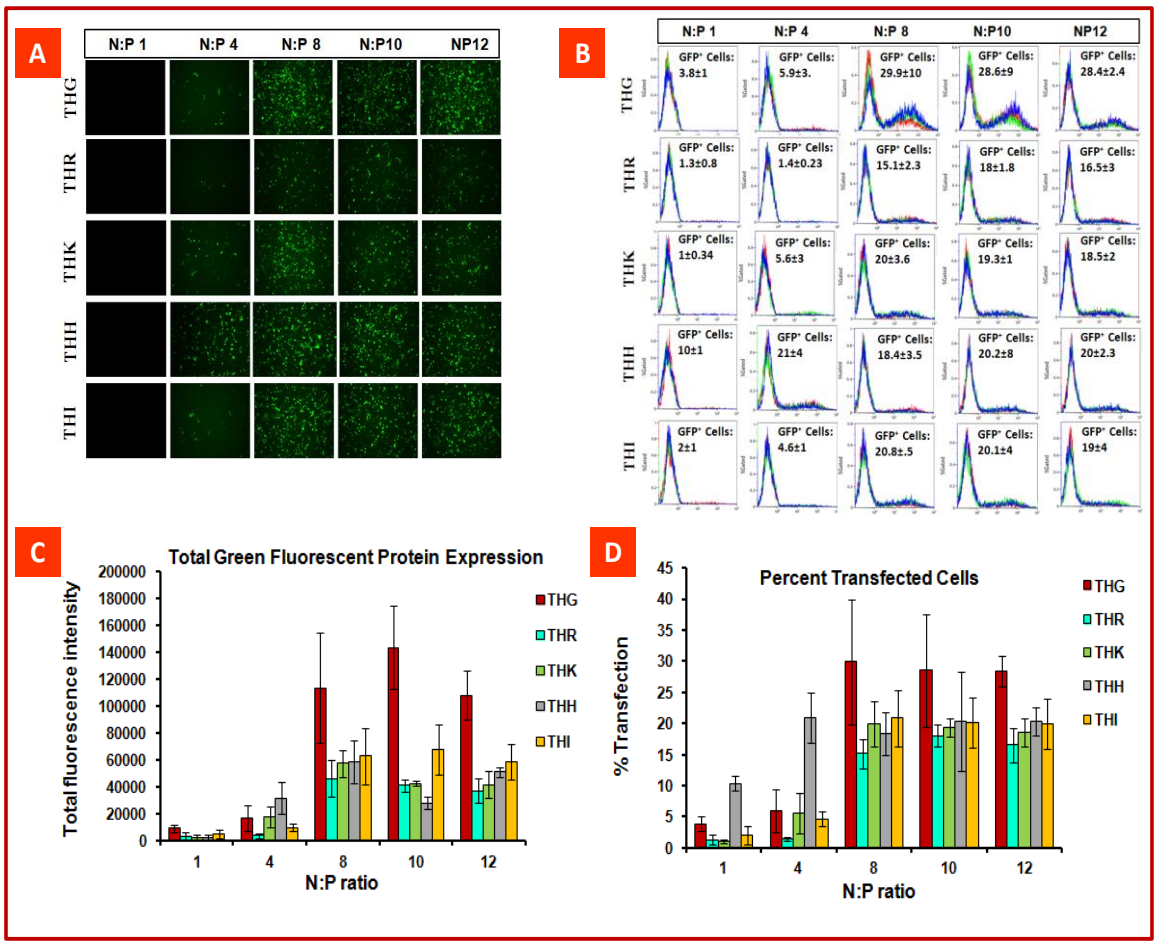

Figure 6.4: Comparison of transfection efficiency of all five biopolymers. A) epifluorescent microscope images of transfected SKOV-3 cells with different biopolymers at different N:P ratios. B) Flowcytometry plots of transfected GFP positive SKOV-3 cells with biopolymers at different N:P ratios. Each plot is the overlay of three independent replicates. C) A bar chart that quantitatively demonstrates total green fluorescence intensity of transfected SKOV-3 cells with biopolymer/pEGFP complexes. D) A bar chart that quantitatively demonstrates percent transfected cells with biopolymer/pEGFP complexes at different N:P ratios.

It is well-understood that the major factors that may affect transfection efficiencies of vectors are particle size and charge, lytic activity of the fusogenic peptides in the vector structure, particle shape, and vector related toxicity. To better understand the reason behind this observation, we examined the above mentioned factors one by one. The results of particle size and charge analysis **(Figure 6.3)** have already shown us that there are no significant differences in terms of surface properties among the nanoparticles (i.e., particle size and charge). Therefore, these two factors could not be a major contributor to the observed significant difference in transfection efficiency. Next, we investigated the ability of the FPs in the biopolymers' structures to lyse cell membranes at low pH. Because all five biopolymers are targeted and can enter SKOV-3 cells via receptor mediated endocytosis, they would end up inside endosomes. Therefore, it is important for fusogenic peptides in the biopolymers to be able to interact with endosomal membranes and disrupt their integrity facilitating their escape into cytosol. We performed a hemolytic assay to examine the fusogenic activity of the biopolymers at physiologic pH 7.4 and low endosomal pH 5.5. The results of this study showed that at pH 5.5 and in comparison to THG, the THH had slightly higher hemolytic activity (*t-test*, p=0.047) and THI slightly lower (*t-test*, p=0.044). THR and THK had statistically similar hemolytic activity as THG (*t-test*, p>0.05) **(Figure 6.5)**. At pH 7.4, the hemolytic activities of all biopolymers were negligible.

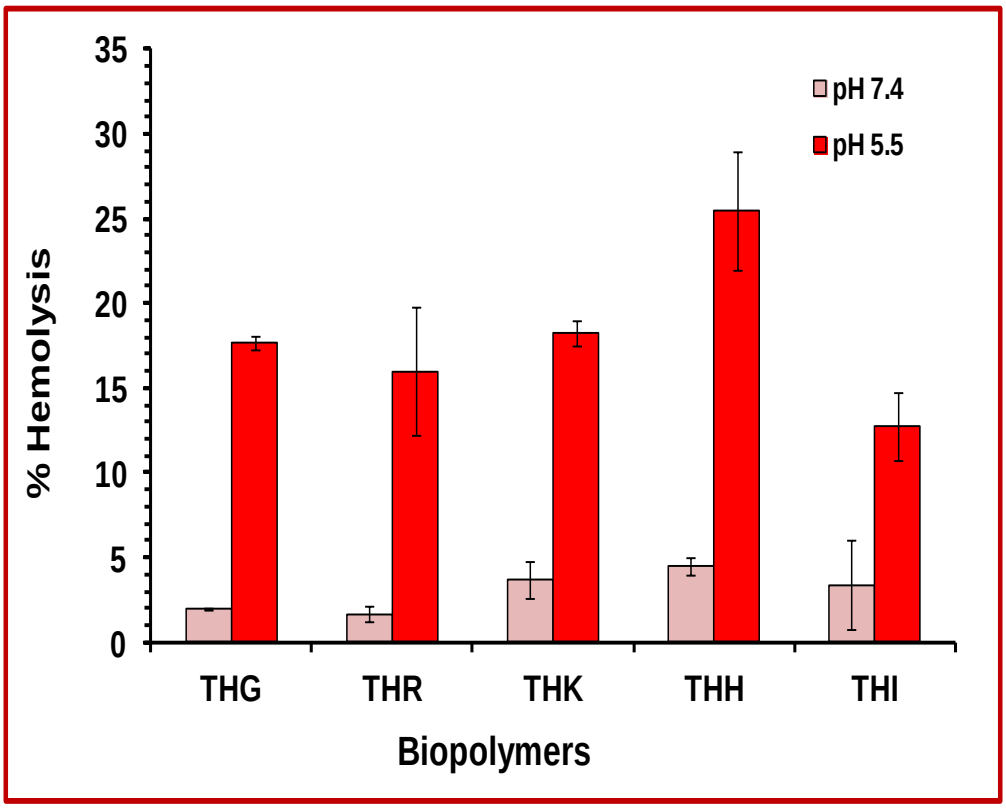

Figure 6.5: Hemolytic activity of THG, THR, THK, THH and THI biopolymers at two different

This was an interesting observation because it shows that even though THH has a slightly better ability to disrupt membranes, its capability to transfect cells is not as high as that for THG. The slightly higher hemolytic activity of THH in comparison to other biopolymers was somewhat expected as it has been previously reported that H5WYG can disrupt membranes via both fusogenic activity and proton sponge effect.[147] However, it is worth mentioning that in our previous studies we have demonstrated that the fusogenic activity of the H5WYG plays a significantly higher role in endosome membrane disruption than its proton sponge effect.[156] Nonetheless, these two additive effects may have contributed to higher rate of THH hemolytic activity in comparison to other biopolymers.

In the next step, to examine whether the escape of biopolymer/pEGFP nanoparticles was pH-dependent, we performed a cell transfection study in the presence of bafilomycin A1. This drug is an inhibitor of the vacuolar ATPase endosomal protein pump.[157] If the nanoparticles entered endosomes, then the inhibition of this pump should reduce the release of the complexes into the cytosol and subsequent gene transfection efficiency. The results of this study illustrated that a low pH was necessary for endosomal escape, as a significant decrease in gene expression was observed for biopolymers when cells were treated with bafilomycin at the time of transfection ($p<0.05$) **(Figure 6.6)**. In addition, transfection in the presence of chloroquine (endosomolytic agent) did not increase transfection efficiency indicating that the nanoparticles could effectively escape from the endosomes **(Figure 6.6)**. In this study, we treated all FPs equally and positioned them at the C-terminal ends of biopolymers followed by fusion with histag. In literature it has been mentioned that the influenza virus fusogenic peptide and some of its synthetic

derivatives such as INF-7 and 5HWYG may need to have a free N-terminal end for efficient membrane fusion.[145,147,158] The results of transfection in the presence of chloroquine suggests that the FP free N-terminal end requirement may not be applicable to vector/pDNA nanocomplexes where each particle contains thousands of copies of FPs; thereby, compensating for any potential deficiencies.[145,159] For example, in the past we have demonstrated that regardless of positioning at the N- or C-terminal, 5HWGY is able to help nanoparticles escape from endosomes efficiently. [156,160] While position of FP in the vector structure could potentially impact its fusogenic activity but nanoparticles that contain thousands of FPs in their makeup may efficiently escape from endosomes due to their cooperative activities. Nonetheless, the developed biopolymeric platform allows us to position FPs at any location in the biopolymer structure depending on the needs of a study and examine the outcomes.

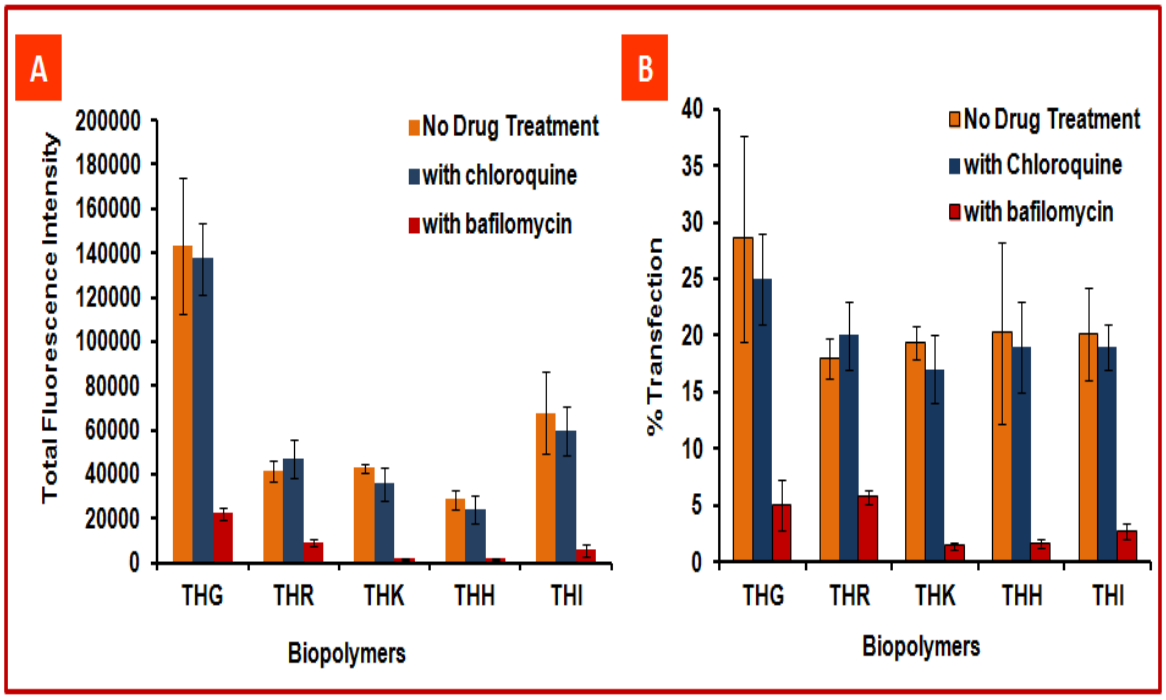

Figure 6.6: A) total green fluorescent protein expression in SKOV-3 cells transfected with biopolymers at N:P 10 in the presence and absence of bafilomycin and chloroquine. B) Percent SKOV-3 cells transfected with biopolymers at N:P 10 in the presence and absence of bafilomycin and chloroquine.

This observation along with the results of the hemolytic assay indicates that biopolymers could effectively disrupt endosome membranes at low pH and escape into cytosol. However, it was still unclear why THG had a significantly higher rate of cell transfection.

We further examined the shape of the nanoparticles created as a result of biopolymer complexation with pEGFP because it has previously been shown that particle geometry significantly affects nanoparticle uptake.[161] Using TEM, the shape of the nanoparticles was studied and it was observed that all biopolymers condensed pEGFP into spherical and somewhat similar floccus nanoparticles **(Figure 6.7)**. Therefore, the differences in transfection efficiencies may not be related to the differences in nanoparticle's geometry. The polydispersity index of the biopolymer/pDNA nanocomplexes at N:P 10 was also measured by dynamic light scattering technique and no significant differences among groups were observed ($p>0.05$)

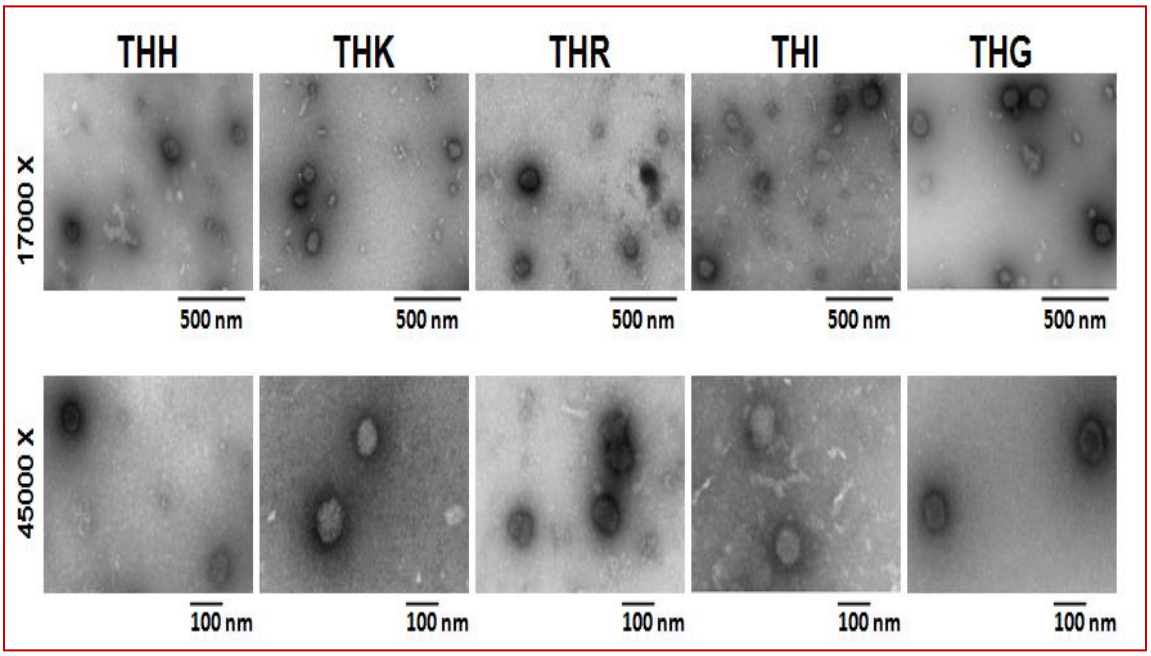

Figure 6.7: Transmission electron microscopy of the negatively stained nanoparticles formed as a result of complexation of THH, THK, THR, THI and THG biopolymers with pEGFP at N:P 10.

Learning that the nanoparticle shape in this case may not have played a significant role in nanoparticle uptake or release from endosomes, we then hypothesized that perhaps different FPs have different cell toxicity profiles and the observed differences in transfection efficiencies could have been influenced by biopolymer toxicities. This hypothesis was formulated based on the results of the biopolymer production studies in E.coli. To examine this hypothesis, a cell toxicity assay was performed to evaluate the impact of biopolymer/pEGFP complexes on SKOV-3 cells viability. The results of this study revealed that the biopolymers with negatively charged FPs (GALA and INF7) had no significant impact on cell viability while the biopolymers with cationic FPs (THH, THK and THR) showed significant toxicity ($p<0.05$) **(Figure 6.8)**.

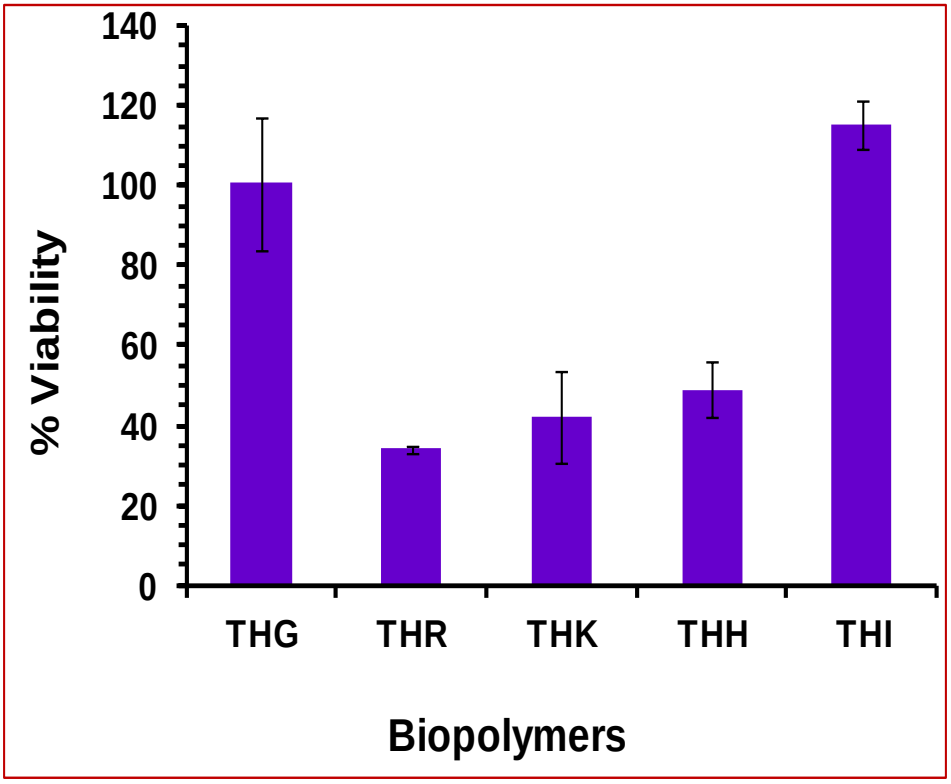

Figure 6.8: cell viability assay for SKOV-3 cells treated with biopolymer/pEGFP complexes at N:P 10. The data is normalized to the viability of untreated cells considered as 100% viable.

While the exact mechanism of cell toxicity for KALA, RALA and H5WYG are unclear, but their toxicity could be due to their sequence similarity to cationic antimicrobial peptides which are generally composed of cationic and lipophilic residues with α-helical β-sheet, loop, or extended peptide structures.[162,163] The cell toxicity of such peptides is attributed to their binding to negatively charged proteins in the cell membrane and disruption of the membrane's integrity.[163] It is also noteworthy that the cytotoxicities of 5HWYG, INF-7 and GALA alone are not reported in literature as such neutral to negatively charged peptides are unable to interact with cell membranes independently and internalize. To evaluate the cytotoxcity of these peptides, a carrier such as the biopolymer shown in this study is required to facilitate their internalization allowing a side-by-side comparison study. Overall, it appears that negatively charged FPs are safer to use as endosomolytic agents in the structure of gene delivery systems. While both THG and THI facilitated endosomal escape efficiently as illustrated in **Figure 6.6** (with chloroquine), but observation of the higher rate of transfection efficiency with THG in comparison to THI (without chloroquine) suggests that perhaps pDNA could be released from THG much easier than THI for transcription in the nucleus. One may speculate that presence of seven negatively charged residues in GALA may have participated in more efficient pDNA release in comparison to INF7 which contains five negatively charged residues in its sequence. Nonetheless, other more complex explanations could be involved with this process which opens the door for more mechanistic studies to shed light on the ambiguities of the impact of FP sequence on efficient gene transfer.

6.3 Conclusion

The results of side by side comparison studies suggest that among the five tested constructs, GALA is the most suitable pH-responsive endosomolytic peptide for enhancing the efficiency of gene delivery systems due to its high endosomolytic activity and lower cytotoxicity. After selecting the best candidate for the fusogenic peptide, we decided to make more modifications on our recombinant vector to improve its efficacy. There are some other strategies which are claimed to be able to improve transfection efficiencies. Cell penetrating peptides and receptor mediated targeting are among the popular approaches which can facilitate cell internalization. In the next step we utilized the above mentioned approaches to examine whether or not they can improve efficiency and toxicity profile of our previously developed recombinant vector.

Chapter 7

Vector Design for Efficient and Safe Gene Delivery to Stem Cells

Stem cells have opened a new window into targeted cancer therapy owing to their unique properties. Their intrinsic tumor tropism along with active penetration into deep sites of the tumor and low immunogenicity tailors them for tumor targeted gene delivery[3]. The vector that is used for stem cell transfection needs to be highly efficient as stem cells in cell culture change or differentiate over time[5]. An efficient vector is able to mitigate the number of passages that is needed to reach the sufficient number of transfected cells which subsequently results in decreasing the in vitro incubation time and probability of change in stem cell properties. In addition to being highly efficient, transfection vectors need to be non-toxic to stem cells; otherwise, it diminishes cell viability during transfection and could potentially transform normal stem cells into cancer initiating cells (CICs) and result in tumor formation.

In order to develop an efficient and safe vector for MSCs transfection, in the first step as it was discussed in chapter six, we employed the recombinant vector previously developed in our lab to compare the fusogenic peptides from different categories. Among all GALA, classified as an anionic fusogenic peptide, was selected as the most efficient one. In the second step that is discussed in more detail in this chapter we decided to make some other modifications on our recombinant vector to evaluate whether these modifications are able to improve its efficiency and cell viability in MSCs transfection.

To achieve this goal, two types of recombinant vectors were prepared: targeted and non-targeted. The targeted vectors are composed of four repeating units of histone H2A to condense DNA, a pH-dependant endosomolytic fusogenic peptide (GALA), and a VEGFR targeting peptide[164]. The reasons behind selecting VEGFR among all various types of receptors are: 1) this receptor is overexpressed on the surface of stem cells and

can facilitate the uptake of the recombinant vector-DNA complexes via receptor mediated endocytosis, 2) VEGFR agonists play a role in protecting stem cells from damage and keeping them healthy, therefore it may not only increase the transfection efficiency but also diminish cytotoxicity, 3) since VEGFR agonists can induce stem cell proliferation, VEGFR targeting could enhance transfection efficiency as the nuclear membrane dissolves during mitosis[165]. Moreover, VEGFR antagonist is also included in this study as the control in order to evaluate the potential positive and negative effects of the sequences on transfection efficiency and cell viability[166].

The non-targeted vectors are consisting of the same motifs as mentioned above but instead of VEGFR targeting peptide contain cell penetrating peptides. Cell-penetrating peptides (CPPs) are among the most promising tools for delivering biologically active molecules into cells. It is broadly reported in the literature that they can overcome intracellular and extracellular barriers and improve delivery of various biomolecules, such as plasmid DNA, proteins and peptides, as well as liposome nanoparticles[167,168]. CPPs are able to facilitate internalization of the vector through stem cell wall. Among most commonly used cell penetrating peptides Pep-1 and MPG were selected. Pep-1 is a tryptophan-rich peptide with high affinity for membranes and MPG is derived from the fusion sequence of the HIV glycoprotein 41[167]. There are four reasons behind choosing these two penetrating peptides among all the ones reported in the literature: 1) non-cationic nature, 2) high efficiency in membrane fusion and cell penetration, 3) low cytotoxicity, and 4) proven ability to enhance transfection efficiency of vectors[169,170]. As it is reported in the literature that these penetrating peptides facilitate cell penetration through direct translocation and not endocytosis dependent pathways, two more

constructs of Pep-1 and MPG was included in this study by elimination of the GALA from the construct in order to get more information regarding their internalization mechanism[170].

All of these constructs were designed, produced and characterized. Then transfection efficiency and cytotoxicity of them on AD-MSCs were evaluated and compared with the recombinant vector without any targeting motif or cell penetrating peptide.

7.1 Methods and Materials

7.1.1 Cloning and Expression of the Recombinant Vectors

The genes encoding 4HG, Pep 1-4H, Pep 1-4HG, MPG-4H, MPG-4HG, $VEGFR_{Ago}$-4HG and $VEGFR_{Anta}$-4HG with C-terminal histags were designed by our group and synthesized by Integrated DNA Technologies (Coralville, IA). A C-terminal NdeI and N-terminal XhoI restriction sites were also designed for cloning purposes. The synthesized genes were double digested with NdeI and XhoI restriction enzymes (New England Biolabs, Ipswich, MA) and cloned into the pET21b expression vector (Novagen, Billerica, MA). After verification by DNA sequencing, each construct was transformed into an Escherichia coli expression host for production. Plasmids encoding 4HG, Pep 1-4H, Pep 1-4HG, $VEGFR_{Ago}$-4HG and $VEGFR_{Anta}$-4HG were transformed into E. coli BL21(DE3) pLysS (Novagen, Billerica, MA), and those encoding MPG-4H and MPG-4HG were transformed into E. coli BL21AI (Invitrogen, Life Technologies, Grand Island, NY).

For 4HG, Pep 1-4H, Pep 1-4HG, VEGFRAgo-4HG and VEGFRAnta-4HG expression, starter cultures were prepared by inoculation of a single fresh colony of

BL21(DE3) pLysS harboring expression plasmids in 5 mL of LB medium containing 50 μg/mL carbenicillin incubated at 37 °C overnight. The next day, 5 mL of the starter culture was used to inoculate 500 mL of Circlegrow medium (MP Biomedicals) containing 50 μg/mL carbenicillin. The culture was grown at 37 °C for 3 h to reach the OD600 of 1.2. Gene expression was induced by isopropyl β-D-1-thiogalactopyranoside (IPTG) 1 mM at 37 °C. The cells were harvested after 4 h by centrifugation at 5000g for 20 min. For MPG-4H and MPG-4HG production, starter cultures were prepared by inoculation of a single fresh colony of BL21AI harboring expression plasmids in 5 mL of LB medium containing 50 μg/mL carbenicillin incubated at 37 °C overnight. The next day, 5 mL of the starter culture was used to inoculate 500 mL of Circlegrow medium (MP Biomedicals) containing 50 μg/mL carbenicillin. The culture was grown at 37 °C for 3 h to reach the OD600 of 1.2. Gene expression was induced by IPTG 1 mM and L-arabinose 0.2% at 37 °C. The cells were harvested after 2 h by centrifugation at 5000g for 20 min

7.1.2 Purification of Recombinant Vectors

All recombinant vectors were purified using Ni-NTA affinity chromatography. The cell pellets were suspended in lysis buffer (urea 8 M, NaCl 2 M, NaH2PO4 100 mM, Tris 10 mM, Triton 1%, imidazole 10 mM) and stirred for 30 min. The lysates were centrifuged at 37000g for 1 h to sediment the insoluble fractions. The supernatant was transferred to another tube and incubated with Ni-NTA resins equilibrated with lysis buffer for 1 h with gentle shaking on ice. The resins were loaded onto a column and first washed with 70 mL of lysis buffer and then 45 mL of wash buffer (urea 5 M, NaCl 1.5 M, NaH2PO4 100 mM, Tris 10 mM, imidazole 40 mM) to remove the impurities.

Finally, the peptides were eluted with elution buffer (urea 3 M, NaCl 0.5 M, NaH2PO4 100 mM, Tris 10 mM, imidazole 200 mM). The purity of the recombinant vectors were analyzed by SDS−PAGE.

7.1.3 Particle Size and Charge Analysis

Prior to use in experiments, the purified biopolymer solutions were desalted. The G-25 Sepharose column (GE Heathcare) was first conditioned with HEPES buffer (100 mM, pH 7.4) and then loaded with the peptide solution. The elute fractions were collected, and the final concentrations of the desalted biopolymers were measured by Bradford method.

Different amounts of each biopolymer were mixed with 0.5 μg of pEGFP (plasmid encoding green fluorescent protein) to make nanoparticles at N:P ratios (the ratio of positive nitrogen atoms in biopolymer to negative phosphate groups in pDNA) of 1, 4, 8, 10, 12 and 16. Therefore, for preparation of nanoparticles at N:P 1, 1.45 μg of 4HG, 1.2 μg of Pep 1-4H, 1.6 μg of Pep 1-4HG, 1.1 μg of MPG-4H, 1.48 μg of MPG-4HG, 1.57 μg of $VEGFR_{Ago}$-4HG and 1.74 μg of $VEGFR_{Anta}$-4HG was used to complex with 0.5 μg of DNA. Desired amounts of biopolymer and pEGFP were diluted each to 50 μL with HEPES buffer (100 mM pH 7.4) in separate tubes. Nanoparticles were formed by addition of biopolymer to pEGFP solution. Nanoparticles were incubated at room temperature for 5 min before measurement of particle size and surface charge using Nano-ZS Zetasizer (Malvern Instruments, U.K). Three independent batches for each N:P ratio were prepared, and the results are presented as mean ± SD (n = 3).

7.1.4 Particle Shape Analysis by Transmission Electron Microscopy

To study the shape of the nanoparticles, one drop of sample was put on a carbon type B coated copper grid (Ted Pella, Redding, CA, USA) for 5 min. The sample was dried, and the grid was stained for 2 min with 1% sodium phosphotungstate solution. The grids were imaged using transmission electron microscope (1200EX electron microscope, JEOL, USA) at RUMDNJ TEM core imaging facility.

7.1.5 Transfection of Stem Cells by Recombinant Vectors

AD-MSCs (Lonza) were seeded in 24-well plate at 12000 cells/well and incubated overnight at 37 °C to reach ca. 80% confluency. At the time of transfection, the old medium was removed and replaced with 200 μL of ADSC growth medium supplemented with insulin, transferrin, selenium, dexamethasone, and fibronectin and incubated at 37 °C for 1 h. Each recombinant vector was complexed with 1 μg of pEGFP at N:P ratios of 8, 10, and 12 to form nanoparticles. They were then added to each well in total volume of 50 μl and incubated with AD-MSCs. After three hours of incubation, the medium was removed and replaced with 500 μL of ADSC growth medium supplemented with 10% FBS.

To visualize green fluorescent protein (GFP) expression, an epifluorescent microscope (Olympus, USA) was used. To prepare the samples for FACS analysis, cells were trypsinized in each well and, after detachment and neutralization, collected by centrifugation at 300g for 6 min. The supernatant was removed, and formaldehyde at 2% in PBS was added to fix the cells. Then, a F500 flow cytometer (Beckman Coulter, USA) was used to measure percent transfected cells as well as GFP expression (transfection efficiency). Each time, 1000 cells were counted and the total fluorescence intensity of

positive cells was normalized against the total fluorescence intensity of untransfected cells (background control). The data are presented as mean ± SD (n = 3).

7.1.6 Cell Viability Assay for Stem Cells Transfected with Recombinant Vectors

For WST-1 assay AD-MSCs were seeded in 24-well plates at 12000 cells/well. 4HG construct was complexed with 1 μg of pEGFP and used to transfect AD-MSCs as mentioned above. After 24 h incubation, WST-1 reagent was added to the cells. Cytotoxicity was evaluated by measuring the absorbance of each well at 450 nm after 3 hours. The absorbance of untransfected cells was considered as %100 viable. Data are reported as mean ± SD (n = 3).

7.2 Results and Discussion

To develop a more efficient and less toxic vector for stem cell transfection we designed and developed seven different recombinant vectors. The constructs and amino acid sequence of each is depicted in **Figure 7.1**. We then characterized them in terms of particle size and charge, particle morphology, transfection efficiency and toxicity.

4HG Insert: NdeI-4HP-GALA-Hisx6-XhoI

MSGRGKQGGKARAKAKTRSSRAGLQFPVGRVHRLLRKSGRGKQGGKARAKAKTRSSRAGLQFPVGRVHRLLR
KGSRGKQGGKARAKAKTRSSRAGLQFPVGRVHRLLRKSGRGKQGGKARAKAKTRSSRAGLQFPVGRVHRLLR
KGGGWEAALAEALAEALAEHLAEALAEALEALAAHHHHHH

PEP 1-4H Insert: NdeI-PEP1-4HP-Hisx6-XhoI

MMKETWWETWWTEWSQPKKRKVSGRGKQGGKARAKAKTRSSRAGLQFPVGRVHRLLRKSGRGKQGGKAR
AKAKTRSSRAGLQFPVGRVHRLLRKGSRGKQGGKARAKAKTRSSRAGLQFPVGRVHRLLRKSGRGKQGGKAR
AKAKTRSSRAGLQFPVGRVHRLLRKGGGHHHHHH

PEP 1-4HG Insert: NdeI-PEP1-4HP-GALA-Hisx6-XhoI

MMKETWWETWWTEWSQPKKRKVSGRGKQGGKARAKAKTRSSRAGLQFPVGRVHRLLRKSGRGKQGGKAR
AKAKTRSSRAGLQFPVGRVHRLLRKGSRGKQGGKARAKAKTRSSRAGLQFPVGRVHRLLRKSGRGKQGGKAR
AKAKTRSSRAGLQFPVGRVHRLLRKGGGWEAALAEALAEALAEHLAEALAEALEALAAHHHHHH

MPG-4H Insert: NdeI-MPG-4HP-Hisx6-XhoI

MGALFLGFLGAAGSTMGAWSQPKKKRKVSGRGKQGGKARAKAKTRSSRAGLQFPVGRVHRLLRKSGRGKQGG
KARAKAKTRSSRAGLQFPVGRVHRLLRKGSRGKQGGKARAKAKTRSSRAGLQFPVGRVHRLLRKSGRGKQGG
KARAKAKTRSSRAGLQFPVGRVHRLLRKGGGHHHHHH

MPG-4HG Insert: NdeI-MPG-4HP-GALA-Hisx6-XhoI

MGALFLGFLGAAGSTMGAWSQPKKKRKVSGRGKQGGKARAKAKTRSSRAGLQFPVGRVHRLLRKSGRGKQGG
KARAKAKTRSSRAGLQFPVGRVHRLLRKGSRGKQGGKARAKAKTRSSRAGLQFPVGRVHRLLRKSGRGKQGGK
ARAKAKTRSSRAGLQFPVGRVHRLLRKGGGWEAALAEALAEALAEHLAEALAEALEALAAHHHHHH

$VEGFR_{AGO}$-4HG INSERT: NdeI-$VEGFR_{AGO}$-Linker-4HP-GALA-Hisx6-XhoI

MKLTWQELYQLKYKGIGGGSGGGSGGGSGRGKQGGKARAKAKTRSSRAGLQFPVGRVHRLLRKSGRGKQGG
KARAKAKTRSSRAGLQFPVGRVHRLLRKGSRGKQGGKARAKAKTRSSRAGLQFPVGRVHRLLRKSGRGKQGG
KARAKAKTRSSRAGLQFPVGRVHRLLRKGGGWEAALAEALAEALAEHLAEALAEALEALAAHHHHHH

$VEGFR_{ANTA}$-4HG Insert: NdeI-$VEGFR_{ANTA}$-Linker-4HP-GALA-Hisx6-XhoI

MNGYEIEWYSWVTHGMYGGGSGGGSGGGSGRGKQGGKARAKAKTRSSRAGLQFPVGRVHRLLRKSGRGKQ
GGKARAKAKTRSSRAGLQFPVGRVHRLLRKGSRGKQGGKARAKAKTRSSRAGLQFPVGRVHRLLRKSGRGKQ
GGKARAKAKTRSSRAGLQFPVGRVHRLLRKGGGWEAALAEALAEALAEHLAEALAEALEALAAHHHHHH

Figure 7.1: Amino acid sequence of recombinant vectors designed and developed for MSC transfection.

First, the genes encoding the recombinant vectors were constructed and cloned into the pET21b expression vector. The cloned vectors were then transformed into suitable expression hosts (i.e., BL21AI or BL21(DE3) pLysS) for expression. All constructs were expressed as soluble proteins and purified. SDS-PAGE confirmed the expression and purity of biopolymers after Ni-NTA affinity chromatography **(Figure 7.2)**.

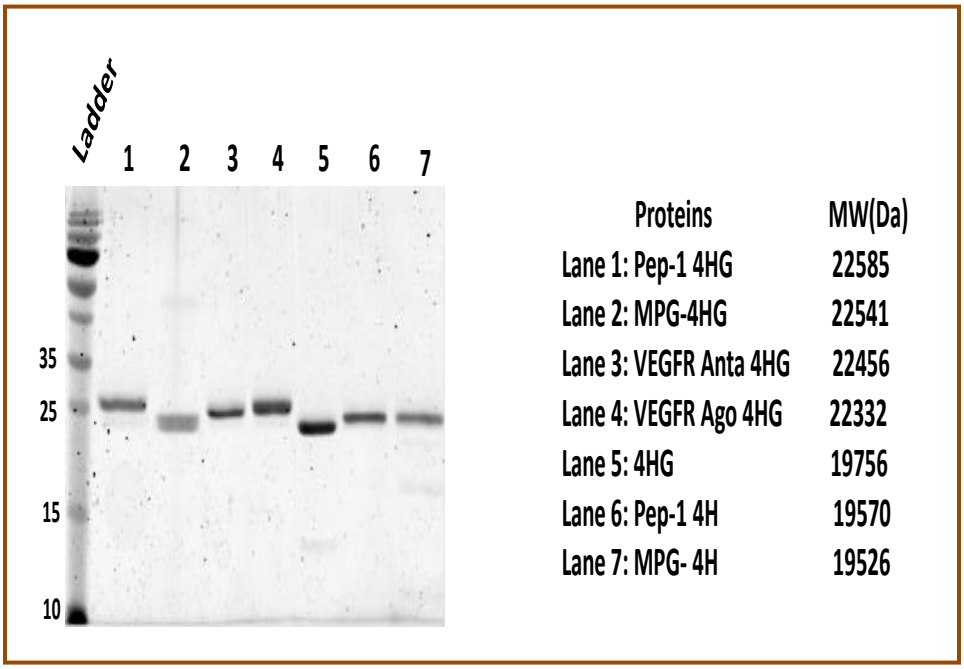

Figure 7.2: SDS PAGE of the purified recombinant vectors.

In the next step, all seven recombinant vectors were desalted to remove the excess salt. To examine the ability of the vectors to condense pDNA into nanosize particles, they were used to complex with pEGFP at various N:P ratios, which were then characterized in terms of hydrodynamic particle size and charge **(Figure 7.3)**. The results of this study revealed that the sizes of the nanoparticles formed at N:P ratios of 8, 10, 12, and 16 were below 100 nm in HG constructs. It is noteworthy that nanoparticles in this size range (<150nm) are known to be suitable for receptor mediated endocytosis as they can fit into clathrin-coated vesicles[35]. In contrast, H constructs i.e. Pep 1-4H and MPG-4H demonstrated higher size range. GALA is an anionic fusogenic peptides bearing negative charges on its surface, hence it cannot participate in condensing DNA. However it appears that is can mediate forming smaller nanoparticles through some other interactions.

The results of the zeta potential study revealed that the nanoparticles' surface charge increased to a stable ca. +6 mV for Pep-1 constructs and ca. +10 to +12 mV for the rest of the constructs at N:P ratios 8 or higher **(Figure 7.3).** It has been reported that as the nanoparticle's surface positive charge increases (>+20mV), the potential for genetic aberrations (genotoxicity) enhances[171]. This could become notably problematic when dealing with stem cells because they could potentially transform into cancer initiating cells (CIC).

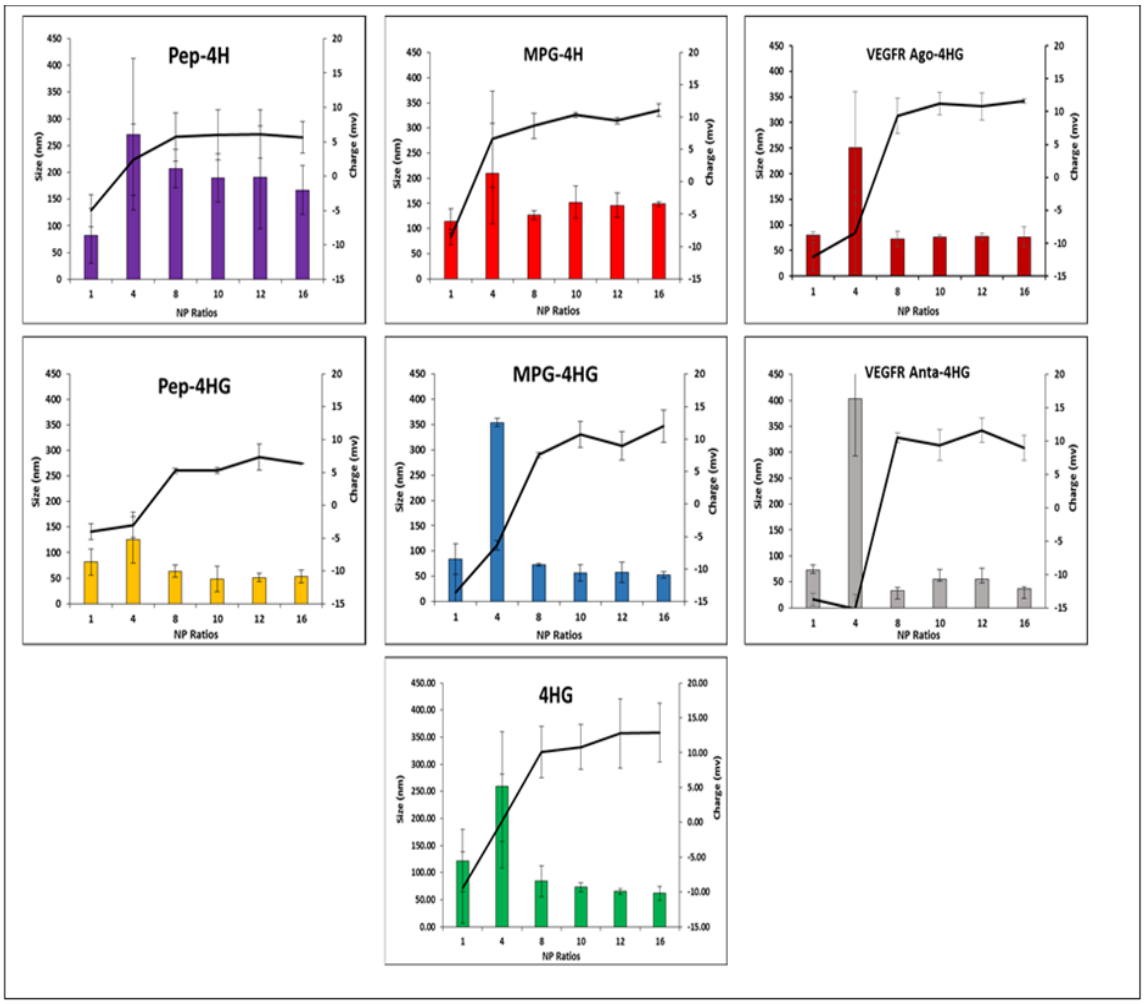

Figure 7.3: Particle size and charge analysis of recombinant vectors in complexation with pEGFP at various N:P ratios.

We further examined the shape of the nanoparticles created as a result of recombinant vectors complexation with pEGFP because it has previously been shown that particle geometry significantly affects nanoparticle uptake. Using TEM, the shape of the nanoparticles was studied and it was observed that all biopolymers condensed pEGFP into spherical and somewhat similar floccus nanoparticles **(Figure 7.4)**. Therefore, the differences in transfection efficiencies may not be related to the differences in nanoparticle's geometry.

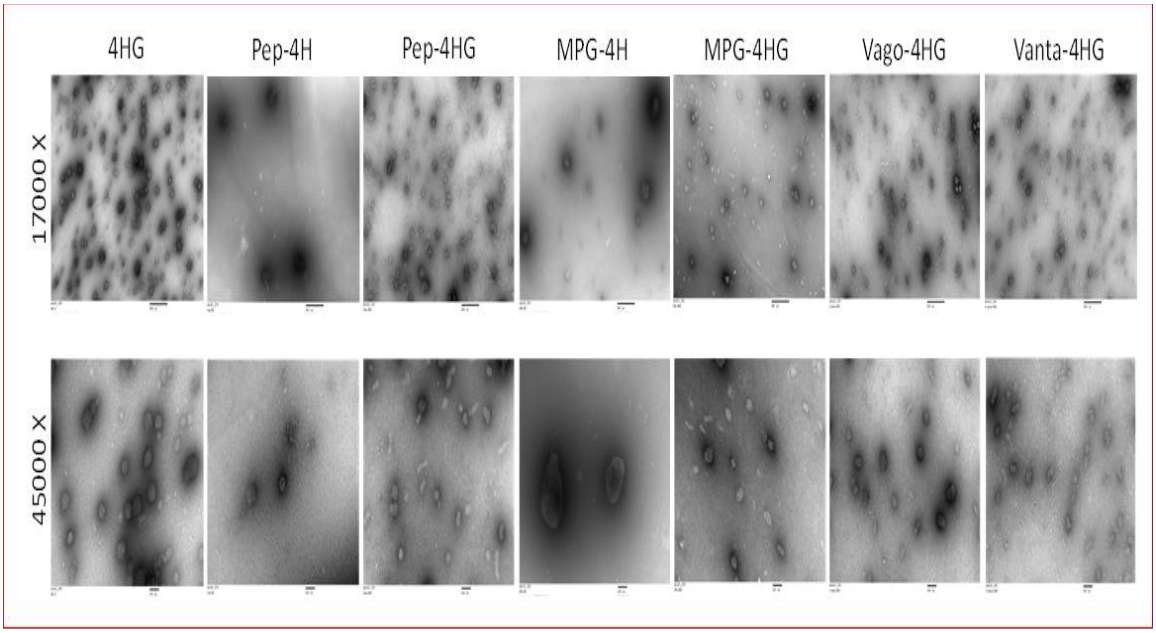

Figure 7.4: Transmission electron microscopy of the negatively stained nanoparticles formed as a result of complexation of recombinant vectors with pEGFP at N:P 10.

We then investigated the ability of all seven recombinant vector/pEGFP nanocomplexes to internalize and transfect AD-MSCs. In order to find the N:P ratio at which the nanoparticles have the highest rate of transfection efficiency, we transfected AD-MSCs cells with recombinant vectors/pEGFP complexes at N:P ratios of 8, 10 and 12. The transfection efficiency was evaluated in the first step by epiflouorescence microscopy **(Figure 7.5)**. The images demonstrated no fluorescence signal for Pep 1-4H and MPG-4H constructs meaning that these two vectors were not able to make any transfection in the absence of GALA. Although all the HG constructs showed some fluorescence signal, it was very low in Pep 1-4HG and $VEGFR_{Ago}$-4HG as depicted in Figure 7.5. Therefore, only 4HG, MPG-4HG and $VEGFR_{Anta}$-4HG that showed higher signal were prepared for FACS study. It is reported in the literature that the mechanism through that MPG and Pep-1 deliver their cargo does not involve the endosomal pathway and therefore obviates them from endosomolytic agents[167]. It was in conflict with our study as we did not observe any transfection in Pep 1-4H and MPG-4H constructs, whereas there were some in Pep 1-4HG and MPG-4HG. Our study revealed that in our recombinant vectors Pep-1 and MPG are not able to penetrate via endocytosis independent pathways and they need fusogenic peptides such as GALA which can facilitate endosomal escape. It worth to emphasize that different cellular uptake mechanism are reported for CPPs in different studies. However, for most CPPs, the cellular uptake mechanism is still controversial and needs to be confirmed, partly due to the fact that different methods, which are carried out in different labs, have been utilized for this purpose. In most of the cases the tracking of CPPs inside the cell is based on fluorescein-labelled CPPs with the probability that fluorescent label may alter the uptake

mechanism or stimulate an unusual cell entry pathway[172]. Particle size, molar ratio of the CPP/cargo and the procedure to prepare the cargo are among the factor altering the penetration pathway[167].

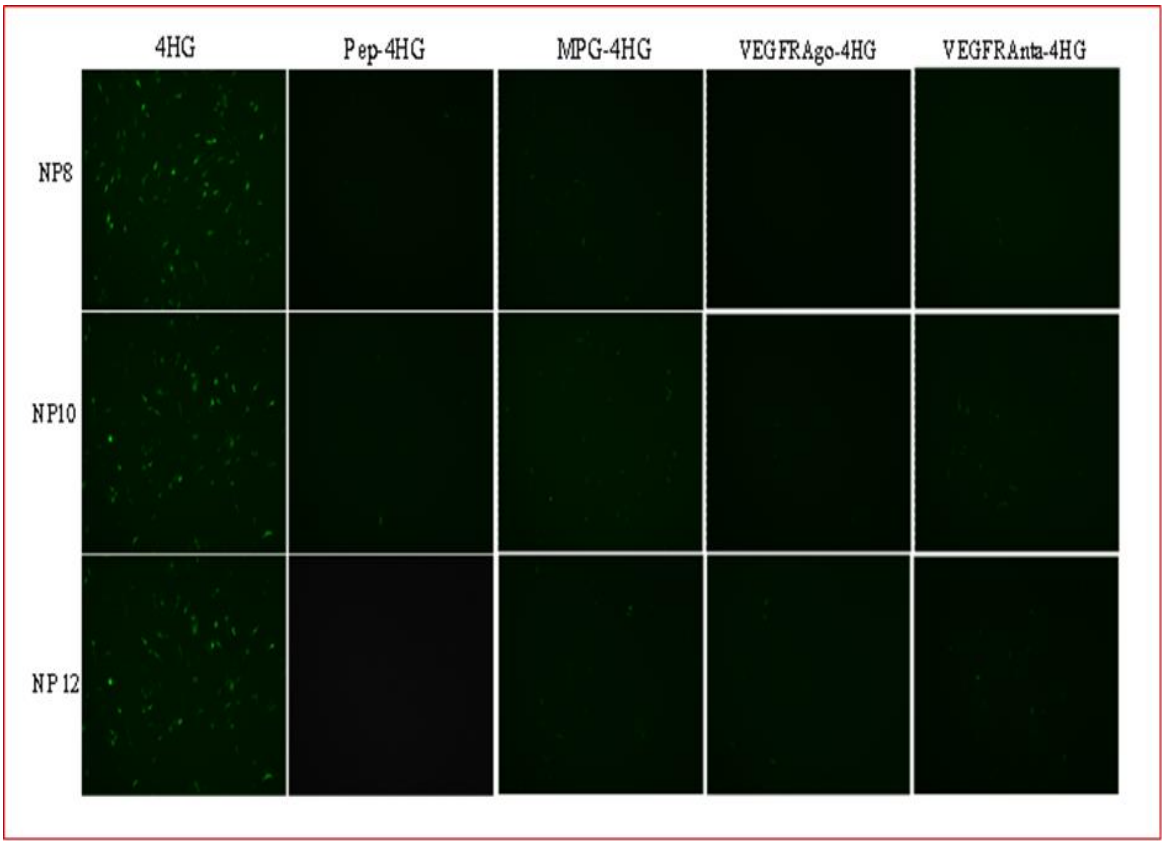

Figure 7.5: Epifluorescence images of AD-MSCS transfected with 4HG, Pep-4HG, MPG-4HG, VEGFRAgo-4HG and VEGFRAnta-4HG complexed with pEGFP in NP 8, 10 and 12.

As illustrated in the graph plotted by using FACS data, 4HG showed the highest transfection efficiency with total fluorescence intensity (TFI) of ca. 27000 to 32000 unit in different NP ratios which didn't have any significant difference with GeneIn^{TM} as the most efficient commercial transfection reagent **(Figure 7.6)**. In contrast, MPG-4HG and $VEGFR_{Anta}$-4HG displayed lower than 5000 unit TFI in different NP ratios that was in accordance with the epifluorescence pictures.

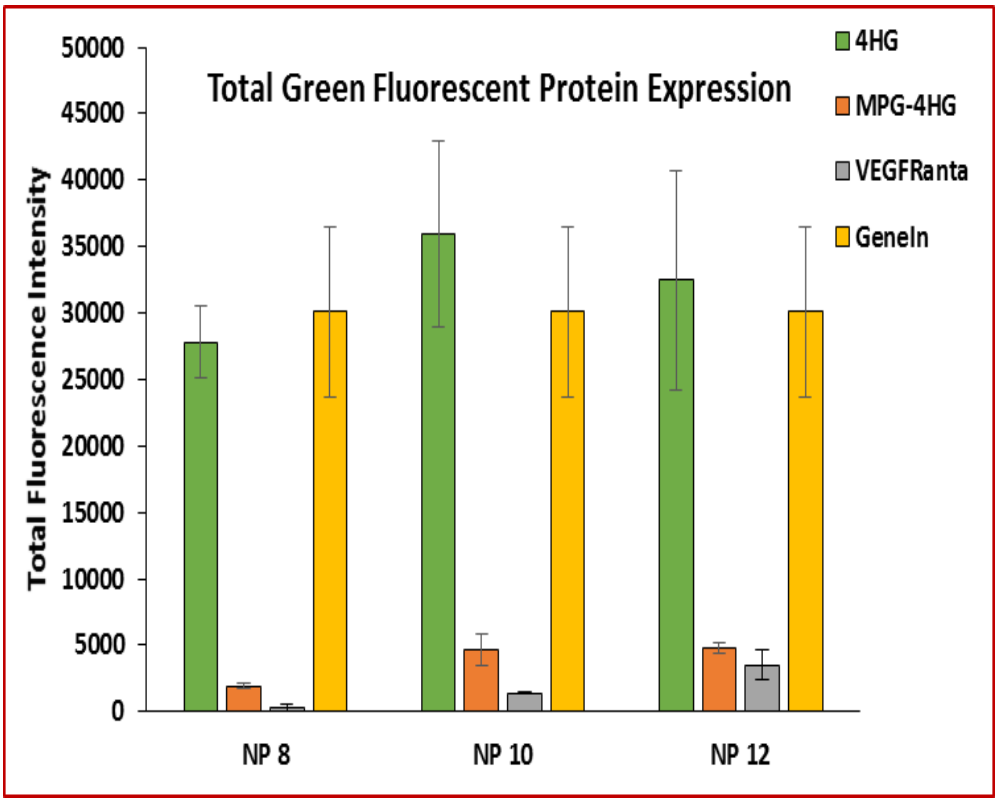

Figure 7.6: Quantitatively demonstration of total green fluorescence intensity of transfected AD-MSCs with recombinant vector/pEGFP complexes by use of FACS study.

As it is depicted in the figure 7.5 and 7.6, addition of Pep-1 and MPG penetrating peptides to our recombinant vector has mitigated its transfection efficiency dramatically. Given that the appearance of the cells after transfection with the constructs containing CPPs resembles healthy cells this drop could not be due to the cytotoxicity effect of penetrating peptides on the cells. The other point that might clarify this observation is both the fusogenic peptides such as GALA and penetrating peptides such as Pep-1 or MPG needs to acquire the right conformation to exert its biological effects. It is feasible that these two motifs have interference with each other in forming the right conformation and this issue has diminished their efficiency in constructs containing both the GALA and CPP.

We also developed a targeted recombinant vector containing $VEGFR_{Ago}$ as the targeting motif to facilitate vector internalization through receptor mediated endocytosis. VEGFR is overexpressed on the surface of MSCs and VEGFR agonists are able to increase proliferation of the cells. We speculated that this effect also might be advantageous to increase transfection as the nuclear membrane dissolves during mitosis. As the control we also included a construct that contains $VEGFR_{Anta}$ instead of $VEGFR_{Ago}$. As demonstrated in epifluorescence pictures and graph, transfection efficiency for both the agonist and antagonist constructs is very low relative to 4HG. While the efficacy of the $VEGFR_{Ago}$ sequence as a functional agonist is demonstrated in some studies[164,173], it appears it is not able to exert improving effect on the transfection efficiency of our recombinant vectors when produced as a part of a multifunctional single peptide.

Overall, 4HG displayed the highest transfection efficiency among all recombinant vectors. Its efficiency was not also significantly different from GeneIn™ that was selected as the most efficient commercial vector in our previous study. In the last step we examined the cytotoxicity effect of 4HG on AD-MSCs to see whether it is more or less toxic compared to GeneIn™.

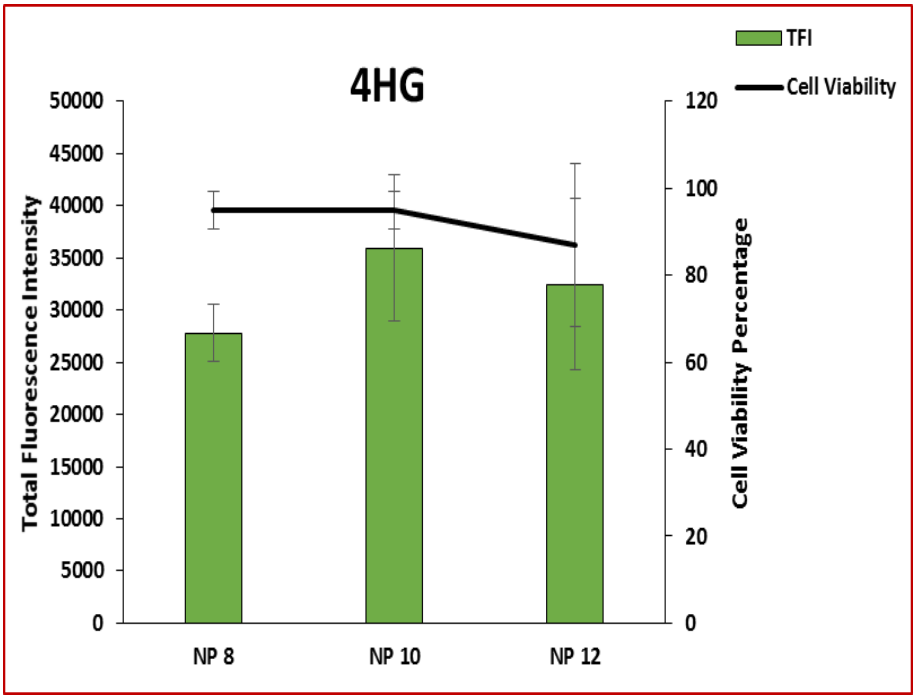

Figure 7.7: Total fluorescence intensity vs cell viability of AD-MSCs transfected with 4HG in different NP ratios.

As it is depicted in the graph, the highest transfection efficiency of 4HG at NP 10 is correlated to ca. 100% cell viability **(Figure 7.7)**. It appears that, in contrast to GeneIn™ which has cytotoxic effect on AD-MSCs in effective doses, 4HG is a safe vector for stem cell transfection.

7.3 Conclusion

We designed and developed different biopolymers for MSCs transfection by taking advantage of fusogenic peptides, penetrating peptides and receptor targeted motifs. The transfection and cytotoxicity studies revealed that 4HG consisting of four Histone H2A repeats as the DNA condensing motif and GALA as the fusogenic peptide is the most qualified candidate for MSCs transfection owing to its high efficiency and no toxicity. 4HG transfection efficiency was similar to GeneIn ™ as one of the most efficient commercial vectors; however; its significantly lower toxicity puts it in the higher level of eligibility compared to GeneIn™.

While metabolic activity assays such as WST-1 is one tool to evaluate toxicity but it does not tell the whole story. More in depth toxicity analysis is required to evaluate the true toxicity especially when the intension is to use stem cells as a tool for treating cancer. To date, there has been no comprehensive study that has closely looked at the impact of gene transfer agents on genotoxicity, up-regulation of oncogenes and other damages to stem cells. These crucial toxicity studies need to be done sooner rather than later. Our lab is continuing this project to provide more relevant data regarding the toxicity profile of the commercial vectors and 4HG.

References

1. McCormick F. Cancer gene therapy: fringe or cutting edge? Nature reviews Cancer 2001;1:130-41.
2. Karjoo Z, Chen X, Hatefi A. Progress and problems with the use of suicide genes for targeted cancer therapy. Advanced drug delivery reviews 2015.
3. Cihova M, Altanerova V, Altaner C. Stem cell based cancer gene therapy. Mol Pharm 2011;8:1480-7.
4. Teo GS, Ankrum JA, Martinelli R, et al. Mesenchymal stem cells transmigrate between and directly through tumor necrosis factor-alpha-activated endothelial cells via both leukocyte-like and novel mechanisms. Stem Cells 2012;30:2472-86.
5. Li C, Xu Y, Song L, Fu Q, Cui L, Yin S. Preliminary experimental study of tissue-engineered urethral reconstruction using oral keratinocytes seeded on BAMG. Urologia internationalis 2008;81:290-5.
6. Wang Y, Canine BF, Hatefi A. HSV-TK/GCV cancer suicide gene therapy by a designed recombinant multifunctional vector. Nanomedicine : nanotechnology, biology, and medicine 2011;7:193-200.
7. He XH, Wang Y, Yan XT, et al. Transduction of PEP-1-heme oxygenase-1 fusion protein reduces myocardial ischemia/reperfusion injury in rats. Journal of cardiovascular pharmacology 2013;62:436-42.
8. Simeoni F, Morris MC, Heitz F, Divita G. Insight into the mechanism of the peptide-based gene delivery system MPG: implications for delivery of siRNA into mammalian cells. Nucleic acids research 2003;31:2717-24.
9. DeVita VT, Jr., Chu E. A history of cancer chemotherapy. Cancer research 2008;68:8643-53.
10. Liu J, Zhang C, Hu W, Feng Z. Tumor suppressor p53 and its mutants in cancer metabolism. Cancer letters 2015;356:197-203.
11. van Horssen R, Ten Hagen TL, Eggermont AM. TNF-alpha in cancer treatment: molecular insights, antitumor effects, and clinical utility. The oncologist 2006;11:397-408.
12. van der Meel R, Vehmeijer LJ, Kok RJ, Storm G, van Gaal EV. Ligand-targeted particulate nanomedicines undergoing clinical evaluation: current status. Advanced drug delivery reviews 2013;65:1284-98.
13. Portsmouth D, Hlavaty J, Renner M. Suicide genes for cancer therapy. Molecular aspects of medicine 2007;28:4-41.
14. Dorer DE, Nettelbeck DM. Targeting cancer by transcriptional control in cancer gene therapy and viral oncolysis. Advanced drug delivery reviews 2009;61:554-71.
15. Kianmanesh AR, Perrin H, Panis Y, et al. A "distant" bystander effect of suicide gene therapy: regression of nontransduced tumors together with a distant transduced tumor. Human gene therapy 1997;8:1807-14.
16. Lammers T, Kiessling F, Hennink WE, Storm G. Drug targeting to tumors: principles, pitfalls and (pre-) clinical progress. J Control Release 2012;161:175-87.
17. Nicholas TW, Read SB, Burrows FJ, Kruse CA. Suicide gene therapy with Herpes simplex virus thymidine kinase and ganciclovir is enhanced with connexins to improve gap junctions and bystander effects. Histology and histopathology 2003;18:495-507.
18. Ardiani A, Johnson AJ, Ruan H, Sanchez-Bonilla M, Serve K, Black ME. Enzymes to die for: exploiting nucleotide metabolizing enzymes for cancer gene therapy. Current gene therapy 2012;12:77-91.

19. Preuss E, Muik A, Weber K, Otte J, von Laer D, Fehse B. Cancer suicide gene therapy with TK.007: superior killing efficiency and bystander effect. Journal of molecular medicine 2011;89:1113-24.
20. Black ME, Kokoris MS, Sabo P. Herpes simplex virus-1 thymidine kinase mutants created by semi-random sequence mutagenesis improve prodrug-mediated tumor cell killing. Cancer research 2001;61:3022-6.
21. Ostertag D, Amundson KK, Lopez Espinoza F, et al. Brain tumor eradication and prolonged survival from intratumoral conversion of 5-fluorocytosine to 5-fluorouracil using a nonlytic retroviral replicating vector. Neuro-oncology 2012;14:145-59.
22. Stolworthy TS, Korkegian AM, Willmon CL, et al. Yeast cytosine deaminase mutants with increased thermostability impart sensitivity to 5-fluorocytosine. Journal of molecular biology 2008;377:854-69.
23. Shi DZ, Hu WX, Li LX, Chen G, Wei D, Gu PY. Pharmacokinetics and the bystander effect in CD::UPRT/5-FC bi-gene therapy of glioma. Chinese medical journal 2009;122:1267-72.
24. Greco O, Dachs GU. Gene directed enzyme/prodrug therapy of cancer: historical appraisal and future prospectives. Journal of cellular physiology 2001;187:22-36.
25. Green LK, Storey MA, Williams EM, et al. The Flavin Reductase MsuE Is a Novel Nitroreductase that Can Efficiently Activate Two Promising Next-Generation Prodrugs for Gene-Directed Enzyme Prodrug Therapy. Cancers 2013;5:985-97.
26. Green LK, Syddall SP, Carlin KM, et al. Pseudomonas aeruginosa NfsB and nitro-CBI-DEI--a promising enzyme/prodrug combination for gene directed enzyme prodrug therapy. Molecular cancer 2013;12:58.
27. Stribbling SM, Friedlos F, Martin J, et al. Regressions of established breast carcinoma xenografts by carboxypeptidase G2 suicide gene therapy and the prodrug CMDA are due to a bystander effect. Human gene therapy 2000;11:285-92.
28. Mohit E, Rafati S. Biological delivery approaches for gene therapy: strategies to potentiate efficacy and enhance specificity. Molecular immunology 2013;56:599-611.
29. Thomas CE, Ehrhardt A, Kay MA. Progress and problems with the use of viral vectors for gene therapy. Nature reviews Genetics 2003;4:346-58.
30. McCarthy HO, Wang Y, Mangipudi SS, Hatefi A. Advances with the use of bio-inspired vectors towards creation of artificial viruses. Expert opinion on drug delivery 2010;7:497-512.
31. Gao X, Kim KS, Liu D. Nonviral gene delivery: what we know and what is next. The AAPS journal 2007;9:E92-104.
32. Ambegia E, Ansell S, Cullis P, Heyes J, Palmer L, MacLachlan I. Stabilized plasmid-lipid particles containing PEG-diacylglycerols exhibit extended circulation lifetimes and tumor selective gene expression. Biochimica et biophysica acta 2005;1669:155-63.
33. Ishida T, Ichihara M, Wang X, et al. Injection of PEGylated liposomes in rats elicits PEG-specific IgM, which is responsible for rapid elimination of a second dose of PEGylated liposomes. Journal of controlled release : official journal of the Controlled Release Society 2006;112:15-25.
34. Judge A, McClintock K, Phelps JR, Maclachlan I. Hypersensitivity and loss of disease site targeting caused by antibody responses to PEGylated liposomes. Molecular therapy : the journal of the American Society of Gene Therapy 2006;13:328-37.
35. Rejman J, Oberle V, Zuhorn IS, Hoekstra D. Size-dependent internalization of particles via the pathways of clathrin- and caveolae-mediated endocytosis. The Biochemical journal 2004;377:159-69.
36. Fischer D, Li Y, Ahlemeyer B, Krieglstein J, Kissel T. In vitro cytotoxicity testing of polycations: influence of polymer structure on cell viability and hemolysis. Biomaterials 2003;24:1121-31.
37. Fenske DB, MacLachlan I, Cullis PR. Long-circulating vectors for the systemic delivery of genes. Current opinion in molecular therapeutics 2001;3:153-8.

38. Palucka K, Ueno H, Fay J, Banchereau J. Dendritic cells and immunity against cancer. Journal of internal medicine 2011;269:64-73.
39. Palucka K, Ueno H, Roberts L, Fay J, Banchereau J. Dendritic cell subsets as vectors and targets for improved cancer therapy. Current topics in microbiology and immunology 2011;344:173-92.
40. Altaner C, Altanerova V, Cihova M, et al. Complete regression of glioblastoma by mesenchymal stem cells mediated prodrug gene therapy simulating clinical therapeutic scenario. International journal of cancer Journal international du cancer 2014;134:1458-65.
41. Allen TM, Cullis PR. Drug delivery systems: entering the mainstream. Science 2004;303:1818-22.
42. Peer D, Karp JM, Hong S, Farokhzad OC, Margalit R, Langer R. Nanocarriers as an emerging platform for cancer therapy. Nat Nanotechnol 2007;2:751-60.
43. Yao X, Yoshioka Y, Morishige T, et al. Systemic administration of a PEGylated adenovirus vector with a cancer-specific promoter is effective in a mouse model of metastasis. Gene Ther 2009;16:1395-404.
44. Yao XL, Yoshioka Y, Ruan GX, et al. Optimization and internalization mechanisms of PEGylated adenovirus vector with targeting peptide for cancer gene therapy. Biomacromolecules 2012;13:2402-9.
45. Reddy LH. Drug delivery to tumours: recent strategies. J Pharm Pharmacol 2005;57:1231-42.
46. Matsumura Y, Maeda H. A new concept for macromolecular therapeutics in cancer chemotherapy: mechanism of tumoritropic accumulation of proteins and the antitumor agent smancs. Cancer research 1986;46:6387-92.
47. Zhao D, Najbauer J, Garcia E, et al. Neural stem cell tropism to glioma: critical role of tumor hypoxia. Mol Cancer Res 2008;6:1819-29.
48. Ren C, Kumar S, Chanda D, et al. Cancer gene therapy using mesenchymal stem cells expressing interferon-beta in a mouse prostate cancer lung metastasis model. Gene Ther 2008;15:1446-53.
49. Stagg J, Lejeune L, Paquin A, Galipeau J. Marrow stromal cells for interleukin-2 delivery in cancer immunotherapy. Human gene therapy 2004;15:597-608.
50. Ciavarella S, Grisendi G, Dominici M, et al. In vitro anti-myeloma activity of TRAIL-expressing adipose-derived mesenchymal stem cells. Br J Haematol 2012;157:586-98.
51. Khan Z, Knecht W, Willer M, et al. Plant thymidine kinase 1: a novel efficient suicide gene for malignant glioma therapy. Neuro-oncology 2010;12:549-58.
52. Studeny M, Marini FC, Champlin RE, Zompetta C, Fidler IJ, Andreeff M. Bone marrow-derived mesenchymal stem cells as vehicles for interferon-beta delivery into tumors. Cancer research 2002;62:3603-8.
53. Uhl M, Weiler M, Wick W, Jacobs AH, Weller M, Herrlinger U. Migratory neural stem cells for improved thymidine kinase-based gene therapy of malignant gliomas. Biochem Biophys Res Commun 2005;328:125-9.
54. Benedetti S, Pirola B, Pollo B, et al. Gene therapy of experimental brain tumors using neural progenitor cells. Nat Med 2000;6:447-50.
55. Kucerova L, Matuskova M, Pastorakova A, et al. Cytosine deaminase expressing human mesenchymal stem cells mediated tumour regression in melanoma bearing mice. J Gene Med 2008;10:1071-82.
56. Salem HK, Thiemermann C. Mesenchymal stromal cells: current understanding and clinical status. Stem Cells 2010;28:585-96.
57. Belmar-Lopez C, Mendoza G, Oberg D, et al. Tissue-derived mesenchymal stromal cells used as vehicles for anti-tumor therapy exert different in vivo effects on migration capacity and tumor growth. BMC Med 2013;11:139.

58. Ringe J, Strassburg S, Neumann K, et al. Towards in situ tissue repair: human mesenchymal stem cells express chemokine receptors CXCR1, CXCR2 and CCR2, and migrate upon stimulation with CXCL8 but not CCL2. J Cell Biochem 2007;101:135-46.
59. Ponte AL, Marais E, Gallay N, et al. The in vitro migration capacity of human bone marrow mesenchymal stem cells: comparison of chemokine and growth factor chemotactic activities. Stem Cells 2007;25:1737-45.
60. Pendleton C, Li Q, Chesler DA, Yuan K, Guerrero-Cazares H, Quinones-Hinojosa A. Mesenchymal stem cells derived from adipose tissue vs bone marrow: in vitro comparison of their tropism towards gliomas. PLoS One 2013;8:e58198.
61. Frank RT, Edmiston M, Kendall SE, et al. Neural stem cells as a novel platform for tumor-specific delivery of therapeutic antibodies. PLoS One 2009;4:e8314.
62. Mercapide J, Rappa G, Anzanello F, King J, Fodstad O, Lorico A. Primary gene-engineered neural stem/progenitor cells demonstrate tumor-selective migration and antitumor effects in glioma. International journal of cancer Journal international du cancer 2010;126:1206-15.
63. Zhao Y, Lam DH, Yang J, et al. Targeted suicide gene therapy for glioma using human embryonic stem cell-derived neural stem cells genetically modified by baculoviral vectors. Gene Ther 2012;19:189-200.
64. Lee DH, Ahn Y, Kim SU, et al. Targeting rat brainstem glioma using human neural stem cells and human mesenchymal stem cells. Clin Cancer Res 2009;15:4925-34.
65. Kidd S, Spaeth E, Dembinski JL, et al. Direct evidence of mesenchymal stem cell tropism for tumor and wounding microenvironments using in vivo bioluminescent imaging. Stem Cells 2009;27:2614-23.
66. Dwyer RM, Potter-Beirne SM, Harrington KA, et al. Monocyte chemotactic protein-1 secreted by primary breast tumors stimulates migration of mesenchymal stem cells. Clin Cancer Res 2007;13:5020-7.
67. Komarova S, Kawakami Y, Stoff-Khalili MA, Curiel DT, Pereboeva L. Mesenchymal progenitor cells as cellular vehicles for delivery of oncolytic adenoviruses. Mol Cancer Ther 2006;5:755-66.
68. Bexell D, Gunnarsson S, Svensson A, et al. Rat multipotent mesenchymal stromal cells lack long-distance tropism to 3 different rat glioma models. Neurosurgery 2012;70:731-9.
69. Song C, Xiang J, Tang J, et al. Thymidine kinase gene modified bone marrow mesenchymal stem cells as vehicles for antitumor therapy. Human gene therapy 2011;22:439-49.
70. Loebinger MR, Eddaoudi A, Davies D, Janes SM. Mesenchymal stem cell delivery of TRAIL can eliminate metastatic cancer. Cancer Res 2009;69:4134-42.
71. Kim SW, Kim SJ, Park SH, et al. Complete regression of metastatic renal cell carcinoma by multiple injections of engineered mesenchymal stem cells expressing dodecameric TRAIL and HSV-TK. Clin Cancer Res 2013;19:415-27.
72. Chao P, Deshmukh M, Kutscher HL, et al. Pulmonary targeting microparticulate camptothecin delivery system: anticancer evaluation in a rat orthotopic lung cancer model. Anticancer Drugs 2010;21:65-76.
73. Xia X, Ji T, Chen P, et al. Mesenchymal stem cells as carriers and amplifiers in CRAd delivery to tumors. Molecular cancer 2011;10:134.
74. Kucerova L, Altanerova V, Matuskova M, Tyciakova S, Altaner C. Adipose tissue-derived human mesenchymal stem cells mediated prodrug cancer gene therapy. Cancer research 2007;67:6304-13.
75. Zhao D, Najbauer J, Annala AJ, et al. Human neural stem cell tropism to metastatic breast cancer. Stem Cells 2012;30:314-25.
76. Aboody KS, Bush RA, Garcia E, et al. Development of a tumor-selective approach to treat metastatic cancer. PLoS One 2006;1:e23.

77. Hung SC, Deng WP, Yang WK, et al. Mesenchymal stem cell targeting of microscopic tumors and tumor stroma development monitored by noninvasive in vivo positron emission tomography imaging. Clin Cancer Res 2005;11:7749-56.
78. Yang J, Lam DH, Goh SS, et al. Tumor tropism of intravenously injected human-induced pluripotent stem cell-derived neural stem cells and their gene therapy application in a metastatic breast cancer model. Stem Cells 2012;30:1021-9.
79. Luetzkendorf J, Mueller LP, Mueller T, Caysa H, Nerger K, Schmoll HJ. Growth inhibition of colorectal carcinoma by lentiviral TRAIL-transgenic human mesenchymal stem cells requires their substantial intratumoral presence. J Cell Mol Med 2010;14:2292-304.
80. Eggenhofer E, Benseler V, Kroemer A, et al. Mesenchymal stem cells are short-lived and do not migrate beyond the lungs after intravenous infusion. Front Immunol 2012;3:297.
81. Mukherjee A, Tipnis S, Sarma HD, et al. Radiolabeling of umbilical cord-derived mesenchymal stem cells for in vivo tracking. Cancer Biother Radiopharm 2012;27:614-9.
82. Doucette T, Rao G, Yang Y, et al. Mesenchymal stem cells display tumor-specific tropism in an RCAS/Ntv-a glioma model. Neoplasia 2011;13:716-25.
83. Kim SM, Oh JH, Park SA, et al. Irradiation enhances the tumor tropism and therapeutic potential of tumor necrosis factor-related apoptosis-inducing ligand-secreting human umbilical cord blood-derived mesenchymal stem cells in glioma therapy. Stem Cells 2010;28:2217-28.
84. Ziadloo A, Burks SR, Gold EM, et al. Enhanced homing permeability and retention of bone marrow stromal cells by noninvasive pulsed focused ultrasound. Stem Cells 2012;30:1216-27.
85. Nystedt J, Anderson H, Tikkanen J, et al. Cell surface structures influence lung clearance rate of systemically infused mesenchymal stromal cells. Stem Cells 2013;31:317-26.
86. Ruan J, Song H, Li C, et al. DiR-labeled Embryonic Stem Cells for Targeted Imaging of in vivo Gastric Cancer Cells. Theranostics 2012;2:618-28.
87. Lin S, Xie X, Patel MR, et al. Quantum dot imaging for embryonic stem cells. BMC Biotechnol 2007;7:67.
88. Muller-Borer BJ, Collins MC, Gunst PR, Cascio WE, Kypson AP. Quantum dot labeling of mesenchymal stem cells. J Nanobiotechnology 2007;5:9.
89. Bouvet M, Wang J, Nardin SR, et al. Real-time optical imaging of primary tumor growth and multiple metastatic events in a pancreatic cancer orthotopic model. Cancer Res 2002;62:1534-40.
90. Jiguet-Jiglaire C, Cayol M, Mathieu S, et al. Noninvasive near-infrared fluorescent protein-based imaging of tumor progression and metastases in deep organs and intraosseous tissues. J Biomed Opt 2014;19:16019.
91. Togel F, Yang Y, Zhang P, Hu Z, Westenfelder C. Bioluminescence imaging to monitor the in vivo distribution of administered mesenchymal stem cells in acute kidney injury. Am J Physiol Renal Physiol 2008;295:F315-21.
92. Close DM, Xu T, Sayler GS, Ripp S. In vivo bioluminescent imaging (BLI): noninvasive visualization and interrogation of biological processes in living animals. Sensors (Basel) 2011;11:180-206.
93. Nouri FS, Wang X, Hatefi A. Genetically engineered theranostic mesenchymal stem cells for the evaluation of the anticancer efficacy of enzyme/prodrug systems. J Control Release 2015;200:179-87.
94. Wang H, Cao F, De A, et al. Trafficking mesenchymal stem cell engraftment and differentiation in tumor-bearing mice by bioluminescence imaging. Stem Cells 2009;27:1548-58.
95. Collins JW, Meganck JA, Kuo C, Francis KP, Frankel G. 4D multimodality imaging of Citrobacter rodentium infections in mice. J Vis Exp 2013.
96. Kuo C, Coquoz O, Troy TL, Xu H, Rice BW. Three-dimensional reconstruction of in vivo bioluminescent sources based on multispectral imaging. J Biomed Opt 2007;12:024007.

97. Li SC, Tachiki LM, Luo J, Dethlefs BA, Chen Z, Loudon WG. A biological global positioning system: considerations for tracking stem cell behaviors in the whole body. Stem Cell Rev 2010;6:317-33.
98. Aoki I, Wu YJL, Silva AC, Lynch RM, Koretsky AP. In vivo detection of neuroarchitecture in the rodent brain using manganese-enhanced MRI. Neuroimage 2004;22:1046-59.
99. Zhang SJ, Wu JC. Comparison of imaging techniques for tracking cardiac stem cell therapy. J Nucl Med 2007;48:1916-9.
100. Liu J, Cheng EC, Long RC, et al. Noninvasive monitoring of embryonic stem cells in vivo with MRI transgene reporter. Tissue Eng Part C Methods 2009;15:739-47.
101. Li Z, Suzuki Y, Huang M, et al. Comparison of reporter gene and iron particle labeling for tracking fate of human embryonic stem cells and differentiated endothelial cells in living subjects. Stem Cells 2008;26:864-73.
102. Nohroudi K, Arnhold S, Berhorn T, Addicks K, Hoehn M, Himmelreich U. In vivo MRI stem cell tracking requires balancing of detection limit and cell viability. Cell Transplant 2010;19:431-41.
103. Diana V, Bossolasco P, Moscatelli D, Silani V, Cova L. Dose dependent side effect of superparamagnetic iron oxide nanoparticle labeling on cell motility in two fetal stem cell populations. PLoS One 2013;8:e78435.
104. Thu MS, Najbauer J, Kendall SE, et al. Iron labeling and pre-clinical MRI visualization of therapeutic human neural stem cells in a murine glioma model. PLoS One 2009;4:e7218.
105. Lee HJ, Doo SW, Kim DH, et al. Cytosine deaminase-expressing human neural stem cells inhibit tumor growth in prostate cancer-bearing mice. Cancer letters 2013;335:58-65.
106. Boersma HH, Tromp SC, Hofstra L, Narula J. Stem cell tracking: reversing the silence of the lambs. J Nucl Med 2005;46:200-3.
107. Daldrup-Link HE, Rudelius M, Metz S, et al. Cell tracking with gadophrin-2: a bifunctional contrast agent for MR imaging, optical imaging, and fluorescence microscopy. Eur J Nucl Med Mol Imaging 2004;31:1312-21.
108. Jiang H, Cheng Z, Tian M, Zhang H. In vivo imaging of embryonic stem cell therapy. Eur J Nucl Med Mol Imaging 2011;38:774-84.
109. Hofmann M, Wollert KC, Meyer GP, et al. Monitoring of bone marrow cell homing into the infarcted human myocardium. Circulation 2005;111:2198-202.
110. Gu E, Chen WY, Gu J, Burridge P, Wu JC. Molecular imaging of stem cells: tracking survival, biodistribution, tumorigenicity, and immunogenicity. Theranostics 2012;2:335-45.
111. Love Z, Wang F, Dennis J, et al. Imaging of mesenchymal stem cell transplant by bioluminescence and PET. J Nucl Med 2007;48:2011-20.
112. Miletic H, Fischer Y, Litwak S, et al. Bystander killing of malignant glioma by bone marrow-derived tumor-infiltrating progenitor cells expressing a suicide gene. Molecular therapy : the journal of the American Society of Gene Therapy 2007;15:1373-81.
113. Zhang G, Lan X, Yen TC, et al. Therapeutic gene expression in transduced mesenchymal stem cells can be monitored using a reporter gene. Nucl Med Biol 2012;39:1243-50.
114. Dwyer RM, Ryan J, Havelin RJ, et al. Mesenchymal Stem Cell-mediated delivery of the sodium iodide symporter supports radionuclide imaging and treatment of breast cancer. Stem Cells 2011;29:1149-57.
115. Frangioni JV, Hajjar RJ. In vivo tracking of stem cells for clinical trials in cardiovascular disease. Circulation 2004;110:3378-83.
116. Stojanov K, de Vries EF, Hoekstra D, van Waarde A, Dierckx RA, Zuhorn IS. [18F]FDG labeling of neural stem cells for in vivo cell tracking with positron emission tomography: inhibition of tracer release by phloretin. Mol Imaging 2012;11:1-12.

117. Wang XY, Ju S, Li C, et al. Non-invasive imaging of endothelial progenitor cells in tumor neovascularization using a novel dual-modality paramagnetic/near-infrared fluorescence probe. PLoS One 2012;7:e50575.
118. Aboody KS, Najbauer J, Metz MZ, et al. Neural stem cell-mediated enzyme/prodrug therapy for glioma: preclinical studies. Sci Transl Med 2013;5:184ra59.
119. Cavarretta IT, Altanerova V, Matuskova M, Kucerova L, Culig Z, Altaner C. Adipose tissue-derived mesenchymal stem cells expressing prodrug-converting enzyme inhibit human prostate tumor growth. Molecular therapy : the journal of the American Society of Gene Therapy 2010;18:223-31.
120. Matuskova M, Hlubinova K, Pastorakova A, et al. HSV-tk expressing mesenchymal stem cells exert bystander effect on human glioblastoma cells. Cancer letters 2010;290:58-67.
121. Gu C, Li S, Tokuyama T, Yokota N, Namba H. Therapeutic effect of genetically engineered mesenchymal stem cells in rat experimental leptomeningeal glioma model. Cancer letters 2010;291:256-62.
122. Kosaka H, Ichikawa T, Kurozumi K, et al. Therapeutic effect of suicide gene-transferred mesenchymal stem cells in a rat model of glioma. Cancer gene therapy 2012;19:572-8.
123. Yi BR, Hwang KA, Aboody KS, Jeung EB, Kim SU, Choi KC. Selective antitumor effect of neural stem cells expressing cytosine deaminase and interferon-beta against ductal breast cancer cells in cellular and xenograft models. Stem Cell Res 2014;12:36-48.
124. Karjoo Z, Ganapathy V, Hatefi A. Gene Directed Enzyme Prodrug Cancer Therapy. In: Lattime EC, Gerson SL, eds. Gene Therapy of Cancer. 3rd ed: Elsevier Inc.; 2013:77-91.
125. Prosser GA, Copp JN, Syddall SP, et al. Discovery and evaluation of Escherichia coli nitroreductases that activate the anti-cancer prodrug CB1954. Biochem Pharmacol 2010;79:678-87.
126. Shi DZ, Hu WX, Li LX, Chen G, Wei D, Gu PY. Pharmacokinetics and the bystander effect in CD::UPRT/5-FC bi-gene therapy of glioma. Chin Med J (Engl) 2009;122:1267-72.
127. Grohmann M, Paulmann N, Fleischhauer S, Vowinckel J, Priller J, Walther DJ. A mammalianized synthetic nitroreductase gene for high-level expression. BMC Cancer 2009;9:301.
128. Luetzkendorf J, Mueller LP, Mueller T, Caysa H, Nerger K, Schmoll HJ. Growth inhibition of colorectal carcinoma by lentiviral TRAIL-transgenic human mesenchymal stem cells requires their substantial intratumoral presence. J Cell Mol Med 2010;14:2292-304.
129. Fischer UM, Harting MT, Jimenez F, et al. Pulmonary passage is a major obstacle for intravenous stem cell delivery: the pulmonary first-pass effect. Stem Cells Dev 2009;18:683-92.
130. Xiao J, Zhang G, Qiu P, et al. Tanshinone IIA increases the bystander effect of herpes simplex virus thymidine kinase/ganciclovir gene therapy via enhanced gap junctional intercellular communication. PLoS ONE 2013;8:e67662.
131. Belmar-Lopez C, Mendoza G, Oberg D, et al. Tissue-derived mesenchymal stromal cells used as vehicles for anti-tumor therapy exert different in vivo effects on migration capacity and tumor growth. BMC Med 2013;11:139.
132. Tang MH, Helsby NA, Goldthorpe MA, Thompson KM, Al-Ali S, Tingle MD. Hepatic nitroreduction, toxicity and toxicokinetics of the anti-tumour prodrug CB 1954 in mouse and rat. Toxicology 2007;240:70-85.
133. Green LK, Storey MA, Williams EM, et al. The Flavin Reductase MsuE Is a Novel Nitroreductase that Can Efficiently Activate Two Promising Next-Generation Prodrugs for Gene-Directed Enzyme Prodrug Therapy. Cancers (Basel) 2013;5:985-97.
134. Wiewrodt R, Amin K, Kiefer M, et al. Adenovirus-mediated gene transfer of enhanced Herpes simplex virus thymidine kinase mutants improves prodrug-mediated tumor cell killing. Cancer Gene Ther 2003;10:353-64.

135. Ardiani A, Sanchez-Bonilla M, Black ME. Fusion enzymes containing HSV-1 thymidine kinase mutants and guanylate kinase enhance prodrug sensitivity in vitro and in vivo. Cancer gene therapy 2010;17:86-96.
136. Rath P, Shi H, Maruniak JA, Litofsky NS, Maria BL, Kirk MD. Stem cells as vectors to deliver HSV/tk gene therapy for malignant gliomas. Current stem cell research & therapy 2009;4:44-9.
137. van Putten EH, Dirven CM, van den Bent MJ, Lamfers ML. Sitimagene ceradenovec: a gene-based drug for the treatment of operable high-grade glioma. Future Oncol 2010;6:1691-710.
138. Garcia-Sanchez F, Pizzorno G, Fu SQ, et al. Cytosine deaminase adenoviral vector and 5-fluorocytosine selectively reduce breast cancer cells 1 million-fold when they contaminate hematopoietic cells: a potential purging method for autologous transplantation. Blood 1998;92:672-82.
139. Wiethoff CM, Middaugh CR. Barriers to nonviral gene delivery. Journal of pharmaceutical sciences 2003;92:203-17.
140. Haider M, Hatefi A, Ghandehari H. Recombinant polymers for cancer gene therapy: a minireview. Journal of controlled release : official journal of the Controlled Release Society 2005;109:108-19.
141. Goparaju GN, Satishchandran C, Gupta PK. The effect of the structure of small cationic peptides on the characteristics of peptide-DNA complexes. International journal of pharmaceutics 2009;369:162-9.
142. Wang Y, Mangipudi SS, Canine BF, Hatefi A. A designer biomimetic vector with a chimeric architecture for targeted gene transfer. Journal of controlled release : official journal of the Controlled Release Society 2009;137:46-53.
143. Khalil IA, Hayashi Y, Mizuno R, Harashima H. Octaarginine- and pH sensitive fusogenic peptide-modified nanoparticles for liver gene delivery. J Control Release 2011;156:374-80.
144. Wang Y, Mangipudi SS, Canine BF, Hatefi A. A designer biomimetic vector with a chimeric architecture for targeted gene transfer. J Control Release 2009;137:46-53.
145. Plank C, Oberhauser B, Mechtler K, Koch C, Wagner E. The influence of endosome-disruptive peptides on gene transfer using synthetic virus-like gene transfer systems. J Biol Chem 1994;269:12918-24.
146. Wyman TB, Nicol F, Zelphati O, Scaria PV, Plank C, Szoka FC, Jr. Design, synthesis, and characterization of a cationic peptide that binds to nucleic acids and permeabilizes bilayers. Biochemistry 1997;36:3008-17.
147. Midoux P, Kichler A, Boutin V, Maurizot JC, Monsigny M. Membrane permeabilization and efficient gene transfer by a peptide containing several histidines. Bioconjug Chem 1998;9:260-7.
148. Laue M. Electron microscopy of viruses. Methods Cell Biol 2010;96:1-20.
149. Midoux P, Monsigny M. Efficient gene transfer by histidylated polylysine/pDNA complexes. Bioconjug Chem 1999;10:406-11.
150. Kashiwada A, Matsuda K, Mizuno T, Tanaka T. Construction of a pH-responsive artificial membrane fusion system by using designed coiled-coil polypeptides. Chemistry 2008;14:7343-50.
151. Rittner K, Benavente A, Bompard-Sorlet A, et al. New basic membrane-destabilizing peptides for plasmid-based gene delivery in vitro and in vivo. Mol Ther 2002;5:104-14.
152. Midoux P, Pichon C, Yaouanc JJ, Jaffres PA. Chemical vectors for gene delivery: a current review on polymers, peptides and lipids containing histidine or imidazole as nucleic acids carriers. Br J Pharmacol 2009;157:166-78.
153. Nygren PA. Alternative binding proteins: affibody binding proteins developed from a small three-helix bundle scaffold. The FEBS journal 2008;275:2668-76.
154. Orlova A, Magnusson M, Eriksson TL, et al. Tumor imaging using a picomolar affinity HER2 binding affibody molecule. Cancer Res 2006;66:4339-48.

155. Khalil IA, Kogure K, Akita H, Harashima H. Uptake pathways and subsequent intracellular trafficking in nonviral gene delivery. Pharmacol Rev 2006;58:32-45.
156. Canine BF, Wang Y, Hatefi A. Biosynthesis and characterization of a novel genetically engineered polymer for targeted gene transfer to cancer cells. J Control Release 2009;138:188-96.
157. Bowman EJ, Siebers A, Altendorf K. Bafilomycins: a class of inhibitors of membrane ATPases from microorganisms, animal cells, and plant cells. Proc Natl Acad Sci U S A 1988;85:7972-6.
158. Huang Q, Sivaramakrishna RP, Ludwig K, Korte T, Bottcher C, Herrmann A. Early steps of the conformational change of influenza virus hemagglutinin to a fusion active state: stability and energetics of the hemagglutinin. Biochimica et biophysica acta 2003;1614:3-13.
159. Han X, Bushweller JH, Cafiso DS, Tamm LK. Membrane structure and fusion-triggering conformational change of the fusion domain from influenza hemagglutinin. Nat Struct Biol 2001;8:715-20.
160. Mangipudi SS, Canine BF, Wang Y, Hatefi A. Development of a genetically engineered biomimetic vector for targeted gene transfer to breast cancer cells. Mol Pharm 2009;6:1100-9.
161. Herd H, Daum N, Jones AT, Huwer H, Ghandehari H, Lehr CM. Nanoparticle geometry and surface orientation influence mode of cellular uptake. ACS Nano 2013;7:1961-73.
162. Hancock RE. Peptide antibiotics. Lancet 1997;349:418-22.
163. Hilchie AL, Doucette CD, Pinto DM, Patrzykat A, Douglas S, Hoskin DW. Pleurocidin-family cationic antimicrobial peptides are cytolytic for breast carcinoma cells and prevent growth of tumor xenografts. Breast Cancer Res 2011;13:R102.
164. D'Andrea LD, Iaccarino G, Fattorusso R, et al. Targeting angiogenesis: structural characterization and biological properties of a de novo engineered VEGF mimicking peptide. Proceedings of the National Academy of Sciences of the United States of America 2005;102:14215-20.
165. Brusselmans K, Bono F, Collen D, Herbert JM, Carmeliet P, Dewerchin M. A novel role for vascular endothelial growth factor as an autocrine survival factor for embryonic stem cells during hypoxia. The Journal of biological chemistry 2005;280:3493-9.
166. El-Mousawi M, Tchistiakova L, Yurchenko L, et al. A vascular endothelial growth factor high affinity receptor 1-specific peptide with antiangiogenic activity identified using a phage display peptide library. The Journal of biological chemistry 2003;278:46681-91.
167. Morris MC, Deshayes S, Heitz F, Divita G. Cell-penetrating peptides: from molecular mechanisms to therapeutics. Biology of the cell / under the auspices of the European Cell Biology Organization 2008;100:201-17.
168. Milletti F. Cell-penetrating peptides: classes, origin, and current landscape. Drug discovery today 2012;17:850-60.
169. Deshayes S, Morris MC, Divita G, Heitz F. Interactions of amphipathic carrier peptides with membrane components in relation with their ability to deliver therapeutics. Journal of peptide science : an official publication of the European Peptide Society 2006;12:758-65.
170. Deshayes S, Gerbal-Chaloin S, Morris MC, et al. On the mechanism of non-endosomial peptide-mediated cellular delivery of nucleic acids. Biochimica et biophysica acta 2004;1667:141-7.
171. Shah V, Taratula O, Garbuzenko OB, et al. Genotoxicity of different nanocarriers: possible modifications for the delivery of nucleic acids. Current drug discovery technologies 2013;10:8-15.
172. Heitz F, Morris MC, Divita G. Twenty years of cell-penetrating peptides: from molecular mechanisms to therapeutics. British journal of pharmacology 2009;157:195-206.
173. Santulli G, Ciccarelli M, Palumbo G, et al. In vivo properties of the proangiogenic peptide QK. Journal of translational medicine 2009;7:41.